Incorporation of Functional Considerations in Highway Pavement Design and Operations

CHU LONGJIA
(B.Eng & M.Sc)

A THESIS SUBMITTED
FOR THE DEGREE OF DOCTOR OF PHILOSOPHY
DEPARTMENT OF CIVIL & ENVIRONMENTAL ENGINEERING
NATIONAL UNIVERSITY OF SINGAPORE

2017

Supervisors:
Professor Fwa Tien Fang, Main Supervisor
Professor Tan Kiang Hwee, Co-Supervisor

Examiners:
Professor Meng Qiang
Associate Professor Tan Siew Ann
Professor Zhang Zhanmin, University of Texas at Austin

DECLARATION

I hereby declare that the thesis is my original work and it has been written by me in its entirety. I have duly acknowledges all the sources of information which have been used in the thesis.

This thesis has also not been submitted for any degree in any university previously.

Chu Longjia

18 Jan, 2017

ACKNOWLEDGEMENTS

I would like to express my utmost appreciation and gratitude to my supervisors, Professor Fwa Tien Fang and Professor Tan Kiang Hwee, for their constant guidance, support and encouragement throughout the research. They do not only teach me the knowledge necessary for doing the research, but also cultivate me to look at a fact in different views, discover problems, and find a way to solve.

Special thanks are given to the National University of Singapore for providing me the NUS Research Scholarship for my PhD study. Thanks are also extended to my fellow research students, Ms. Fu Rao, Ms. Xu Min, Ms. Hua Wen, Mr. Wang Yadong and Mr. Zhao Kangjia for their kind help and friendship. Thanks are also accorded to Mr. Foo Chee Kiong, Mr. Goh Joon Kiat, Mrs. Yap-Chong Wei Leng, and Mr. Santhasamy Martin of the Transportation Engineering Laboratory.

Finally, I would like to express my heartfelt thanks and gratitude to my parents and my brother for their tremendous care, support and encouragement all the time.

TABLE OF CONTENTS

SUMMARY

The main objective of pavement design is to provide a smooth, safe, quiet, durable and environmentally sustainable pavement structure to serve the road users with a high level of service. To meet this objective, a pavement must be designed to satisfy both structural and functional requirements. Unfortunately, the current pavement design methods are based on structural analysis to provide a pavement with an adequate structural capacity against specified design failure modes. The considerations for pavement roughness, skid resistance, hydroplaning, and tire-pavement noise are not fully considered.

This study aims to develop a design framework to incorporate function performance requirements into a pavement structural design process. The scope of this study can be divided into two parts. The first part addresses travel safety requirements related to pavements, and the second part is concerned with porous pavement properties related to both safety requirements and tire-pavement noise reduction.

The first part stresses how to incorporate skid resistance and hydroplaning consideration into current pavement design and pavement management systems. In the design phase, a three-dimensional skid resistance simulation model is employed to evaluate the adequacy of a gradation design of aggregates to fulfil wet-weather driving safety requirements. The analysis is based on the consideration of hydroplaning and skid resistance, taking into account the deterioration of pavement microtexture and macrotexture caused by traffic loading. Next, considering the operation phase, a procedure for determining the terminal rut depth based on wet-weather driving safety

consideration is proposed for pavement maintenance planning in a pavement management system.

Another travel safety issue related to pavement management is how to set the maximum safe speed limit during wet weather. A procedure for determining the safe speed limit is presented based on the consideration of stopping sight distance and the minimum skid resistance set by highway agency concerned. It is of significance to note that central to the wet-weather driving safety analyses in these applications in the first part is the introduction of the concept of skid resistance intervention curve, which is an improvement to the conventional concept of single-point minimum skid resistance intervention level.

The second part deals with the safety and noise reduction properties of porous pavements. Porous pavements are widely used in different parts of the world because of their benefits in noise reduction and enhanced wet-weather driving safety. Both benefits are heavily dependent on the high porosity of porous pavement structures. Unfortunately, porous pavements are prone to clogging which causes the pavements to lose much of its beneficial properties. The current porous pavement maintenance procedure is unable to provide pavement engineers enough information about when a maintenance treatment should be activated. This research proposes a engineering procedure, based on the consideration of wet-weather skid resistance requirements, to determine the terminal service state of a porous pavement affected by clogging. This part of the research also presents a laboratory procedure to evaluate the impact of the degree of clogging on the sound absorption characteristics of porous asphalt pavements, and to estimate their contributions to tire-pavement noise reduction.

LIST OF TABLES

LIST OF FIGURES

LIST OF SYMBOLS

A	Force attributed to adhesive/ cohesive effects
BPN	British Pendulum Number
$C_{1\varepsilon}$	Numerical constant equal to 1.44
$C_{2\varepsilon}$	Numerical constant equal to 1.92
C_{μ}	Numerical constant equal to 0.09
D	Stopping distance
D_R	Reaction distance
D_B	Braking distance
E_{ij}	Stress tensor
F	Friction force
G	Roadway grade
g	Gravitational acceleration
k	Kinetic energy of water
L_R	Reflected sound intensity in dBA
L_I	Incident sound intensity in dBA
N	Normal force at the contact surface
NRC	Noise reduction coefficient
P_{ref}	Reference sound pressure equal to 2×10^{-5} Pa
p	Sound pressure in Pa
S	Sight distance

SAA	Sound absorption average
SN	Skid number
SN_0	Skid number at zero speed
t	Time
U	Velocity vector
V_0	Vehicle speed at time 0
$V(t)$	Vehicle speed at time t
α	Sound absorption coefficient of the pavement
ε	Viscous dissipation of water
μ	Coefficient of friction
ρ	Density of water
σ_k	Numerical constant equal to 1.00
σ_ε	Numerical constant equal to 1.30

CHAPTER 1 INTRODUCTION

1.1 Historical Development of Pavement Design Methodology

One of the earliest forms of engineering design of pavement was the Corps of Engineers' method. The Corps of Engineers' interest in developing a rational design procedure for airfield pavements began in 1940 (Ahlvin, 1991), due to the urgent need for airfield construction to meet wartime operational needs. With the recognition that developing a rational method based on limiting stresses and strains in various pavement layers was not possible with the theoretical knowledge and analytical tools available then, the Corps of Engineers concluded that an empirical highway design method should be adopted and further developed. Furthermore, due to the difficulties in developing theoretical means for analyzing load-induced behavior of flexible pavements, empirical approaches were adopted to characterize pavement behavior.

The provision of a structurally adequate pavement was the primary consideration in the early days. Toward the end of 1950s and early 1960s, there was an increasing concern for the functional role of highway pavements. This led to the introduction of the concept of pavement serviceability at the AASHO Road Test in late 1960s (Carey and Irick, 1960). This concept was adopted in the 1972 Interim Pavement Design Guide (AASHO, 1961; AASHTO, 1972). A pavement was considered failed when it no longer satisfactorily served the function to provide a smooth and safe travelled surface for efficient traffic operations. This was also the basis for the AASHTO design guides of 1985 (AASHTO, 1985) and 1993 (AASHTO, 1993). Unfortunately, due to the empirical nature of the thickness design relationships, this design concept was

abandoned and gave way to the mechanistic-empirical pavement design methodology proposed by AASHTO in its latest Mechanistic-Empirical Pavement Design Guide (MEPDG) (AASHTO, 2008a).

The mechanistic–empirical approach essentially designs pavement structure against selected load induced failure modes based on mechanistically derived stresses and strains. This is the approach that has been adopted by a number of pavement design guidelines such as the design guides of Australia (Austroads, 2004), France (LCP and SETRA, 1997), India (IRC, 2001), Asphalt Institute (1999), and South Africa (Theyse et al., 1996). Experience based empirical pavement design approaches are still being used by some other organizations, including Japan Road Association (1989), United Kingdom (1970), and Germany (RstO, 2000).

The current pavement design methods described above are based on structural analysis to provide a pavement with an adequate structural capacity against specified design failure modes. The considerations for roughness, skid-resistance, hydroplaning, and excess noise are either ignored or taken as ancillary pavement design considerations. This is not satisfactory as the functional service life may be much shorter than the structural design life.

1.2 Requirements of Pavement Design and Management

In pavement design and management, the main objective is to design and maintain a road providing a smooth, safe, quiet, durable and environmentally sustainable pavement structure to provide the road users with a high level of service. To meet this objective, a pavement must be designed and managed to satisfy both structural and functional requirements.

Practically all current pavement design procedures focus on structural design. If the structural design of a pavement has no effect on its functional performance, then it is acceptable to perform structural design independently from functional design of the pavement. The reality is that pavement structural design has important impacts on many aspects of the functional performance of a pavement, including major performance indicators such as riding comfort, driving safety, traffic noise, and environmental sustainability. Hence a comprehensive pavement design procedure must also incorporate functional requirements of a pavement in addition to the structural requirements addressed by conventional design procedures.

The conventional pavement management practices do not have a comprehensive treatment of the functional requirements of a pavement. For instance, for driving safety assessment, the only piece of information that highway agencies rely on is the measurement of skid resistance conducted according to a standard test procedure. Many highway agencies adopt a subjectively determined minimum skid resistance as the reference for checking the adequacy of pavement skid resistance (Henry, 2000; New Zealand Transport Agency, 2010; Ohio Department of Transportation, 2008; UK Design Manual, 2006). The minimum skid resistance threshold is usually determined from past experience or engineering judgement, based on statistical records of road accidents or values used by other highway agencies for similar pavement sections. As for traffic noise, there have not been any requirements for pavement management agencies to monitor how traffic noise varies with the type of pavement and the age of pavement. There are obviously needs for highway agencies to incorporate functional considerations in their pavement

management systems to provide a better service to the motorists and the general public.

1.3 Important Functional Requirements to be Considered in Pavement Design and Management

A key aspect of pavement structural design involves selection of pavement materials and paving mix design, to meet the requirements of providing efficient, safe, quiet, durable and environmentally sustainable pavements. The following functional requirements of a highway pavement are relevant in pavement design and management:

(a) Highway operational efficiency;

(b) Safe traffic operation; and

(c) Environmental sustainability.

1.3.1 Highway Operation Efficiency

The operational efficiency of a highway is dependent on the operating speeds of the traffic, which in turn are affected by the geometric design of highway and riding comfort of the traveled surface. Both of these two aspects are affected by certain properties of the pavement materials selected for the surface course. Therefore, there is a need to incorporate the relevant requirements of highway geometric design and roadway riding comfort in pavement design, the design of surface course mixture in particular.

To achieve the design traffic speed or traffic operating speed with the chosen geometric design of a highway, the pavement must be designed with the required properties to provide a safe and efficient operation of the highway. The geometric design of highway assumes a friction coefficient in the design of the following elements for a given design vehicle speed: (i) minimum sight distance,

(ii) minimum radius of horizontal curvature, and (iii) percent super-elevation of horizontal curves. The frictional requirements of pavement for each of these aspects should logically be part of the considerations in pavement design. Unfortunately, such requirements are not considered in any of the pavement design procedures currently used in practice.

The importance of riding comfort was first given due recognition in pavement design in the early 1960s by the then AASHO (American Association of State Highway Officials) in its interim pavement design guide (AASHO, 1961; AASHTO, 1972). The effect of riding comfort was introduced through the concept of pavement serviceability and evaluated in terms of the Pavement Serviceability Index (PSI). PSI is a key governing factor in the thickness determination of pavement layers in the AASHO design procedure. It is a main parameter in the pavement layer thickness equation of the interim AASHTO pavement design guide (AASHTO, 1972) and the subsequent AASHTO pavement design guide (AASHTO, 1993).

In the new Mechanistic-Empirical Pavement Design Guide (MEPDG) design procedure published by AASHTO (2008), the consideration of riding comfort remains but its importance is reduced to become one of a number of performance conditions to be checked after a trial structural design has been selected based on traffic loading analysis. Riding comfort is measured in terms of the International Roughness Index (IRI), which is estimated based on the predicted values of other pavement distresses. The predicted IRI values of the trial design are checked against pre-selected threshold limits. If the predicted performance does not meet the IRI criteria at a specified reliability level, the

trial pavement structural design (i.e. pavement thickness and material types) is modified until the performance criteria are satisfied.

Compared with the PSI based structural thickness design equations of 1972 AASHTO design guide procedure, the MEPDG trial and error approach of checking pavement smoothness performance of trial pavement thickness designs carries more promise as a rational pavement design procedure of incorporating the effects of other functional requirements of pavement as well. The main weakness of the MEPDG method of considering the requirements of pavement smoothness lies with the empirical nature of deriving the roughness development trend with time under the action of traffic loading. This is certainly an area in need for further research to develop a mechanistic model of roughness development as a function of traffic loading.

1.3.2 Safe Traffic Operation

Safe traffic operation of a highway pavement is affected by pavement design in terms of hydroplaning and skidding risks, especially in wet-weather driving. The selection of materials and mix design of the pavement surface course must therefore take into consideration the skid resistance and hydroplaning potential of the pavement surface.

While adequate structural strength for safe operation is already taken care of through structural design of pavements, a safe vehicular traveled surface requires special considerations not covered by conventional pavement design procedures. The two most important pavement-related safety considerations for vehicular traffic are the hydroplaning potential and skidding risks of the pavement design.

Hydroplaning and skidding are wet-weather driving safety concerns. Both are the results of interaction among tire, pavement surface and water on pavement surface. Hydroplaning of a vehicle refers to the situation when water on a wet pavement is not displaced at a rate fast enough from the tire-pavement contact area of a rolling or a locked sliding tire, resulting in the tire not making contact with the pavement surface over its complete footprint area. When hydroplaning occurs, the driver will lose steering and directional control of the vehicle, as well as the ability to reduce vehicle speed and bring the vehicle to a complete stop, due to the absence of friction force available to the tire. The pavement related factor that significantly influences the magnitude of hydroplaning risk is pavement surface macrotexture, which is largely governed by the choice of pavement mix design.

Skidding of vehicles during wet-weather driving is often caused by reduced skid resistance due to the presence of water on pavement surface. The magnitude of the available skid resistance at a given speed on a wet pavement is a function of the initial low-speed skid resistance and rate of decrease in skid resistance with speed. The decrease in skid resistance with speed is a function of the pavement surface macrotexture which governs the rate at which pavement surface water can be displaced from the tire-pavement contact area. The higher the rate of water dissipation, the lower is the rate of decrease in the skid resistance.

Vehicle hydroplaning risk on a wet pavement is determined mainly by the macrotexture of the pavement surface, which could be either the surface texture of the compacted pavement or artificially created surface texture when the as-compacted surface texture is inadequate to guard against hydroplaning.

The available skid resistance on a pavement surface is dependent on both the microtexture of the pavement surface materials, and the macrotexture of the pavement surface. At low vehicle speeds, the skid resistance is basically contributed by the microtexture of pavement surface materials. At higher vehicle speeds, the presence of macrotexture is important to control the loss of skid resistance by facilitating speedy discharge of pavement surface water from the tire-pavement contact area.

1.3.3 Environmental Sustainability

The environmental sustainability issues that are closely associated with pavement design are the source and recyclability of pavement materials, risk of environment contamination by pavement materials during construction and service, and traffic noise generated by tire-pavement interaction, in particular, the following five aspects have received much attention:

- Use of construction wastes or any other forms of waste as pavement materials – The use of waste materials for pavement production helps to enhance environmental sustainability of pavement development. This course of action can lead to two major environmental benefits: (i) Reduce waste disposal problems such as the demand for landfill area or pollution caused by the waste materials; (ii) Eliminate the need for quarrying of new materials, thereby helping to preserve natural materials and landscape, and avoid pollution created by quarry operation.
- Recycling of waste pavement materials for new pavement construction – This measure has the same beneficial effects to the environment as the use of waste materials for pavement production. In the case of pavement

construction employing in-situ recycling, it has the additional energy-saving benefit of eliminating the need for hauling.

- Use recyclable pavement materials in pavement design – This measure ensures that the materials used in pavement construction can be recycled in the subsequent rehabilitation or reconstruction of the pavement. It has the same environmental benefits as the preceding measure of recycling pavement materials.
- Use of materials that possess no risk of causing environmental pollution – Materials used in pavement construction must not create any risks in environmental pollution. Such risks include pollution potential during the pavement production and laying operations, as well as possible pollution caused by leaching of pavement materials during service.
- Use of paving mixture that helps to reduce traffic noise – Traffic noise is a major source of man-made environmental nuisance to human beings. It has been estimated that traffic noise dominates more than 70% of the environmental noise in urban areas (Newton et al., 2001). The mix design of pavement surface course can have a significant effect on the magnitude of tire-pavement noise generated through the dynamic interaction of pavement surface and tires. Choosing a quiet pavement design mix can help to reduce tire-pavement interaction noise, and hence the overall traffic noise.

1.4 Coverage and Organization of Thesis

This research study addresses selected aspects of the requirements for safe traffic operation (see Section 1.3.2) and environmental sustainability (see Section 1.3.3) for integration with the conventional structural requirements to

develop a comprehensive pavement design framework. For safe traffic operation of a highway pavement, the issues considered are the effects of mix design on hydroplaning and skidding risks on both rutted and non-rutted pavements, and also the safe wet-weather speed limits. For environmental sustainability, the effects of pavement design on traffic noise are studied. This research proposes new concepts and procedures to incorporate these functional requirements in the conventional structural design of asphalt pavements.

Chapter 2 reviews the literature on topics related to the current research areas: effects of pavement design on functional traffic operations and tire-pavement noise, characteristics and mechanisms of tire-pavement skid resistance and hydroplaning, and outstanding research issues relating to inadequacy of current pavement design procedures in meeting the functional safety and traffic noise control requirements. The literature review will conclude with a highlight of some major areas that require research efforts to further improve the current pavement design methods in order to better meet the needs of highway authorities and road users.

The remainder of this thesis covers research on topics that can be categorized into the following two parts: the first part (Chapter 3 to 5) focuses on the development new procedures to correct three specific inadequacies of current pavement design and pavement maintenance management practices. The second part (Chapter 6 and 7) conducts research on selected aspects of porous pavement design and maintenance that can help to reduce traffic noise and enhance wet-weather driving safety through maintaining sufficient drainage capacity.

Chapter 3 proposes a procedure to incorporate skid resistance consideration in the determination of the terminal rut depth in pavement structural design based on a functional control of minimum skid resistance level, and a maintenance activation threshold for wet-weather travel safety control in pavement management.

Chapter 4 highlights the limitations of the current practice of aggregate polishing tests and recommends an improved procedure to relate laboratory polishing test of asphalt mixture to the terminal pavement skid resistance in the field, and assess if the mix design could meet the functional safety requirement of skid resistance and hydroplaning risk.

Chapter 5 proposes a procedure to determine the safe speed limit during wet weather as a part of pavement management operations. This procedure is capable of considering the friction value which varies with the thickness of water film on pavement surface, thereby allowing the safe speed limits under different wet-weather conditions to be determined more accurately.

Chapter 6 highlights the limitations of the current porous pavement management system and proposes a procedure to determine the terminal service state of a porous pavement affected by clogging. This will provide the pavement engineers with adequate information to determine when to active de-clogging treatment of a clogged porous pavement.

Chapter 7 examines the contributions to tire-pavement noise reduction by the porous structure of a pavement. The sound absorption of common pavement materials are studied, and the noise reduction performance of porous pavement at different clogged states are examined.

Chapter 8 summarizes the main findings and conclusions of the research study and makes recommendations for further research.

CHAPTER 2 LITERATURE REVIEW

2.1 Introduction

Current pavement design methods fall short of offering a comprehensive mechanistic procedure which is capable of providing engineers a design tool to address all the required structural and functional requirements in a systematic and cohesive manner. Chapter 1 has stressed the needs for incorporating functional considerations in pavement design and management. The main aim of this research is to demonstrate how pavement design and management practices can be improved by incorporating some important functional requirements. This chapter presents a review of the existing literature on the major functional requirements of highway operations that are affected by the choice of pavement design and management practice, with emphasis on safety and road traffic noise control requirements which are the main focuses of this research.

The literature review in this chapter is organized into two main parts: Part I deals with skid resistance and hydroplaning risk of highways, which are a key highway safety concern that is closely related to pavement design and management practice, and Part II addresses tire-pavement noise which is a major component of road traffic noise.

PART I SKID RESISTANCE AND HYDROPLANING

2.2 Mechanism of Tire-Pavement Skid Resistance

The skid resistance available to a vehicle traveling on a road pavement derives from the friction at the tire-pavement interface between vehicle tires and the pavement surface. Pavement friction is the force that resists the relative motion between a vehicle tire and a pavement surface (Hall et. al, 2009).

Pavement friction plays a very critical role in keeping vehicles on the road, as it gives drivers the ability to control their vehicles in a safe manner, in both the longitudinal and lateral directions.

The friction force, as illustrated in Figure 2-1, is generated as a tire rolls or slides on the pavement surface. This friction force existing between tire and pavement is generally described by a coefficient of friction, which is the ratio of the tangential force at the tire-pavement contact surface to the vertical force on the wheel. This section presents the current understanding of the mechanism of tire-pavement friction with and without the presence of water, and the evaluation of pavement properties that affect tire-pavement skid resistance.

2.2.1 Mechanism for Dry Tire-Pavement Friction

2.2.1.1 Classical Friction Theories

The concept of contact friction was first mentioned by Leonardo Da Vinci in the 15th century (MacCurdy, 1938). In 1699, Amontons mentioned of friction due to surface irregularities, which was further elaborated subsequently by Coulomb (1785). The main contribution of Coulomb's work covered the following four aspects: nature of the materials in contact and their surface coatings; extent of contact surface area; normal pressure or load at the contact area; and the length of time that the surfaces remained in contact.

Amontons and Coulomb's findings formed the following five classical laws of friction: (i) Friction force is proportional to load; (ii) Coefficient of friction is independent of apparent contact area; (iii) Static coefficient of friction is greater than kinetic coefficient of friction; (iv) The coefficient of friction is independent of sliding speed; and (v) The coefficient of friction is material dependent.

The first two are also known as Amontons-Coulomb laws. The last three laws of friction were conceived by Coulomb based on Amontons' research. Combining the studies conducted by Amontons (1699) and Desaguliers (1734), Coulomb (1785) presented a relationship of friction which is shown in Equation 2-1,

$$F = A + \mu N \quad (2\text{-}1)$$

where F is the friction force, A is the force attributed to adhesive /cohesive effects, μ is the coefficient of friction, N is the normal force at the contact surface, and μN represents the deformation effect.

Equation (2-1) is able to explain the surface contact mechanism without the presence of water or lubricant at the macroscopic level. Moore (1975) pointed out that these five friction classical laws are not valid for the case of a lubricated contact surface, or when rubber is one of the contact materials.

2.2.1.2 Theories of Friction involving Rubber

Friction mechanism is much more complicated when one of the contact materials is rubber, such as vehicle tire. When rubber is involved, the coefficient of friction is highly related to the contact area, normal load, and velocity (Brown, 1996). The research conducted by Williams et al. (1955) found that the coefficient of friction varied with temperature and speed. Gough (1958) pointed out that friction force and sliding speed affected the magnitude of friction.

Another important aspect of contact friction involving rubber is the presence of adhesion and hysteresis as two distinct components of contact friction (Moore and Geyer, 1972; Hall et al., 2009). Adhesion is the friction generated from the small-scale bonding and interlocking between rubber and an other surface. It is a function of the interface shear strength and contact area.

The hysteresis component of frictional force is generated during the occurrences of the bulk deformation of rubber and the energy lost. When a rubber tire contacts a pavement surface, there will be compression in the tire. This compression generates a deformation energy which is stored within the rubber. When the load is removed and the tire relaxes, part of the energy stored in the rubber is released, and the remaining part of the energy is lost in the form of heat (hysteresis) which is irreversible. This loss provides a net frictional force that helps resist the forward motion of the tire.

Besides adhesion and hysteresis, there are also other components of tire-pavement friction, such as tire rubber shear. But compared to adhesion and hysteresis, other components of pavement friction are insignificant. Thus, friction can be described by Equation (2-2).

$$F = F_A + F_H \tag{2-2}$$

where F_A and F_H are the friction due to adhesion and hysteresis respectively. Both of these frictional components are dependent on the contact area between tire and pavement surface, pavement surface characteristics, and tire properties. Sliding speed also has a significant effect on these two components.

Adhesion is mostly contributed by the microtexture of the pavement surface materials, coarse aggregate particles in particular for the case of asphalt pavement. Compared to adhesion, hysteresis is developed by tire deformation, and is most responsive to the macrotexture of pavement surface materials. Figure 2-2 provides a schematic diagram of the contributions of adhesion and hysteresis to the friction factor. At low speed, friction is dominated by adhesion. At high speed, the contribution of hysteresis becomes more significant.

2.2.2 Contact Mechanism for Wet Tire Pavement Friction

When water is present on a pavement surface, the mechanism of tire-pavement friction differs significantly from the case of dry pavement. The mechanism now involves the interaction of tire, fluid (i.e. water), and pavement surface. The following characteristics of wet tire-pavement have been observed and reported in the literature.

(1) The friction value of a pavement suffers a significant reduction when the pavement is wet, even at very low vehicle speed or near-zero speed, regardless of the thickness of water film on the pavement surface (Wu and Nagi, 1995).

(2) Given a water film thickness on a pavement surface, the friction between tire and pavement decreases as the vehicle speed increases (Henry, 2000).

(3) The tire-pavement friction value at a given vehicle speed is lower when the water film thickness becomes thicker (Chakroborty, 2003).

(4) The tire-pavement friction value at a given vehicle speed and water film thickness is affected by temperature of the tire and pavement. The higher the temperature, the lower is the friction value (Jayawickrama and Thomas, 1998).

(5) The wet tire-pavement friction at near-zero or low vehicle speed is a function of the microtexture of the pavement surface (Hogervorst, 1974).

(6) The wet tire-pavement friction at high vehicle speeds (higher than about 40 km/h) is significantly affected by the macrotexture of the pavement surface. The better the macrotexture (i.e. higher texture depth), the higher is the friction value (Hogervorst, 1974).

(7) At a given water film thickness, the rate of tire-pavement friction loss with increasing vehicle speed is lower for a pavement surface with a better macrotexture (Hogervorst, 1974).

(8) At a constant vehicle speed, the rate of tire-pavement friction loss with increasing water film thickness is less for a pavement surface with a better macrotexture (Hogervorst, 1974).

Past researchers have attempted to explain the above behaviors of wet tire-pavement friction using different mechanisms. Some have applied lubrication theories (Reynolds, 1886; Moore, 1975) but without much success. The three-zone model presented by Gough (1959) and Moore (1966) is most commonly employed by pavement researchers to explain the mechanism of wet tire-pavement friction, as illustrated in Figure 2-3. Zone C is the Traction zone with an intimate contact between the tire and pavement. No free water exists between the tire and pavement in this zone. The size of area of zone C is governed by water film thickness and vehicle speed. As the vehicle speed increases, Zone A would extend and eventually occupy the entire contact area, causes the tire to either skid or hydroplane on the film of water (Balmer and Gallaway, 1983).

2.3 Factors Affecting Tire-Pavement Friction

There are three main categories of factors that affect pavement friction: pavement surface properties, tire properties and environmental factors (Wallman and Astrom, 2001). Table 2-1 lists the factors of each category. Past research has identified pavement surface texture and chemical composition of pavement surface materials to be the most important pavement factors that influence the magnitude of tire-pavement friction (Wallman and Astrom, 2001).

This is of high practical significance to pavement engineers because both factors are dependent on pavement mix design and the designer's choice of pavement materials.

2.3.1 Pavement Surface Texture

Pavement texture is the vertical unevenness of a pavement surface with reference to an absolutely even surface. The World Road Association (PIARC) defines different categories of pavement texture based on wave length as shown in Figure 2-4 (Hall et al., 2009). According to PIARC there are four wave length categories of the pavement texture (Rasmussen et al., 2011):

(i) Microtexture with a wave length of 1 μm -0.5 mm: microtexture contributes to the adhesion component of tire-pavement friction. It is a surface roughness quality at the sub-visible or microscopic level; and is a function of the properties of aggregate in the pavement surface. When newly constructed, pavement microtexture is harsh. Under the effect of repeated traffic, the microtexture becomes polished. The polishing susceptibility of microtexture is a function of the mineral and chemical composition of the aggregates. Polishing reduces microtexture's contribution to tire-pavement friction.

(ii) Macrotexture with a wave length of 0.5 to 50 mm: Macrotexture affects pavement friction by influencing the drainage of water present in pavement surface, especially at high vehicle speed (PIARC, 1991). Pavement macrotexture serves as many mini-flow channels in pavement surface to facilitate drainage that helps to relieve the fluid pressure and hydrodynamic uplift force acting on the tire. As a result, a pavement

with better macrotexture (i.e. higher mean texture depth) would experience a lower rate of pavement friction loss with vehicle speed.

(iii) Megatexture with a wave length of 50 to 500 mm: This is an undesirable property of a pavement and its value increases with the presence of pavement defects such as potholes, raveling, bridge joints, and pavement marking, etc. Megatexture is known to play a small role in providing pavement friction but it plays an important role in rolling resistance and the noise levels created by tire-pavement interactions (Shaffer, 2006).

(iv) Unevenness or roughness with a wave length of 500 mm to 100 m: Pavement surface irregularities in this range affects riding comfort. Its value would also increase with the presence of various forms of pavement distresses such as rutting, cracking, raveling and surface distortions, etc (Shaffer, 2006). Unevenness or roughness has an insignificant role in generating tire-pavement friction.

Pavement microtexture and macrotexture are the two key forms of surface texture that affect pavement friction (Henry, 2000). Megatexture and roughness are the major players that influence ride quality. Microtexture depends primarily on aggregate surface characteristics, while macrotexture is a function of aggregate shape, aggregate gradation mix properties and compaction method (Kandhal and Parker 1998; Crouch et al., 1995; Luce et al., 2007; Forster, 1989).

Table 2-2 lists the factors affecting the microtexture and macrotexture of asphalt pavements. The factors listed in this table are explained below.

- Maximum aggregate dimensions — The size of the largest aggregates contained in asphalt pavement materials affects the sizes of voids

formed in pavement surface and the spacing of the voids. Both factors change the wavelength of pavement surface unevenness.

- Coarse aggregate type — The type of coarse aggregate used in asphalt mix has effect on its angularity, shape and surface characteristics. These properties will directly influence both the microtexture and macrotexture of pavement surface.
- Fine aggregate type — As only a small number of fine aggregates are exposed in pavement surface, their effect on pavement microtexture will be limited. Their effect on pavement macrotexture is also limited.
- Binder viscosity and content — Bleeding may occur in asphalt mixtures prepared with binders of low viscosities and when the binder content is high. High binder content will also lead to low texture depth and poor pavement surface macrotexture.
- Mix gradation — Mix gradation has direct effects on the size and spacing of voids in pavement surface. Fine graded and dense graded mixes in general tend to produce poorer macrotexture than gap graded, coarse graded and open graded mixes.
- Mix air voids — Increasing air void content in an asphalt mix increases water drainage which can improve wet pavement skid resistance.

2.3.2 Porosity of Pavement Surface Course

Porous surface courses have been widely used in different parts of the world because of their various functional benefits, such as enhanced wet-weather driving safety, lower tire-pavement noise, improved control of storm water runoff and other favorable environmental effects (FCPA, 1990; Agostinacchio and Cuomo, 2006; Shimeno et al., 2010). It is important to note

that these benefits of porous pavements are due to the relatively high porosity and permeability of the pavement surface materials. Higher porosity and permeability level will lead to a higher friction available; lower porosity and permeability level will reduce its friction value. The porosity and permeability level are the most important factors affecting the functional performance of the porous pavement.

When the porous layer becomes partially or totally clogged, the porosity level and the permeability of the porous pavement will be significantly affected. As a result, some agencies have specified that the porous pavement surface permeability should be at least 8 inches per hour (203mm/h) in order to maintain its high skid resistance during wet weather (DCCD, 2012). Several other recommendations have been made by other researchers and institutions. Sandberg and Ejsmont (2002) and Liu and Cao (2009) recommended that 15% void content be taken as the lower limiting state for a porous pavement. Izevbekhai and Maloney (2011) indicated that the porosity of porous pavements should be kept at around 18-22%.

2.3.3 Chemical Properties of Pavement Surface Materials

Aggregate Adhesion

Many past studies have pointed out that aggregate adhesion is a key affecting factor of pavement friction (Moore and Geyer, 1972; NCHRP Project 01-43). Adhesion is the friction generated from the small-scale bonding/ interlocking between the vehicle tire rubber and the pavement surface when they contact each other. It is a function of the interface shear strength and contact area, as well as the molecular properties of the two contact surfaces.

Resistance to stripping

Stripping is defined as "the breaking of the adhesive bond between the aggregate surface and the asphalt cement" (Asphalt Institute, 1981). The phenomena of stripping is determined by many variables, including the types of aggregates and binder, aggregate properties, environment and so on. The occurrence of stripping can heavily affect the cohesion resistance and in turn affect the friction provided by the pavement (Tarrer et al., 1991). The presence of water at the pavement surface is the most direct inducting factor to all stripping problem which can cause the breaking of aggregate bond and lead to the disintegration of the pavement.

2.3.4 Physical Properties of Pavement Surface Materials

It has long been recognized by many researchers that the angularity, sharpness, and polish resistance of aggregates are positive attributes to pavement skid resistance (Rose and Havens, 1971).

Polish Resistance

The term "polishing" has been widely used in pavement engineering to describe the loss of microtexture due to smoothing and rounding of aggregates in asphalt pavement surface caused by repeated traffic movements. Hence, the polishing effect will directly influence the tire-pavement friction. Aggregate polishing was already recognized as early as the 1930s as a property of aggregates that influences skid resistance (Dillard and Alwood, 1957). The coarse aggregates near the surface of a pavement surface course are exposed after the binder is worn away by traffic. The exposed aggregates will be subject to polishing effect under the action of repeated road traffic. In order to maintain a high level of the skid resistance during the whole service life, appropriate

types of aggregate with high polishing resistance need to be chosen. Past researches have concluded that aggregates polishing at different rates are mainly caused by their mineralogy (McDaniel and Coree, 2003; Kowalski, 2009). Mineralogy is generally believed to be the most critical factor to retain the microtexture of aggregates.

Angularity and Fractured Faces

It has long been recognized by pavement researchers and engineers that aggregate angularity and fracture faces have an enhancing effect on pavement frictional performance (Dahir et al., 1974; Emery et al., 1982). Angularity affects pavement frictional performance by establishing points of contact with tire rubber, and the presence of fractured faces helps to maintain a high coefficient of friction when in contact with the tire. An aggregate will be able to maintain a high level of tire-pavement friction if under the action of traffic, it retains its angularity or produces fracture to expose new sharp edges and fractured faces.

Hardness of Aggregate

Hardness of an aggregate is desirable if it is resistant to the abrasive actions of traffic and does not become smoothened. Instead, it is able to retain the angularity and fractured faces of the aggregate. The retention of angularity is determined by the mineralogical composition and hardness of aggregates.

Presence of Hard Grains in Matrix Structure

Some natural aggregates as well as some artificially manufactured aggregates contain small-size hard grains cemented in a softer matrix. The hard grains offer the needed frictional resistance. If there is an abundant supply of these hard grains in the structure that are continuously exposed in the process

of abrasive traffic actions, a high level of frictional performance can be maintained throughout the entire service life. When the cementing matrix is strong, the individual grains will be tightly held and consequently polished by traffic. The rate of polish depends on the hardness of the grains, the frequency of contacts with traffic, and the type of abrasive materials on the roadway surface (Beaton, 1976).

Differential Wear

For aggregates that contain more than one mineral, the differential in hardness between minerals could contribute to durable skid resistance (Mullen et al., 1974). Dahir and Mullen (1971) pointed out that without a differential in hardness among minerals, the hardest rock types would still polish and not provide sufficient friction of a pavement surface. A harder mineral will provide a longer rate of polishing (Webb, 1970). Furbush and Styers (1972) concluded that good microtexture of aggregates could be achieved by a differential of polishing rates between minerals with different hardness. To produce durable skid resistance, Dahir and Mullen (1971) suggested a proportion of 50~70% hard minerals to 50~30% soft minerals, while Smith et al. (1977) indicated that 40~70% hard minerals would produce the highest resistance to aggregate polishing.

Impurities in Aggregate

Impurities in an aggregate could have an important effect on pavement frictional performance. Burnett et al. (1968) found that most limestone and dolomite aggregates had a coefficient of friction less than 0.32 after 5 million vehicular passes, but some still retained high coefficients to provide sufficient skid resistance after 10 million vehicular passes. It was observed that impurities

in the form of quartz grains within the matrix had a sand paper-like texture and led to higher skid resistance. West and Cho (2000) also reported good skid resistance performance of limestone and dolomite aggregates that contained impurities. Gray and Renninger (1966) observed that insoluble residue influenced the skid resistance of aggregates in the same manner.

2.3.5 Structural Properties of Pavement Materials

Pavement rutting is a major form of distress in asphalt pavements. It is caused by cumulative permanent deformation of pavement materials under the action of repeated traffic loading. Ruts typically develop along pavement wheelpaths. Rutting along wheel paths affects traffic speeds and ease of vehicle operations in two major aspects: (i) Ruts could cause steering difficulties for vehicles, particularly the overtaking, cornering or lane changing movements of vehicles. The presence of ruts is likely to cause some reduction in traffic speeds. (ii) In wet weather, ruts could collect water and lead to ponding that would increase skidding and hydroplaning risks to traffic.

2.3.6 Environmental Factors

Temperature and contamination of road surface are the two most important environmental factors influencing tire-pavement friction. Runkle and Mahone (1980) reported that water temperature and pavement temperature were highly related to tire-pavement skid resistance. The magnitude of skid resistance decreases with the increased temperature due to changes in tire properties and viscosity of water (Ibrahim, 2007).

Reduced pavement skid resistance during wet weather is of great concern to road safety agencies because of the significant loss of skid resistance compared with dry condition (Tyfour, 2009). It has been observed that after a

dry period, accidents rates would increase with the coming of wet weather (Tyfour, 2009).

2.4 Hydroplaning

2.4.1 Mechanism of Hydroplaning

Hydroplaning refers to the situation at which the tires of a moving vehicle are separated from pavement surface by the water on the pavement. Under this situation, the driver would lose steering and directional control and braking capability of the vehicle. Hydroplaning occurs when the total hydrodynamic lift force acting on the tire equals the sum of the weight plus the downward vertical loading upon it (Browne, 1975).

The most common form of hydroplaning on roads is dynamic hydroplaning that occurs when the hydrodynamic force developed in the fluid is large enough to separate the tires of a moving vehicle from a pavement surface (Horne and Dreher, 1963; Browne, 1975). This happens when the vehicle speed is high enough so that the inertial force developed in the fluid is comparable to the tire inflation pressure, thereby causing the tire surface to buckle and producing a large region of fluid capable to support the loaded tire.

2.4.2 Factors Affecting Hydroplaning

The vehicle speed at which hydroplaning occurs when a vehicle travels on a pavement is known as the hydroplaning speed for the given operating conditions, including pavement surface characteristics and environmental factors. The hydroplaning risk of the pavement is low when the hydroplaning speed is high, and vice versa. As in the case of skid resistance, the occurrence of hydroplaning is affected by three main categories of factors: pavement

surface properties, tire properties, and environmental factors. The following sub-sections describes the effects of these factors.

2.4.2.1 Pavement Surface Properties

Pavement microtexture and macrotexture are the two key forms of surface texture that affect skid resistance and hydroplaning. A study by Balmer and Gallaway (1983) presented an extensive list of illustrations of how pavement texture can be applied to reduce the risk of hydroplaning and skidding. It was suggested that microtexture are asperities on the pavement surface consisting of thousands of small, pointed projections. When a water film exists on the pavement surface, these asperities break through the water film and enable direct contact between the tire and pavement. The number and spacing of the asperities have a direct influence on how effective the microtexture of a pavement surface help to reduce hydroplaning risk.

Macrotexture refers to larger scale surface roughness with wavelengths in the range of 0.5 to 50 mm. In wet weather, macrotexture functions as channels for drainage of surface runoff. When the water film on pavement surface is thin, a rough macrotexture helps to discharge the water and maintain contact between the tire and pavement surface. When the water film is thick and floods the pavement surface, a rough macrotexture serves the important role of relieving the building up of hydrodynamic pressure at the interface between a moving tire and the pavement surface, thereby reducing the risk of hydroplaning. In general, the rougher the macrotexture, the more effective it is in lowering hydroplaning risk by raising the vehicle speed at which hydroplaning occurs.

2.4.2.2 Porosity of Pavement Surface Course

Porous pavement can be employed to practically eliminate hydroplaning and to reduce skid resistance loss during wet weather (NAVFAC, 1997). The connected pores of a porous pavement allow surface runoff to flow through its structure and reduce water accumulation on the pavement surface. An adequately designed porous pavement will allow rapid removal of surface water through its porous structure, thereby preventing building up of hydrodynamic pressure under moving vehicle tires. The net result is the ability to achieve little loss of skid resistance in wet weather and elimination of hydroplaning risk within the practical range of vehicle operating speeds.

It is important to note that the skid resistance and hydroplaning benefits of a porous pavement are derived from its porous structure. These benefits will be lost if the pores in the porous pavement are clogged. Clogging is one of the leading distress forms encountered in the maintenance management of porous pavements. Preventive maintenance measures must be taken to ensure that sufficient porosity is maintained so that the risk of hydroplaning is kept below a desirable level.

2.4.2.3 Tire Properties

The properties of vehicle tire are an important factor that can be controlled to limit the occurrence of hydroplaning. The important tire properties include tire inflation pressure, tire load, tire size, and tire tread patterns (Horne and Joyner, 1965). The speed at which a tire hydroplanes is a function of these properties of the tire. The occurrence of the hydroplaning will largely dependent on how fast the water can be discharged from the tire-pavement contact area. A good tire tread design is one with a tread pattern that can effectively channel

surface runoff from the tire's footprint. It is known that even on a well-designed, properly-maintained roadway, a worn or under-inflated tire will experience considerably higher risk of hydroplaning than does a tire in normal operating condition. This is because a worn tire would not have the drainage channels provided by normal tire tread grooves, and an under-inflated tire will produce large tire imprint area that is unfavorable for the escape of water from the tire-pavement contact area.

2.4.2.4 Environmental Factors

The presence of contaminants, such as water, ice, snow, oil or grease, will significantly increase the risk of hydroplaning (Ong, 2006). These contaminants prevent vehicle tires from coming into full or partial contact with the pavement surface. The risk of hydroplaning increases because of the low friction available from the interface between pavement surface and the contaminants. The hydroplaning risk is higher at higher vehicle speeds due to the short contact time that does not permit a contaminant to be forced out of the tire imprint area.

2.5 Pavement Design Approaches to Address Safety Issues

The design of road pavement consists of two main elements, namely the selection of pavement materials and the structural thickness design of the pavement. In the case of asphalt pavement, the selection of pavement materials involves the choice of materials for subbase and base construction, as well as the design of asphalt mixture for the surface course. As explained in Sections 2.2 and 2.3, the selection of surface materials directly influences the microtexture and macrotexture of the pavement surface, and hence the skidding and hydroplaning risks of the pavement. On the other hand, the structural

thickness design of pavement determines the required thickness of various pavement layers to withstand pre-selected design traffic loadings and provide an expected level of structural performance. Weak pavement structures may suffer from settlement, depression and rutting; thereby leading to driving hazards such as ponding and uneven riding surface.

2.5.1 Designing Pavement Mix Surface Texture for Safety Risk Control

In the case of asphalt pavement design, the choice of wearing course materials has a direct safety implication because the skid resistance characteristics of the materials determine the skidding and hydroplaning risks of the vehicles using the road. The following two aspects of the effects of the type and gradation of the aggregates in a pavement wearing course are relevant in road safety analysis:

- Macrotexture of wearing course surface, and
- Microtexture and polishing characteristics of the aggregates.

The macrotexture of an asphalt mixture is a function of the gradation of the aggregates and the top size of the aggregates, as well as the percent binder content. It is an important pavement safety attribute to reduce hydroplaning risk and skid resistance loss at high vehicle speeds. In practice, two common mix design measures have been adopted to control safety risks: (i) control of maximum binder content; and (ii) control of polish susceptibility of pavement surface materials. A review of current practices is presented in the following sub-sections.

2.5.1.1 Safety Risk Control by Controlling Binder Content

The choice of binder content in asphalt paving mix design can have major effects on the wet-weather driving risk of a pavement. In a well designed

asphalt mixture, the asphalt binder content is adequate to serve its intended role of coating the aggregates and providing cohesion to enhance the structural stability of the mixture. Too much or too little binder will not only adversely affect the structural capacity of the mixture, but will also negatively affect driving safety (Brosseaud et al., 1993; Karol et al., 2010).

If the asphalt binder content is too low, the structural capacity will be affected since there would not be sufficient binder to coat the aggregates and hold them firmly together under traffic loading. Raveling may take place and the loose particles and fragments could become driving hazards if not removed or repaired in time. When the asphalt binder content is too high, the following driving safety issues might arise:

- Bleeding of binder onto the pavement surface could occur to form a smooth patch of low-friction binder-covered area, and become a potential hydroplaning hazard of due to its low friction and poor drainage.
- An asphalt mixture with a high binder content tends to have lower surface macrotexture, which is unfavorable as the surface drainage properties will be adversely affected.
- An asphalt mixture with too high a binder content may suffer from severe rutting which could become a wet-weather driving hazard when flooded.

2.5.1.2 Skid Resistance Control Based on Laboratory Tests on Polished Aggregates

The importance of considering the microtexture related polishing characteristics of aggregates in asphalt pavement mix design was well recognized as early as the 1960s (Bloem, 1971; Nichols et al., 1957; Gray and Renninger, 1965; Balmer and Colley, 1966; Csathy et al., 1968; Moore, 1969). Polishing of aggregates refers to the smoothening of sharp edges of surface aggregates and the loss of small asperities (or microtexture) of a pavement surface. In the meantime, wearing, which is defined as the loss of surface irregularities (or macrotexture), also takes place under the action of traffic. Table 2-3 shows a typical example of such specifications where the minimum values of polished aggregate skid resistance values for different road types are specified.

The following three types of laboratory polishing equipment have been developed for polishing aggregates: the Accelerated Wheel Polishing Machine, the Michigan Indoor Wear Track, and the Micro-Deval Device.

Accelerated Wheel Polishing Machine

This is probably the most widely adopted standardized procedures for assessing the polished skid resistance of aggregates for asphalt pavements. It measures the polished stone value, PSV (ASTM, 2013; British Standard, 1989). The procedures first polishes the coarse aggregates tested for a specific time (normally 9 hours), followed by measuring British Pendulum Number (BPN) of the polished aggregates with the British Pendulum Tester (Road Research Laboratory, 1960; ASTM, 2013b). The BPN value associated with accelerated polishing is defined as the polished stone value (PSV), which is a quantitative representation for the aggregates' terminal frictional characteristics. A larger PSV value represents a higher resistance to polish.

Michigan Indoor Wear Track

This device uses full-scale smooth tires to polish coarse aggregate specimens (Masad et al., 2009). Following the process of polishing, the friction of specimens is measured by ASTM towed friction tester (ASTM, 2000). The sample preparation procedure is very cumbersome and costly since a circular wear track is required. It is rarely used by highway agencies outside of Michigan.

Micro-Deval Device

The Micro-Deval test evaluates aggregate capability to resist abrasion in a wet environment (Masad et al., 2009). In this test, a steel container is loaded with 5,000 gm of steel balls and 150 gm of an aggregate sample in the range of 4.75mm to 16mm, and 2,000 ml of tap water. After polishing, the skid resistance of the aggregates is tested with any suitable friction tester.

For the above methods that rely on polishing coarse aggregates, the major drawbacks are that they only test the deterioration of microtexture property of the coarse aggregates. Since the skid resistance of a pavement surface is the combined effect of the microtexture and macrotexture properties of the surface materials, the polished property of coarse aggregates alone does not allow one to calculate the skid resistance actually available on an in-service pavement.

2.5.1.3 Skid Resistance Control based on Laboratory Tests on Polished Asphalt Mixtures

To overcome the limitation of aggregate polishing machines, the following asphalt mixture polishing devices have been developed:

- Penn State Reciprocating Polishing Machine (ASTM, 1996)
- Wehner/Schulze Polishing Machine (BSI, 2014)

- North Carolina State University (NCSU) Wear and Polishing Machine, also known as the Small-Wheel Circular Track Wear and Polishing Machine (ASTM, 2011b)
- NCAT Polishing Machine (Vollor and Hanson, 2006)
- ODOT Polisher (Liang, 2013).

Penn State Reciprocating Polishing Machine (ASTM, 1996)

This machine moves a rubber pad (3.5 inch by 3.5 inch or 89×89mm) in a back-and-forth reciprocating motion, under a load over a specimen surface to be polished (Nitta et al., 1990). During the polishing treatment, abrasive slurry is fed to the specimen surface. This machine is portable and easy to use. This method can be used both in the laboratory and in the field to polish aggregates or asphalt mixtures. The skid resistance of the polished surface is measured with the British Pendulum Tester. This method was withdrawn by ASTM in 1997.

Wehner/Schulze Polishing Machine

This machine is described in the European Standard EN 12697-49:2014 (BSI, 2014), commercially known as the Wehner Schulz Polishing machine (Do et al., 2007). The test specimen may either be a cylinder with a diameter 225 mm or a parallelepiped of 320 mm by 260 mm, each with a thickness of not more than 50 mm. The polishing machine has three polishing rollers with a water-quartz powder mixture projection system. The three rollers move on the specimen surface in a circular motion at a rotation speed of 500 ± 5 revolutions per minute, under a static loading force of 392 ± 3 N. The polishing action is stopped after 90,000 passes, and the friction of the polished specimens is next measured using a friction measuring device that has three rubber sliding blocks

spaced at angles of 120 ± 5 °. The device rotates on the specimen surface at an initial speed of 100 ± 5 km/h under a constant static force of 253 ± 3 N. The moment generated by the contact between the rubber sliders is continuously measured until the measuring head comes to a standstill. The friction is calculated from the moment measured at 60 km/h.

North Carolina State University (NCSU) Wear and Polishing Machine

This test is described in ASTM Standard E660-90 (ASTM, 2011b) as a Small-Wheel Circular Track Wear and Polishing Machine. Polishing is achieved with four smooth-tread 11x6.00x5 pneumatic tires without using abrasives or water. Tire pressure is maintained at 20 psi (138 kPa). The circular track measures 36 in. (914 mm) in diameter to the center of the wheel travel path. Twelve trapezoidal or cylindrical specimens at least 6 in. (152 mm) in diameter are mounted at equal spacing on the track. A wheel load of 72 lb. (320 N) is applied to each wheel. At a rotation speed of 30 revolutions per minute or 7200 wheel passes per hour, terminal polish is usually achieved after approximately 8 h of exposure. Friction measurement can be made with any device that will operate to within the center 3.5 in. by 5.06 in. (89mm by 129mm) portion of a 6 in. (15-mm) diameter specimen.

NCAT Polishing Machine

The NCAT (National Centre for Asphalt Technology) Three-Wheel Polishing Device (TWPD) (Vollor and Hanson, 2006) is a laboratory device specially designed to allow the friction and surface texture depth of polished test specimens to be measured by the Dynamic Friction Tester (ASTM, 2009a) and Circular Texture Meter (ASTM, 2015b) respectively. It has three 8 in. by 3 in. (203 mm by 76 mm) caster wheels that track in an 11.1875 in. (284 mm)

diameter circle on the 20 in. (508 mm) square test specimen. The tire pressure for the pneumatic tires is maintained at 50 psi (345 kPa). The test speed and applied load on the wheels are adjustable, with a normal test load of 105 lb (467 N), and a test speed of 60 revolution per minute. Water is sprayed during polishing to wash away abraded particles. The test specimens are tested up to 100,000 cycles to reach the terminal friction condition. This machine was subsequently adopted by a number of researchers in skid resistance studies of asphalt pavements (Erukulla, 2011; Rozaei et al., 2011; Subedi, 2015).

Ohio Department of Transportation Polisher (Liang, 2013)

The machine is designed to polish the top face of a 6 in. (52 mm) diameter specimen of 4 or 6 in. (102 or 152 mm) thick. Polishing is achieved with a 6 in. (152 mm) diameter rubber pad rotating at approximately 30 revolutions per minute under a constant load of 280 lb. (1,245 N). Tap water is fed to lubricate the test specimen during polishing at a rate of 100 ml/min. Polishing is performed for 8 h and the polished friction value is measured using the British pendulum tester (ASTM, 2013b).

Table 2-4 summarizes the strengths and weaknesses of the polishing machines introduced above. These test methods have been developed for the purpose of testing the polishing resistance of aggregates. No efforts were made to relate the test results to the functional requirements of the road pavements subsequently constructed. As such, the test results could not be used to assess the safety risks of an actual in-service pavement.

2.5.2 Pavement Structural Design for Safety Risk Control

Virtually all engineering approaches for pavement structural design are developed to provide adequate structural capacity against the following two

most prevalent modes of structural failures of pavements: pavement cracking and excessive pavement deformation. Of these two modes of failure, pavement deformation is the one that can have significant implications on traffic safety.

Rutting is the key form of structural deformation along the two wheel paths of a traffic lane under repeated loadings. This form of pavement distress has an important traffic safety implication in that flooded rut could present a skidding or hydroplaning hazard to vehicles. Except for empirical pavement design procedure, most mechanistic or semi-mechanistic (including mechanistic-empirical) design procedures consider rutting as a major form of structural defect to be addressed in pavement design. Unfortunately, none of the existing pavement design procedures have included the required skid resistance and hydroplaning risk of flooded ruts as a consideration in the determination of pavement thickness design.

2.5.3 Surface Drainage Consideration in Pavement Design

Pavement surface drainage properties affect the thickness of water film on a pavement surface during wet weather. Besides allowing for cross slope in pavement geometric design, some improvements in surface drainage can be achieved by means of designing a surface mix with good macrotexture of deep texture depth to facilitate surface drainage. Texturing or surface grooving, which is commonly done in concrete pavements but not usually in asphalt pavements, can also be created to achieve the same purpose. A much more effective way of reducing surface water film thickness is by the use of porous pavement surface layer.

The term "porous asphalt" was first specified by the European Committee for Normalization to unify the names used in different countries

(Nicholls, 1998). Porous asphalt is a bituminous paving material characterized by its high porosity. The air void content of porous asphalt mixtures is typically 20% or more by volume (Anderson et al., 1998). It is widely reported in experimental studies that the wet skid resistance of porous asphalt pavement surfaces are considerably higher than those on dense-graded asphalt concrete or Portland cement concrete pavements, and are less speed-sensitive (NCHRP, 1978; Isenring et al., 1990). A detailed analysis by Zhang et al. (2013) indicated that, compared with dense-graded asphalt surfaces, porous asphalt surface courses can result in a lower fluid uplift force, better tire-pavement contact, higher traction and less tire deformation. All these properties are essential to achieving a good skid resistance.

While it is clear that the use of porous asphalt can lead to improved skid resistance and lower hydroplaning risk, these beneficial effects in the functional performance have not been quantified and incorporated in the pavement design porous asphalt pavements.

PART II TIRE-PAVEMENT NOISE

2.6 Characteristics of Tire-Pavement Noise

Tire-pavement noise has long been recognized as one of the dominant factors of the overall vehicle noise (Ponniah et al., 2010; Rasmussen et al., 2007). It is estimated that more than 70% of the traffic noise is attributed to tire-pavement noise (Newton et al., 2001). The most significant impact of traffic noise is the annoyance it causes to humans and the associated negative effects which can adversely affect work productivity, quality of life and people's health. To reduce tire-pavement noise, it is essential to study its mechanism and take measures to minimize the effect of traffic noise on human beings. To reduce

traffic noise, engineers have made much progress in reducing the noise from wind turbulence noise and power unit noise. In the early 1980s, tire-pavement noise has become the major contributor of the overall vehicle noise (Ulf Sandberg, 1982). Sandberg and Ejsmont (2002) reported that tire-pavement dominates traffic noise at speeds over 40 km/hr for passenger cars and 60 km/hr for trucks.

This part of the literature review examines the generation, amplification and propagation mechanisms of tire-pavement noise, and the effects of pavement properties on tire-pavement noise.

2.7 Generation Mechanisms of Tire-Pavement Noise

The generation mechanisms of tire-pavement noise can be divided into mechanisms related to the generation of noise, the amplification of the noise, and the propagation of noise. The noise generation mechanism includes air pumping, impact-induced vibrations and friction induced vibrations. The noise amplification mechanism includes horn effect, cavity resonance, pipe resonance, helmholtz resonance. Propagation of noise refers to the transmission of acoustic energy through the air medium.

2.7.1 Air Pumping

Air pumping is one of the dominant sources of tire-pavement noise (Sandberg and Ejsmont, 2002). It occurs within the contact patch when the passages and grooves in the tire are compressed and distorted. The air entrained in these passages is compressed and pumped in and out of the passages, and aerodynamically generated sound is created, as shown in Figure 2-5 (Nilsson et al., 1980).

Air pumping is affected by both tread pattern and pavement textures. Many researchers concluded that increasing pavement porosity or pavement roughness may reduce air pumping noise by allowing a path for air to escape when compressed (Descornet and Sandberg, 1980; Nilsson, 1982; Fujikawa et al., 2006)

2.7.2 Impact-Induced Vibration

When air is blocked in the contact patch, vibrations are also induced due to sudden displacements of tread elements when a tire impacts the road surface (Sandberg and Ejsmont, 2002). The vibrations generated can be classified into the following modes: radial, tangential, axial and sidewall impact-induced vibrations.

Radial vibrations are induced when a tread block impacts the pavement, as depicted in Figure 2-6. Vibrations will propagate along the tire carcass or radiate sound to another location. Radial vibrations mostly influence noise at frequencies below 1000 Hz (Nilsson, 1980; Descornet, 1980). Studies have suggested that radial vibrations can be reduced by the following measures: having a soft tread compound, having a thin or worn tread or having a compliant pavement (Nilsson, 1982). The radial vibration normally does not cause sound in the far field, as the flexural mode shapes of the tire make it an ineffective radiator below 400 Hz (Yum et al., 2006; Yum et al., 2004).

Tangential vibrations are induced by a rolling tire causing relative movements of the tread block and pavement in the tangential direction (Kropp, 2011; Larsson, 1999). Sidewall vibrations are found to be excited by circumferential tube resonances (Ruhala and Burroughs, 1998; Dare, 2012) and are a critical mode in the 500-1000 Hz frequency range (Donavan and Oswald,

1980; Eberhardt, 1984) and are most significant near the trailing edge of contact patch (Phillips et al., 1999). Axial vibration are found to be much lower than other forms of vibrations (Bergmann et al., 1980; Erin et al., 2003).

2.7.3 Friction-Induced Vibration

Friction-induced vibration is another important noise generation mechanism. Tread blocks transfer tractive forces from the tire to the pavement during acceleration or braking. As illustrated in Figure 2-7, the action of slipping and sticking happens quite rapidly and generates both noise and vibration (Dare, 2012). The frequency of the stick-slip noise normally occurs at 1-2.5 kHz, depending on the magnitudes of normal force and vehicle speed (Kroger et al., 2004; Ryszard, 2001). Past studies have indicated that the stick-slip noise can be reduced by improving pavement microtexture (Kroger et al., 2004).

Stick-snap occurs when the contact between the tread block and the pavement causes adhesion between the tread block and pavement. When the tire tread surface is sticky and pavement becomes smooth, the strength of adhesive bond increases. As illustrated in Figure 2-8, when the tread block exits the contact patch, the adhesive force holds the tread block. The release of the tread block causes both sound energy and vibration of the tire carcass.

2.8 Noise Amplification Mechanisms

Four different amplification mechanisms of tire-pavement noise can be identified. They are the horn effect, cavity resonance, Helmholtz, and pipe resonance.

2.8.1 Horn Effect

The geometry of tire contact with pavement is a natural horn as shown in Figure 2-9. The horn effect can amplify the sound by 15 dB in the 2000-3000

Hz region and is believed to be the most important amplification mechanism of tire-pavement noise (Schaaf et al., 1982). Porous surfaces are found effective in reducing the horn effect (Iwai et al., 1994; Kropp et al., 2000). The effect can be enhanced by adjusting the porous layer thickness or using a double-layer porous system (Lui and Li, 2004). Narrowing tire width is also found to be another horn effect reduction measure (Lui and Li, 2004).

2.8.2 Cavity Resonance

Noise amplification caused by cavity resonance is more important for interior-vehicle noise emission than for exterior-vehicle noise (Bschorr, 1985; Scavuzzo et al., 1994). Cavity resonance normally does not affect tire vibration characteristics (Bolton et al., 1998). Its frequency is affected by tire and rim geometry, with typical resonance frequencies for passenger car tires of 220-280 Hz while that for heavy truck tires around 150 Hz (Sandberg and Ejsmont, 2002).

2.8.3 Helmholtz Resonance

Helmholtz resonance is a result of mass-spring vibration actions. In the case of tire-pavement noise, the volume of tread cavity caused by a moving tire acts as a spring, and the air present between tread and pavement acts as a mass (Kinsler et al., 2000). The Helmholtz resonance has most of its energy concentrated in the frequency range of 1000-2500 Hz (Nilsson et al., 1979). The effect of helmholtz resonance could be reduced by providing good "ventilation" with the use of porous pavement or a ventilated tread pattern. It is also possible to shift the resonance frequencies by changing the tread cavity volume or altering tire diameter (Sandberg and Ejsmont, 2002).

2.8.4 Pipe Resonance

Pipe resonance occurs within tire tread grooves. All tread grooves are potential pipe resonators when they are in contact with a smooth road surface, and are a major noise amplification for grooved tires on smooth pavements (Koiki et al., 1999). Saemann and Schmidt (2002) reported that a tire with longitudinal grooves was about 3.5 dB (A) noisier when compared to a smooth tire of the same size. The frequency of pipe resonance generally concentrates in high frequency range (Oswald and Arambages, 1983). Pipe resonance can be reduced by avoiding tread patterns with a resonance frequencies close to the impact frequency, and through the efficient ventilating effect of pavement grooves or porous pavement surface (Koiki et al., 1999).

2.9 Propagation Mechanism

After the tire-pavement noise has been generated and amplified, it propagates through the surrounding air medium. Propagation mechanism of noise would be of interest for far field noise measurement and studies. Since the present research deals only with near field tire-pavement noise generation and amplification, the propagation mechanism is not considered in the analysis.

2.10 Factors Affecting Tire-Pavement Noise

2.10.1 Pavement Surface Properties

Unevenness in pavement surface can generate tire-pavement noise through impact-induced vibration, air pumping, and friction-induced pumping; it can also amplify the generated tire-pavement noise through horn effect, cavity resonance, Helmholtz resonance, and pipe resonance. Of the various pavement surface properties, the main factors are size and distribution of surface voids;

size, shape and arrangement of surface aggregates; and porosity of the surface course layer (Tire-Pavement Noise Research Consortium, 2011).

Studies have shown that the pavement surface texture within a wavelength between 12.7mm to 50.8mm contributes the most to tire-pavement noise generation (Tire-Pavement Noise Research Consortium, 2011). In other words, in order to reduce tire-pavement noise, the texture in this range should be reduced or avoided. It has also been suggested by researchers that pavement texture that is negatively oriented, with the sharper ends of the surface voids pointing downward away from the tire, is desirable as it would generate less tire-pavement noise (Tire-Pavement Noise Research Consortium, 2011).

2.10.2 Porosity of Pavement Surface Course

The initial porosity level of a newly constructed porous pavement usually ranges from 18 to 25%. The presence of connected pores in porous pavements helps to weaken the strength of the air pumping by preventing air compression. It also reduces the enhancement potential of the horn, organ pipe, and Helmholtz resonator mechanisms. Another important reason why porous pavement is effective for reducing traffic noise is that the porous structure can absorb part of tire-pavement noise generated. The sound absorption mechanisms of porous pavements are similar to the sound absorption principles of acoustical wall in buildings. This provides an added benefit of reducing traffic noise caused by engine noise of trucks and other sources (Bernhard et al., 2004).

2.11 Pavement Design Approaches to Address Tire-Pavement Noise

The properties of pavement surface course mixtures have the following major effects on the generation of tire-pavement noise of a moving vehicle: (i)

tire vibrations caused by pavement surface macrotexture; (ii) relative movements of tire tread block and pavement surface; and (iii) the noise absorption capability of pavement mixtures. It is a challenge to pavement engineers to design asphalt mixtures with good noise absorption capability and favorable surface properties to produce quiet pavements. A quiet pavement refers to any pavement that creates less noise than the normal form of pavement when vehicles travel on the road surface.

Rasmussen et al. (2007) pointed out that quiet asphalt pavements can be constructed of virtually any nominal mix type: dense-graded, gap-graded (SMA), and open graded (porous). PIARC (2013) has suggested that stone-matrix asphalt, open-graded friction courses, fine-graded surfaces and rubberized asphalt can help reduce highway noise by as much as 7 decibels.

One of the common elements of these quiet pavements as described above is smooth texture. The smooth pavement texture constructed of small size aggregates can lead to reduced vibration of tires. Take European countries as an example, the top size of aggregates used in the surface course is between 6 and 8mm, while the aggregates used in the US pavement mixtures range from 9.5 to 12.5mm (Robert et al., 2007). Asphalt rubber has also been demonstrated by many studies to be quiet (Freitas, 2012).

The surface texture and bulk properties of a pavement govern the contribution of road surface to tire-pavement noise (Domenichini, 1998; Boscaino and Praticò, 2001). To design a quiet road surface, Haider et al. (2007) recommended the adoption of the following mix properties to reduce tire-pavement noise:

- Pavement surface may be provided with sufficiently deep macrotexture making up a random, closely packed, homogenous array of small to medium size aggregates so as to prevent air pumping;
- A porous pavement surface layer can be used to provide favorable sound absorption to reduce tire-pavement noise;
- Minimize megatexture and large-wavelength macrotexture to ensure that macrotexture is fine and homogeneous. This holds for porous surfaces too.

The acoustic performance of porous pavements in noise reduction is well recognized (Gibbs et al., 2005; Abbott et al., 2010). Many field experimental studies have been carried out by researchers to demonstrate the noise reduction benefits of porous pavements (von Meier et al., 1990; Neithalath et al., 2005; Kowalski et al., 2009; Younger et al., 1994).

In United States, the Federal guidelines require noise levels of 67 dB(A) or less at roadside residences. However, pavement surface type has not been used as a noise mitigation strategy by the FHWA. This has resulted in a widespread use of noise barrier walls, especially in urban areas (Kandhal, 2004). In other words, noise control is not a requirement in normal pavement design practices. It only occurs for certain specific areas requiring noise control that the highway agency will investigate the use of different pavement surface types to reduce tire-pavement noise. In USA, some states such as Arizona, California, and Texas have initiated research projects to investigate the use of pavement surface type as a noise mitigation strategy (Kandhal, 2004).

2.12 Summary

2.12.1 Functional Consideration in Pavement Design and Management

The current pavement design and management practices focus on pavement structural and do not adequately consider pavement functional requirements in the process. In pavement structural design, the requirements for operational efficiency, safe traffic operation and environmental sustainability are often not addressed specifically. In pavement management, the functional requirements such as driving safety risk and tire-pavement noise control are not explicitly integrated into the standard management framework. Considering the drawbacks of the current pavement design and management practice, the first part of this chapter reviews the key safety concerns in pavement operation in terms of skid resistance and hydroplaning, including the mechanism of skid resistance and hydroplaning, and the factors affecting skid resistance and hydroplaning. It also reviews those safety-related factors that have impacts on mix design, including the selection of aggregates type and gradation. Next, it describes the safety concerns related to skidding and hydroplaning during wet weather traffic operation, and the approaches in the current practices that attempt to address the safety issues. The second part of this chapter reviews the generation, amplification and propagation mechanisms of tire-pavement noise, the factors affecting tire-pavement noise, and the current status of pavement design and management practices in their consideration of pavement functional requirements.

2.12.2 Research Needs

A major area in need of improvement for the current pavement design and management methods is to integrate the key functional requirements of

pavements fully in the working framework. The literature review on asphalt pavement design and management conducted in this chapter has identified three major aspects where paving mix design, pavement structural design and pavement management could be improved to address the functional requirement of highway pavements. They are operational efficiency, safe traffic consideration and the environmental impacts. For each of three functional requirements, the research needs with respect to the design and management of asphalt pavements are summarized below:

Operations efficiency — The operational efficiency of a highway as characterized by the safe operating speed of the traffic in both dry and wet weather conditions. These speeds, in particular the wet-weather speeds, are affected by the surface characteristics of the pavements of the highway under different operating conditions. Important research needs include the safe operating speed in wet weather, and the effectiveness of pavement maintenance with respect to traffic delays.

Safe traffic operations — The hydroplaning and skidding risks of vehicle operations, especially in wet weather are critically dependent on the surface characteristics of pavements, which in turn are heavily influenced by paving mix design. Further research is needed to study how different paving mix designs, including the selection of aggregate type and aggregate gradation, and different structural designs of pavement, would affect hydroplaning and skidding risks.

Environmental sustainability — The environmental issues that are closely associated with pavement design are (i) the source and recyclability of the pavement materials used, (ii) risk of environment contamination by

pavement materials during operation, and (iii) the traffic noise generated by tire-pavement interaction. Further research is needed to study how the choices of different pavement materials can address these environmental issues.

2.12.3 Scope of Present Research

It is not possible in this research study to develop procedures to incorporate all aspects of functional requirements of highway operations into pavement design and management. Each functional requirement has its own unique set of technical considerations that should be addressed in establishing their relationships with pavement properties, and in analyzing how pavement design and management would improve pavement functional performance during operation. The aim of this research is to demonstrate the overall concept of considering explicitly pavement functional requirements in pavement design and management of asphalt pavements, by presenting proposed procedures to incorporate the following selected pavement functional requirements into the pavement design and management process:

(A) Safe traffic operations and highway operational efficiency consideration – To develop a new procedure to incorporate the terminal rut depth control in structural design of asphalt pavement and pavement maintenance management

Operational safety consideration of rut depth has an important impact on the terminal or threshold rut depth which is likely to be different from the subjectively determined terminal rut depth used in the current structural design and maintenance management practices of asphalt pavements. The present research will examine the safety risk of flooded ruts and propose a procedure by which the terminal rut depth based on operational safety considerations can

be incorporated in the structural design and maintenance management of asphalt pavement.

(B) Safe Traffic Operations and Highway operational efficiency consideration – To determine the maximum wet-weather safe speed limits under different operating conditions

This is another issue that affects both highway operational efficiency and travel safety in wet weather. The current method which is used to determine wet weather speed limits does not take into the consideration of the effects of different water film thicknesses and the changing value of tire-pavement friction available. This study will focus on the determination of the safe speed limit considering different water film thicknesses.

(C) Consideration of safe traffic operations – To develop an improved aggregate selection procedure for asphalt mix design based on functional safety consideration of highway

As presented in the literature review, the microtexture of the aggregates, their polishing resistance, as well as the gradation of aggregates have a significant impact on the skidding resistance and hydroplaning speed of the pavement. Current aggregate selection guidelines for most pavement design procedures are derived from past experience. The guidelines are only indicative in nature, providing no information on the actual skidding and hydroplaning risks. The present research aims to overcome this shortcoming by developing a rigorous analytical procedure to select aggregates based on their properties related to microtexture, polishing resistance and macrotexture, with analysis to calculate quantitatively the level of skidding and hydroplaning risks with respect to a pre-determined design speed of the highway.

(D) Consideration of safe traffic operations – To develop a procedure for the determination of the terminal service state of a porous pavement affected by clogging

The functional benefits of porous pavements are due to the relatively high porosity and permeability of the pavement materials. Unfortunately, porous pavements are prone to clogging which causes the pavements to lose much of its beneficial properties. Current pavement management methods cannot provide pavement engineers with adequate information to monitor the important service performance of porous pavements. This study aims to overcome this limitation by proposing a rational engineering procedure based on the consideration of wet-weather driving safety requirements to determine the terminal service state of a porous pavement affected by clogging.

(E) Consideration of environmental impacts of traffic noise – To develop a laboratory procedure to evaluate the sound absorption characteristics of trial paving mix design as part of the paving mix design process currently used in practice

The current asphalt paving mix design practices do not consider the sound absorption properties of a design mix. This is unsatisfactory because it will be costly to replace a constructed pavement section that does not meet noise control requirements. This research presents an attempt to develop a laboratory procedure and a method of analysis to assist pavement designers in estimating the contribution of tire-pavement noise reduction of a trial asphalt mix design.

Table 2-1 Factors Affecting Pavement Friction (Wallman and Astrom, 2001)

Pavement Factors	Traffic and Environmental Factors	Tire
Macrotexture Microtexture Megatexture Porosity of surface course Surface depressions and ruts Chemistry of surface materials Temperature Thermal conductivity Specific heat	Traffic polishing Water viscosity Temperature Water film thickness	Tread pattern design Rubber composition Inflation pressure Rubber hardness Wheel Load Sliding velocity or rolling speed Temperature Thermal conductivity Specific heat

Table 2-2 Factors Affecting Pavement Micro-texture and Macro-texture
(Sandberg, 2002; Henry, 2000; Rado, 1994; PIARC, 1995; AASTHO, 1976)

Pavement Surface type	Factor	Microtexture	Macrotexture
Asphalt	Maximum aggregate dimensions		X
	Coarse aggregate types	X	X
	Fine aggregate types		X
	Mix gradation		X
	Mix air content		X
	Mix binder		X

Table 2-3 Minimum Polished Stone Value (PSV) Required for Given IL, Traffic Level and Type of Site

(The Highway Agency, 2006)

Site category	Site description	IL	Minimum PSV required for given IL, traffic level and type of site									
			Traffic (cv/lane/day) at design life									
			0-250	251-500	501-750	751-1000	1001-2000	2001-3000	3001-4000	4001-5000	5001-6000	Over 6000
A1	Motorways where traffic is generally free-flowing on a relatively straight line	0.30	50	50	50	50	50	55	55	60	65	65
		0.35	50	50	50	50	50	60	60	60	65	65
A2	Motorways where some braking regularly occurs (eg. on 300m approach to an off-slip)	0.35	50	50	50	55	55	60	60	65	65	65
B1	Dual carriageways where traffic is generally free-flowing on a relatively straight line	0.3	50	50	50	50	50	55	55	60	65	65
		0.35	50	50	50	50	50	60	60	60	65	65
		0.4	50	50	50	55	60	65	65	65	65	68+
B2	Dual carriageways where some braking regularly occurs (eg. on 300m approach to an off-slip)	0.35	50	50	50	55	55	60	60	65	65	65
		0.4	55	60	60	65	65	68+	68+	68+	68+	68+
C	Single carriageways where traffic is generally free-flowing on a relatively straight line	0.35	50	50	50	55	55	60	60	65	65	65
		0.4	55	60	60	65	65	68+	68+	68+	68+	68+
		0.45	60	60	65	65	68+	68+	68+	68+	68+	68+
G1/G2	Gradients >5% longer than 50m as per HD 28	0.45	55	60	60	65	65	68+	68+	68+	68+	HFS
		0.5	60	68+	68+	HFS	HFS	HFS	HFS	HFS	HFS	HFS
		0.55	68+	HFS	HFS	HFS	HFS	HFS	HFS	HFS	HFS	HFS
K	Approaches to pedestrian crossings and other high risk situations	0.5	65	65	65	68+	68+	68+	HFS	HFS	HFS	HFS
		0.55	68+	68+	HFS	HFS	HFS	HFS	HFS	HFS	HFS	HFS
Q	Approaches to major and minor junctions on dual carriageways and single carriageways where frequent or sudden braking occurs but in a generally straight line.	0.45	60	65	65	68+	68+	68+	68+	68+	68+	HFS
		0.5	65	65	65	68+	68+	68+	HFS	HFS	HFS	HFS
		0.55	68+	68+	HFS	HFS	HFS	HFS	HFS	HFS	HFS	HFS
R	Roundabout circulation areas	0.45	50	55	60	60	65	65	68+	68+	HFS	HFS
		0.5	68+	68+	68+	HFS	HFS	HFS	HFS	HFS	HFS	HFS
S1/S2	Bends (radius <500m) on all types of road, including motorway link roads; other hazards that require combined braking and cornering	0.45	50	55	60	60	65	65	68+	68+	HFS	HFS
		0.5	68+	68+	68+	HFS	HFS	HFS	HFS	HFS	HFS	HFS
		0.55	HFS	HFS	HFS	HFS	HFS	HFS	HFS	HFS	HFS	HFS

Table 2-4 Summary of Strengths and Weaknesses of Polishing Machines

Device	Properties	Strengths	Weakness	Specifications
Polishing Devices for Aggregate Samples				
Polished Stone Value Test	Curved aggregate specimens polished by a rotating wheel	Accelerated polishing for lab testing. Bench sized	Coarse aggregate coupons only. Does not affect Macro-texture or mix properties	ASTM D 3319
Michigan Indoor Wear Track	Wheels centered around pivot point, move in circle around track	Close to real world	Time consuming sample preparation. Used for aggregates only.	MDOT
Micro-Deval	Abrasion of aggregates by steel balls in a container	Effective for polishing aggregates in a short time	Not producing purely polishing action. Used for aggregates only.	AASHTO T327-05/Tex-461-A
Polishing Devices for HMA Specimens				
NCAT Polishing Machine	Three pneumatic tires providing scrubbing action for polishing	Sized to match DFT and CTMeter	Time consuming in sample preparation and polishing test	NCAT
ODOT Polisher	Polish surface of cylindrical specimen using 6 in (152 mm) diameter rubber pad with water	Easy sample preparation by gyratory compactor	Polishes a relatively small area.	Specially developed for Ohio Department of Transportation
Polishing Devices for Both				
NCSU Polishing Machine	Four pneumatic tires are adjusted for camber and toe-out to provide scrubbing action for polishing	No water or grinding compounds, can polish aggregate or mixes	Polishes a relatively small area or few number of samples	ASTM E 660
Wehner/Schulze Polishing Machine	Three rollers polish specimen in circular motion under static load	Polishes and measures friction by the same unit	Non-standard friction measurement method	ASTM E 1393
Penn State Recipro-cating Polishing Machine	Reciprocates rubber pad under pressure against specimen surface in slurry of water and abrasives	Portable. Can polish aggregates or mix in lab or field	Polishes a relatively small area. Oscillation obliterates directional polishing. Fallen into disuse	ASTM E 1393

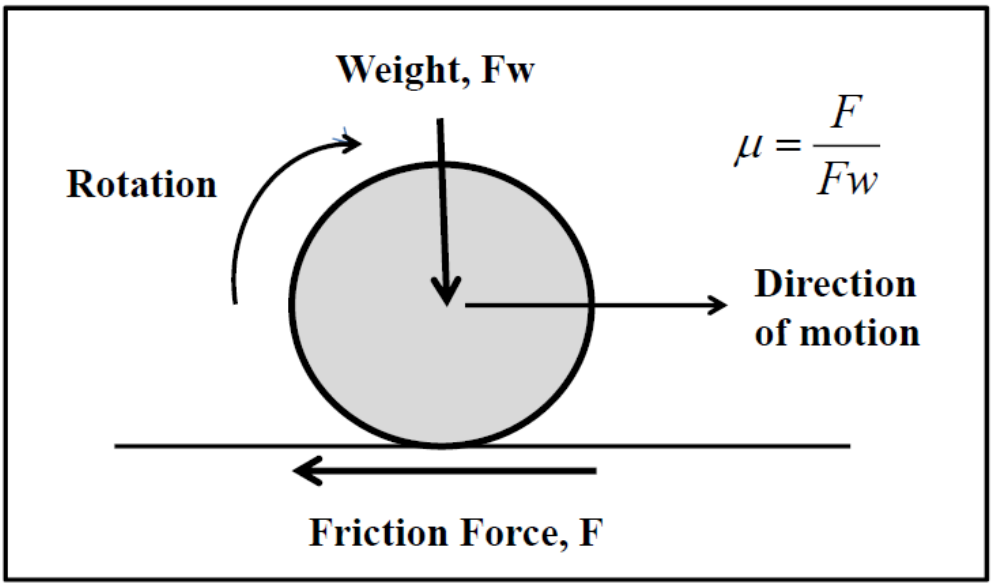

Figure 2-1 Force Body Diagram for Rotating Wheel

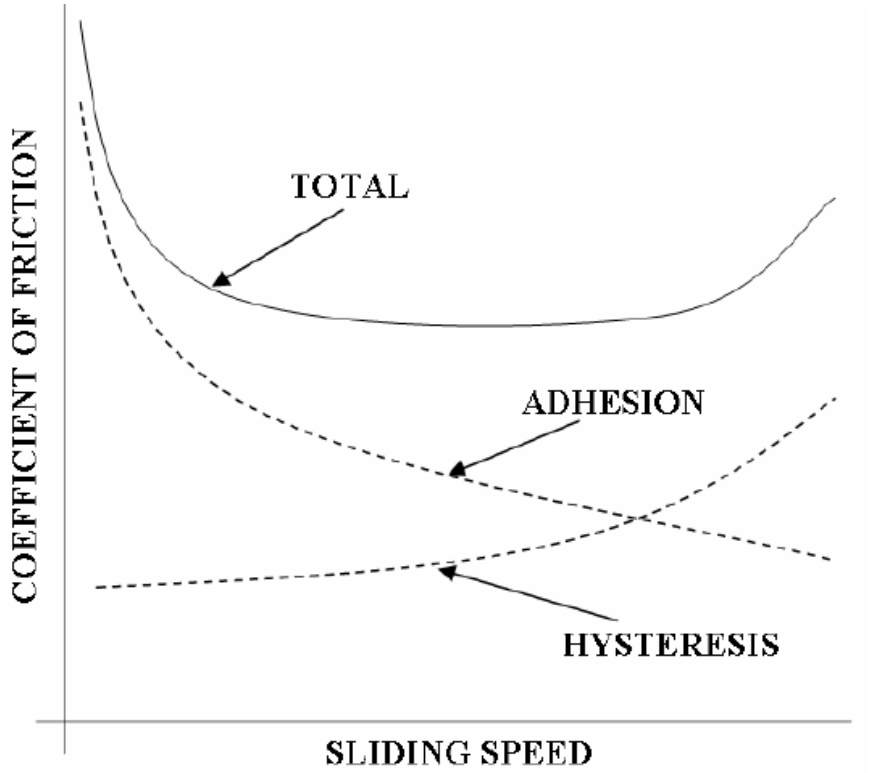

Figure 2-2 The Contribution of Adhesion and Hysteresis to the Friction Factor as a Function of Sliding Speed (Mohammad, 2008)

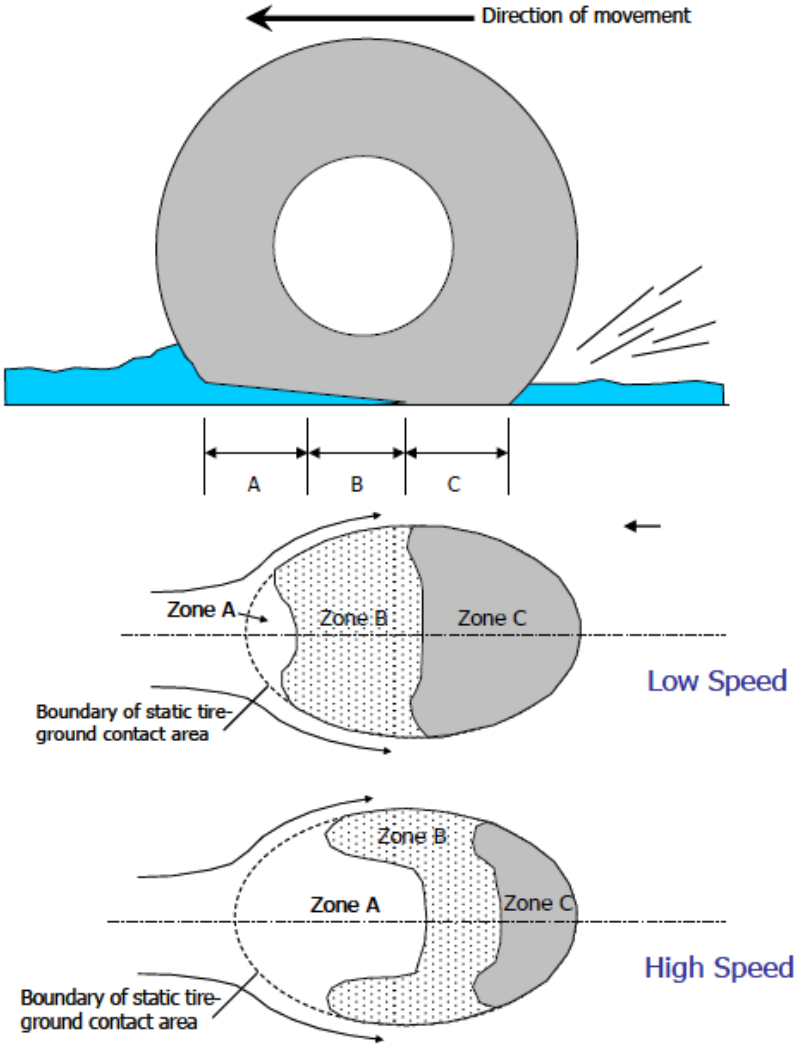

Figure 2-3 Three-zone Model for Sliding Tire on Wet Pavement (Moore, 1996)

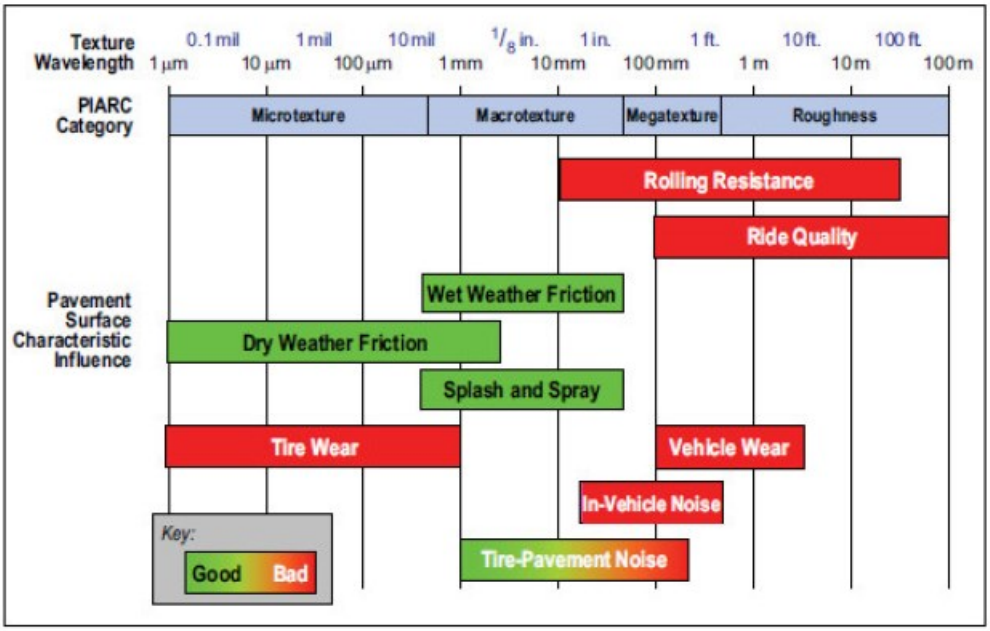

Figure 2-4 Pavement Texture Categories Determined by World Road Association and Their Influence (Rasmussen et al., 2011)

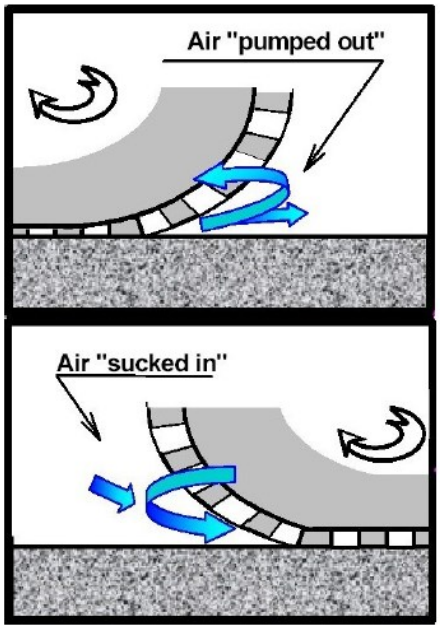

Figure 2-5 Air Pumping at the Entrance and Exit of the Contact Patch (Sandberg and Ejsmont, 2002)

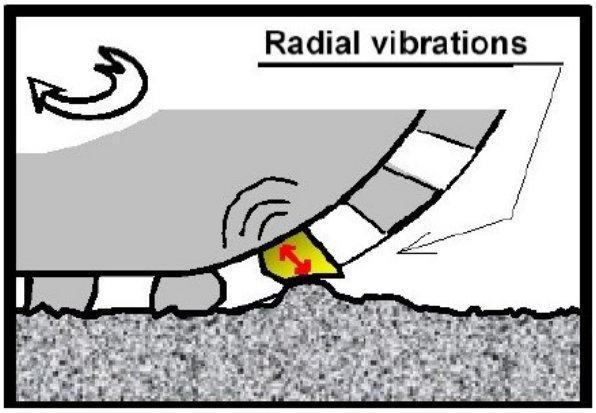

Figure 2-6 Radial Impact-Induced Vibrations (Sandberg and Ejsmont, 2002)

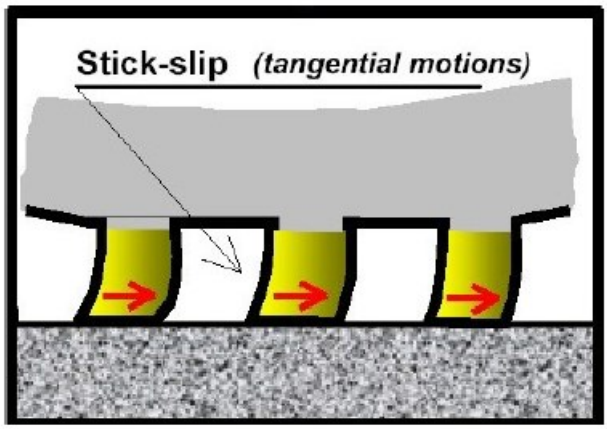

Figure 2-7 Stick-slip Motion of the Tread Block on Pavement

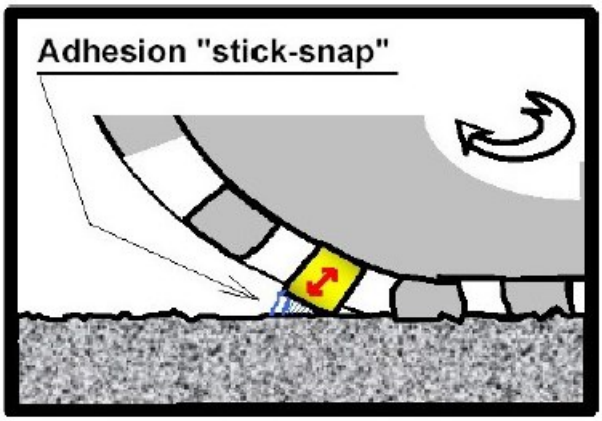

Figure 2-8 Stick-snap Motion of the Tread Block on Pavement

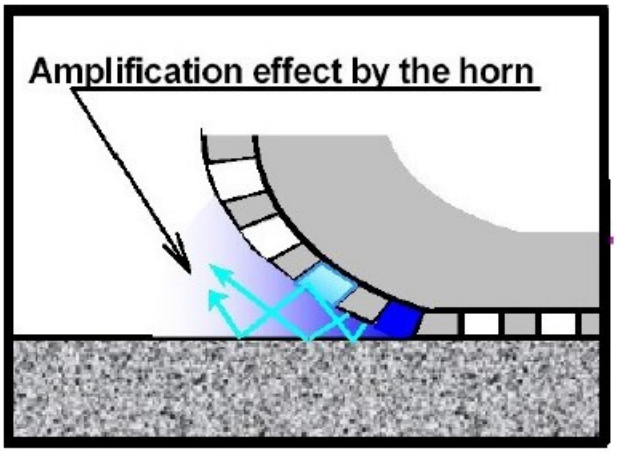

Figure 2-9 The Horn Effect Created by the Tire and Pavement

CHAPTER 3 TERMINAL RUT DEPTH FOR DESIGN AND MANAGEMENT OF ASPHALT PAVEMENT

3.1 Introduction

Pavement rutting is a major form of distress considered in structural design of asphalt pavements (AASHTO, 2008a; Zheng et al., 2001). Ruts typically develop along pavement wheel paths under the action of repeated traffic loading. Although the formation of ruts is load-induced and is related to the structural properties of various pavement layers, it is rare that the structural condition will be the consideration for maintenance or rehabilitation of a rutted pavement. This is because long before the structural condition of a rutted pavement becomes a concern, maintenance or rehabilitation of the pavement would have to be carried out to restore the functional condition of the pavement for safe traffic operations. Pavement ruts affect the functional operation of a highway because they can cause steering instability of vehicles, especially for lane changing or overtaking operations of vehicles (Tomiyama et al., 2010; Jawamura et al., 2001). More importantly, they present a safety risk to vehicles because they collect water during wet weather, leading to reduced skid resistance along the rutted wheel paths due to the presence of water (AASHTO, 1989; Liser et al., 1977).

Past research studies have essentially established a common understanding that safety hazards associated with hydroplaning and skidding during wet weather should be the basis for maintenance treatment or rehabilitation of a rutted pavement (AASHTO, 1989; Lister et al., 1977; Hicks et al., 2000; Barksdale, 1972). There are generally two broad approaches for determining the rut depth intervention level: (i) Theoretical or experimental

studies based on hydroplaning consideration (Lister et al., 1977; Hicks et al., 2000; Barksdale, 1972; Fwa et al., 2012; Sousa et al., 1991), and (ii) Engineering judgement based on field and operational experience (Walker et al., 2002; WSDOT, 1999; ODOT, 2006; CMRPC, 2006; BC MTI, 2009; Shahin, 1994; Caltrans, 2006). The first approach, though theoretically sound, could not be applied directly in practice because it does not take into account the varied field operating conditions in actual highway operations. The second approach, on the other hand, is unsatisfactory because it is based on subjective judgement without a sound quantitative engineering basis.

This chapter presents a study to develop a quantitative engineering procedure for establishing a rut depth maintenance activation level for a rutted pavement (i.e. rut depth intervention level), taking into consideration the actual pavement skid resistance characteristics and traffic operating speeds. The proposed concept of rut depth maintenance activation level is built on the widely practiced concept of intervention level for pavement skid resistance. Based on the skid resistance intervention level identified, a procedure is proposed in this chapter to derive the corresponding rut depth intervention level (i.e. the rut depth at which maintenance treatment to repair the rutted pavement must be activated). This procedure makes use of a theoretically derived finite-element simulation model to determine the maximum ponded rut depth that will still able to provide a skid resistance (computed at an appropriately selected traffic speed) which is equal to the skid resistance intervention level. The detailed concept and procedure of the process of establishing the rut depth intervention level is explained. Numerical examples of computation of rut depth intervention levels for selected operating conditions of pavement and traffic speed are presented

for illustration of the proposed procedure. With the computed critical rut depth, the pavement service life can be re-computed to check against with the design pavement service life.

3.2 Significance of Critical Rut Depth Determination

While it is generally agreed among pavement professionals and researchers that the rut depth threshold for maintenance treatment of a rutted pavement must be set based on safety considerations related to hydroplaning risk and loss of skid resistance encountered in wet-weather driving, there has been no consensus among the results of reported experimental and survey studies on the critical rut depth that will present a definite and unacceptable safety threat to road traffic. Past researchers provided different critical rut depth as shown in Table 3-1. Although many researchers considered 12.7 mm or deeper rut depth to be critical for wet-weather driving safety, rut depths as shallow as 7 and 5.1 mm were also found to present driving safety hazards.

Table 3-2 cites some examples of rut depth severity classifications adopted by selected highway organizations. The differences concerning the severity classification of rut depths are apparent among different organizations. If one considers “high severity” classification as a severity level that deserves maintenance treatment, and that “medium severity” as one that warrants consideration for possible maintenance treatment, then it is logical to say that the “high severity” rut depth represents the critical rut depth, i.e. the maintenance intervention rut depth level. With this interpretation of critical rut depth for “high severity”, we can observe clear discrepancies between the severity classifications in Table 3-2 and the critical rut depth findings in Table 3-1.

The discrepancies between findings of critical rut depth from research studies and those adopted in normal practices in actual pavement management systems are due to the uncertainties involved in establishing a practical rut depth intervention level for maintenance under the actual operating conditions of a given road section. The hydroplaning speed of a road section, which is the speed at which hydroplaning occurs and causes a vehicle to lose braking capability and the driver to lose steering control of the vehicle, is dependent on the following factors: (i) pavement surface characteristics of the road section which is a function of the pavement wearing surface material, (ii) characteristics of vehicles in the traffic stream, such as properties of tires and magnitudes of wheel loads, (iii) vehicle travel speed which is related to the design speed and speed limit of the road section, and (iv) depth of water thickness on the pavement surface. In the case of a ponded rut along a wheel path, the magnitude of the loss of pavement skid resistance will also be affected by these factors which are dependent on pavement properties, vehicle characteristics and traffic operating conditions.

Since both the hydroplaning speed and available skid resistance along a ponded rut vary with the operating conditions of vehicles and pavement surface properties as highlighted in the preceding paragraph, it is easy to understand that the rut depth threshold for maintenance may vary from one road section to another if their vehicle operating conditions and pavement properties are not the same. This is likely the case in practice because a typical road network will consist of different functional classes of highways with different geometric and pavement designs. This being the case, it will not be logical or practical for any highway agency to adopt a uniform set of rut depth threshold for maintenance

in a network level pavement management system, as implied in most research or experimental studies such as those in Tables 3.1 and 3.2.

The procedure for rut depth threshold determination proposed in this chapter recognizes the practical need to take into consideration the road design and operating conditions of each road section in the process. With this procedure, a rut depth maintenance intervention level can be established for each road section according to their unique design and operating conditions. Compared with most of the current practices of setting a uniform rut depth threshold in a network level PMS for the entire road network, the proposed procedure will allow the highway agency and the pavement engineer a more effective pavement management tool to manage the maintenance of rutted pavements at the network level according to their driving safety risks.

3.3 Concept of Proposed Procedure

The proposed procedure aims to determine the critical rut depth at which a rutted pavement must be repaired to ensure driving safety against skidding accidents caused by hydroplaning or loss of skid resistance. This section first looks at the phenomenon of hydroplaning and explains why the experimentally measured or theoretically derived hydroplaning speed cannot be used directly for the determination of the rut depth intervention level for pavement maintenance. Next, it examines the concept of skid resistance intervention level and explains why and how this concept is applicable for rut depth intervention level determination. Finally, the concept of the proposed procedure for rut depth maintenance intervention level is explained.

3.3.1 Hydroplaning Speed and Accident Risk

While travelling on a wet pavement covered with a film of water, a vehicle hydroplanes when its speed is high enough to generate a hydrodynamic uplift beneath its moving tires and cause the tires to be separated from the pavement surface (Fwa et al., 2012, Horne et al., 1963). In other words, a vehicle hydroplanes when the tire-pavement skid resistance becomes zero, and the vehicle speed at which this situation occurs is known as the hydroplaning speed. However, in the real world, the vehicle would have skidded at a low tire-pavement skid resistance before this theoretical situation of hydroplaning (i.e. zero skid resistance) could be reached. This explains why it does not work to simply determine the critical rut depth by computing the hydroplaning speed of a ponded rut and equate it with the speed limit or prevailing traffic speed of the rutted road section.

Another reason why it is practically impossible to determine theoretically the critical ponded rut depth at which accidents will occur, is that besides the pavement and vehicle factors that could be modelled theoretically, there are also the driver factors such as drivers' choice of driving speed and their driving skills. A possible practical approach is to identify a critical rut depth through a field experimental study by analyzing the relationship between accident rates and the depths of ponded ruts in actual highway operations involving rutted pavements. To the knowledge of the author, such information is not available in the literature.

To overcome the difficulties mentioned in the preceding paragraphs, this chapter proposes an alternative rational approach to solve the problem. Instead of attempting to relate ponded rut depths to accident rates directly, it is proposed

to first identify a representative critically low skid resistance based on the relationship between tire-pavement skid resistance and wet-weather accident rates, and select a skid resistance value as the threshold with an acceptably low wet-weather accident risk. This leads to the concept of skid resistance intervention level. The following sub-sections explain the significance of this concept, the basis for applying this concept to the determination of rut depth maintenance intervention level for a rutted pavement section, and the proposed procedure to determine rut depth intervention levels.

3.3.2 Concept of Skid Resistance Intervention Level

Traditionally, it is a common practice in many countries and states to specify a minimum skid resistance value for pavement friction management (Henry, 2000; Hall et al., 2009). Since the early 1990s, the concept of skid resistance investigatory and intervention levels has increasingly been adopted for pavement friction management by highway agencies in different parts of the world (Henry, 2000; Hall et al., 2009; NZ Transport Agency, 2010; Highways England, 2006). The main idea of introducing the two levels is to achieve timely and effective pavement friction maintenance of highway pavement networks for the purpose of keeping wet-weather accidents below an acceptable level.

According to the recommendations of the Federal Highway Administration (FHWA, 2010a) and the American Association of State Highway and Transportation Officials (AASHTO, 2008a), pavement sections with measured friction values at or below an assigned investigatory level are subject to a detailed site investigation to evaluate for friction-related crash potential and determine the need for remedial action. For pavement sections

with friction values at or below the intervention level, some form of remedial action is required to correct the deficiency.

Because of the complex factors and the number of possible situations involved in wet-weather traffic accidents, and differences in the choices of acceptable accident rate, there are differences in the investigatory and intervention level skid resistance values adopted by different highway agencies. Table 3-3 lists some examples of practices adopted by different highway agencies. It is increasingly acknowledged by more and more highway researchers and practitioners that, in view of the varying pavement properties and operating conditions from one road section to another, it is appropriate to have different skid resistance investigatory and intervention levels for different pavement sections in a road network (Henry,2000; Hall et al., 2009). It is also appropriate to adjust the investigatory and intervention levels of pavement sections as and when necessary to more effectively manage pavement friction and reduce accident rates of the road section concerned.

3.3.3 Concept of Rut Depth Investigatory and Intervention Levels

It has been explained earlier that the basis for rut depth control is to ensure adequate driving safety against skidding accidents. This is the same as the basis for the concept of skid resistance investigatory and intervention levels described in the preceding sub-section. This means that it is possible to apply the skid resistance values selected for the skid resistance investigatory and intervention levels to determine the ponded rut depths corresponding to the two levels of skid resistance. By doing so, one is allowed to maintain the same level of accident risk for the rutted and un-rutted pavement sections. This is logical

as it keeps the accident risk unchanged for a given pavement section, whether it is rutted or un-rutted.

In this chapter, a procedure for establishing a rut depth intervention level for a pavement section is proposed with reference to the skid resistance intervention level of the pavement section. The same procedure can be followed in determining rut depth investigatory level based on skid resistance investigatory level, and is not covered in this chapter. Alternatively, after the intervention level has been established, the corresponding rut depth investigatory level can be assigned at a certain rut depth value less than the intervention level so as to permit sufficient time gap for:

- progression monitoring of the rut depth;
- planning of treatment measures and budget for the eventual maintenance intervention.

Figure 3-1 explains schematically the proposed concept of establishing the rut depth intervention level for a pavement section. In this figure, several pavement sections located at different states of conditions are considered. The "intervention skid resistance curve" represents the skid resistance state of the pavement when its skid resistance has deteriorated to the intervention level. At this state, its zero-speed skid resistance has deteriorated to $(SN_0)_I$ and its skid resistance SN_{40} measured at the standard skid resistance test speed is SN_{IL}, which is the skid resistance intervention level. The "skid resistance intervention curve" gives the skid resistance of the pavement section at the intervention state for different vehicle speeds. This curve marks the threshold skid resistance levels for maintenance intervention at different vehicle speeds. It is noted that this intervention curve is measured according to ASTM standard test method

E274 (ASTM, 2011a) at a standard water film thickness of 0.5 mm (Henry, 2000).

The identification of the "skid resistance intervention curve" is useful for establishing a rut depth intervention level that is consistent with the skid resistance intervention level by maintaining a matching accident risk control. This can be explained by considering the state of the in-service pavement in Figure 3-1 with a zero-speed skid resistance of $(SN_0)_{II}$ and a SN_{40} which is higher than the intervention skid resistance SN_{IL}. Since its SN_{40} is higher than the intervention skid resistance, no maintenance intervention is necessary if it is un-rutted. However, if the pavement is rutted, whether or not maintenance intervention is needed is dependent on the possible ponded rut depth of the rutted pavement. If the ponded rut depth is A as shown in Figure 3-1, no maintenance intervention is required because the intervention skid resistance is not violated at any vehicle speed. However, when the ponded rut depth is B, C, D or E, maintenance intervention might be required, depending on the vehicle operating speed.

If the pavement section has a ponded rut depth of B as indicated in Figure 3-1, the intervention skid resistance is reached only when the vehicle speed is 150 km/h, which is considerably higher than the likely highest speed expected on a normal highway and therefore maintenance intervention is not required. The same is the case of ponded rut depth C for most roads. For ponded rut depths D and E, maintenance intervention thresholds are reached at vehicle speeds of 96 and 80 km/h respectively. Whether or not intervention maintenance should be activated for these two cases depends on the profile of wet-weather vehicle speeds of the traffic using the pavement section concerned. If the

number of vehicles with travel speeds higher than 96 km/h is negligible, and the percentage of vehicles travelling at speeds higher than 80 km/h cannot be ignored, then maintenance intervention should be activated for ponded rut depth E, but not for ponded rut depth D.

The reasoning presented in the preceding paragraphs forms the basis for establishing the rut depth intervention level in the procedure proposed in this chapter. Essentially the skid resistance performance curve of a rutted pavement is compared with the "intervention skid resistance curve", and considering the traffic speed characteristics of the pavement section, a ponded rut depth is selected as the rut depth intervention level so that an acceptably small percentage of vehicles will be exposed to the potential driving safety hazard. The detailed procedure of establishing a rut depth intervention level is described in the next section.

3.4 Simulation Model Used In Determining the Critical Rut Depth

In order to develop the procedure of establishing rut depth intervention level, the theoretically derived finite-element skid resistance simulation model needs to be introduced first.

3.4.1 Finite-Element Skid Resistance Simulation Model

Fwa and Ong (2007, 2008) established the finite-element 3D simulation model of a locked wheel sliding on a flooded pavement (see Figure 3-2). This model is capable of computing the resistance force to the sliding motion of the wheel by considering the interaction among the tire, pavement structure and water present on the pavement surface. This model is based on the theories of solid mechanisms and fluid dynamics to analyze tire-fluid interaction, tyre-pavement interaction and fluid-pavement interaction. This theoretical skid

resistance model has been validated for car tires respectively by Fwa and Ong (2008, 2012) using field measured data.

Fluid modelling to correctly compute the hydrodynamic forces in the pavement surface water in contact with the moving vehicle tire in question is crucial in solving the hydroplaning speed problem. This is achieved by applying the complete set of Navier-Stokes equations together with the k-ε turbulence model (Hinze, 1975; Launder and Spalding, 1974) to include the turbulence kinetic energy k and the viscous dissipation ε of the water flow. The final governing equations are given as follows:

$$\frac{\partial(\rho k)}{\partial t} + \nabla \bullet (\rho k \mathbf{U}) = \nabla \bullet \left[\frac{\mu_t}{\sigma_k} \nabla k \right] + 2\mu_t E_{ij} \bullet E_{ij} - \rho\varepsilon \tag{3-1}$$

$$\frac{\partial(\rho \varepsilon)}{\partial t} + \nabla \bullet (\rho \varepsilon \mathbf{U}) = \nabla \bullet \left[\frac{\mu_t}{\sigma_\varepsilon} \nabla \varepsilon \right] + C_{1\varepsilon} \frac{\varepsilon}{k} 2\mu_t E_{ij} \bullet E_{ij} - C_{2\varepsilon} \rho \frac{\varepsilon^2}{k} \tag{3-2}$$

$$\mu_t = \rho C_\mu \frac{k^2}{\varepsilon} \tag{3-3}$$

where:

ρ : density of water,

k : kinetic energy of water,

ε : viscous dissipation of water,

t : time,

U : velocity vector,

σ_k : numerical constant equal to 1.00,

σ_ε : numerical constant equal to 1.30,

$C_{1\varepsilon}$: numerical constant equal to 1.44,

$C_{2\varepsilon}$: numerical constant equal to 1.92,

C_μ : numerical constant equal to 0.09, and

E_{ij} : stress tensor.

Solving the above fluid model and its interaction with vehicle tire and pavement surface, together with appropriate boundary conditions, is performed using the finite element simulation technique. The details of the finite element simulation method for the determination of vehicle hydroplaning speed are presented below.

Tire Sub-Model – The ASTM E524 standard smooth tyre (ASTM, 2000) is adopted as the tire sub-model. This is the tire model used for the standard locked wheel skid resistance test for the determination of skid number SN (ASTM, 2014). It is a G78-15 tire with a cross sectional radius of 393.7 mm and a tread width of 148.6 mm. The tire model consists of three structural components, namely the tire rim, tire sidewalls and tire tread. The elastic moduli of the three components are 100,000, 20 and 90 MPa respectively. The tire is in contact with the pavement surface under a downward concentrated load of 4,800 N acting on the tire rim and a uniformly distributed tire inflation pressure of 165.5 kPa acting on the inside tire walls.

Pavement Sub-Model -- Since the pavement is relatively rigid compared to tire, it is simulated as a rigid surface to support the tire and receive the tire load. In the simulation analysis, it is assigned an elastic modulus of 30 GPa. The contact between tire tread and pavement surface is assumed to follow the Coulomb's theory of friction (Bathe, 1996). The pavement surface is assumed to be water-tight and impervious to flow to water.

Fluid Sub-Model -- In the fluid sub-model, fluid behavior is modeled through the full Navier-Stokes equations (Ong et al., 2007). The standard k-ε

model is adopted for modeling turbulent flow around the tire (Hinze, 1975; Launder, 1974). In the simulation analysis, the wheel is held stationary with the pavement, and water is modeled to move at a specified speed towards the wheel. The final solution is obtained through an iterative process of interaction among the three sub-models, in which the fluid stresses are transferred to the tire and pavement sub-models, and the deformations of tyre are transferred to the fluid sub-model. The properties of water and air at 25°C are used in this study. The density, dynamic viscosity and kinematic viscosity of water are 997.0 kg/m^3, 0.890×10^{-3} Ns/m^3 and 0.893×10^{-6} m^2/s respectively. The density, dynamic viscosity and kinematic viscosity of air at the standard atmospheric pressure and 25°C are 1.184 kg/m^3, 1.831×10^{-5} Ns/m^3 and 1.546×10^{-5} m^2/s respectively.

The simulation model begins with a low vehicle sliding speed which is increased gradually until the hydroplaning speed is reached. The hydroplaning speed is the vehicle sliding speed at which hydroplaning occurs when the inertia forces in the water film are high enough to completely separate the vehicle tires from the pavement surface.

The input data required for the simulation analysis are:

- Tire dimensions: tire radius and width
- Tire inflation pressure
- Tire elastic properties: modulus of elasticity and Poisson's ratio of each of the following three components: tire rim, tire sidewalls, and tire tread
- Magnitude of wheel load
- Physical properties of water: temperature, density, dynamic viscosity, and kinematic viscosity

- Pavement properties: modulus of elasticity, and tire-pavement friction coefficient
- Water film thickness on pavement surface

The output solution would yield the following results:

- Tire deformation profile
- Fluid drag and uplift forces
- Tire-pavement normal reaction
- Traction forces

3.4.2 Method of Back-Calculating SN_0

The central concept of deriving skid resistance performance curve using the finite element skid resistance-hydroplaning simulation model is in a way similar to the two-parameter concepts of the Penn State friction model (Leu and Henry, 1983) and the PIARC International Friction Index (IFI) model (Wambold et al. 1995). The Penn State model uses a skid number for friction coefficient and a term representing percent normalized gradient to describe the friction characteristics of a pavement. The PIARC IFI model characterizes pavement friction performance using a friction number associated with a reference slip-speed value and a speed number associated with the slip-speed gradient of friction.

Following the general two-parameter concept of the Penn State and PIARC models, the proposed concept adopted in this study postulates that the pavement skid resistance performance curve for given vehicle sliding on a given pavement covered with a known thickness of water, can be described by a zero speed skid resistance SN_0 value, and another parameter that describes the variation of skid resistance with vehicle speed. With the finite-element skid

resistance simulation computer program, this representation of the performance curve can be derived if the skid resistance values at two different vehicle speeds are known. This derivation of the skid resistance performance curve, or the calibration of the simulation model to describe the skid resistance of the pavement concerned, is shown in the flow diagram of Figure 3-3. By trial and error, the engineering parameters in the model are calibrated based on the two measured skid resistance values. Once calibrated, the model can generate the skid resistance values at other speeds to provide the complete skid resistance performance curve for the desired range of vehicle speeds.

The proposed approach of deriving the skid resistance performance curve of a pavement is conceptually sound because the derivation is based on the calibration of mechanistic parameters related to engineering properties of tire, water and pavement. In contrast, the parameters in both the Penn State model and the PIARC IFI model are determined by means of statistical techniques. The following are the input parameters required for the simulation analysis:

- Skid resistance $SN(V_1)$ and $SN(V_2)$ at slip speeds V_1 and V_2, respectively
- Water film thickness
- Tire geometry
- Tire structural stiffness
- Wheel load and tire pressure
- Water viscosity

It should be highlighted that, once calibrated, the simulation model could be applied to generate the skid resistance performance curves at other

water film thickness as well. This is the additional capability that cannot be performed by either the Penn State or the PIARC IFI model. It is this capability that makes it possible for the proposed framework and procedure of this study to address the various functional safety requirements of highway operations.

3.5 Procedure of Establishing Rut Depth Intervention Level

The proposed procedure of establishing a rut depth intervention level for an in-service pavement section makes use of the finite-element skid resistance simulation model as introduced in previous section. Figure 3-3 shows that, after SN_0 has been determined, the skid resistance-vehicle speed curve can be derived using the calibrated skid resistance simulation model.

The proposed rut depth intervention level determination procedure consists of the following main steps:

1. Calibrate the finite-element skid resistance simulation model to define the skid resistance-vehicle speed relationship of the in-service pavement section;
2. Identify skid resistance intervention level of the pavement section;
3. Derive the "skid resistance intervention level curve" using the calibrated skid resistance simulation model;
4. Determine the zero-speed wet skid resistance $(SN_0)\pi$ value of the in-service pavement section;
5. Derive the skid resistance-vehicle speed curves for different ponded rut depths of the pavement section;
6. Identify the expected vehicle speed profile of traffic, and
7. Determine the rut depth intervention level.

Step 1: Calibration of Skid Resistance Simulation Model

The calibration of the skid resistance simulation model requires the skid numbers of the pavement section in question at two different speeds to be measured. That is, besides the usual SN_{40} from routine skid resistance survey, the skid number at another speed is needed. With these two skid numbers, the skid resistance simulation model can be calibrated to determine the zero-speed skid number SN_0 and the skid resistance-vehicle speed curve of the in-service pavement section. The detailed calibration procedure, also known as back-calculation procedure, is introduced in last section.

Step 2 and 3: Skid Resistance Intervention Level and Intervention curve

In step (2), the skid resistance intervention level $(SN_0)_{IL}$ is assumed to be known and have been assigned to the pavement section being analysed. In step (3), using $(SN_{40})_{IL}$ and SN_v at another speed v as input, the corresponding zero-speed skid number $(SN_0)_I$ and the "skid resistance intervention curve" (see Figure 3-1) for standard water film thickness of 0.5mm can be back-calculated by applying the calibrated skid resistance simulation model.

Step 4: Determination of Zero-Speed Skid Resistance $(SN_0)_{II}$ of In-Service Pavement

For a given set of vehicle and water film thickness (see the input block of Figure 3-3), the calibrated finite element skid resistance model is able to derive the skid resistance-vehicle speed curve with the knowledge of $(SN_0)_{II}$ and a measured skid resistance at another speed SN_v. $(SN_0)_{II}$ represents the pavement micro-texture effect, while the difference between $(SN_0)_{II}$ and SN_v allows the simulation model to evaluate the changes in skid resistance related to the pavement macro-texture effect. If $(SN_0)_{II}$ is not known, but the skid

resistance values at any two other speeds are known, the simulation model can be used to back-calculate the $(SN_0)_{II}$ value. The steps of back-calculation of $(SN_0)_{II}$ using two other SN values are shown in the iterative loop of Figure 3-3. Once the $(SN_0)_{II}$ has been estimated, and SN_{40} is known, the entire skid resistance-vehicle speed curve can be derived using the calibrated simulation model.

Step 5: Skid Resistance of Ponded Ruts

Before the rut depth intervention level can be determined, the skid resistance-vehicle speed relationships for ponded ruts of different depths must be established. Examples of skid resistance-vehicle speed relationships are schematically represented in Figure 3-1 as skid resistance performance curves for ponded rut depths A, B, C, D and E. These relationships enable one to identify the ponded rut depth and vehicle speed that the skid resistance intervention will be reached.

The method of determining the skid resistance-vehicle speed curve for a ponded rut follows the same procedure described in the preceding sub-section, i.e., the procedure outlined in Figure 3-3. Basically, for a given set of vehicle and water film thickness, one needs to input SN_0 and another SN_v at speed v (usually SN_{40} is known from routine skid resistance survey) to derive the skid resistance-vehicle speed curve. As explained in the preceding section, if SN_0 is not known, it can be back-calculated using SN values measured at two different speeds. Following this procedure, and by setting water film thickness (see input block of Figure 3-3) as the ponded rut depth, a series of skid resistance-vehicle speed curves can be developed for the range of ponded rut depths.

Step 6: Vehicle Speed Profile

After the skid resistance intervention curve and the family of skid resistance-vehicle speed curves have been generated as described in the preceding two paragraphs, the key information required for determining rut depth intervention level (see Figure 3-1) is basically complete. It is now possible to establish a rut depth intervention level following the rationale described under the earlier sub-section entitled "Concept of Rut Depth Investigatory and Intervention Level".

The last piece of information needed is to select a "wet-weather threshold speed" which is the vehicle speed that the skid resistance-vehicle speed curve of the intervention level rut depth intersects the "skid resistance intervention curve" (see Figure 3-1). This "wet-weather threshold speed" defines the speed above which a vehicle will experience a skid resistance that is lower than the skid resistance intervention level. A "wet-weather threshold speed" must be selected such that an acceptably low percentage of vehicles using the pavement section will travel at a speed above it. A possible choice of "wet-weather threshold speed" is the wet-weather speed limit of the road section. A different speed other than the wet-weather speed limit could be chosen as the "wet-weather threshold speed" based on an appropriate analysis of the accident records of the road section in question.

Step 7: Determining Intervention Rut Depth

Having selected the "wet-weather threshold speed", the intervention level rut depth can be defined as the flooded rut depth that will produce a skid resistance-vehicle speed curve that intersects the "skid resistance intervention curve" at a speed equal to the "wet-weather threshold speed". For example,

referring to Figure 3-1, if the "wet-weather threshold speed" is chosen to be 96 km/h, then the intervention level rut depth will be rut depth D.

3.6 Expedient Procedure for Determining Intervention Rut Depth

The steps described in the preceding sub-sections are schematically depicted in Figure 3-4. The procedure for determining intervention rut depth requires repeated analysis using the finite element simulation model. This is impractical because it is time consuming and it requires high level skills and expertise in performing the finite element analysis. For easy and expedient application in network level pavement management, a database of skid resistance-vehicle speed relationships can be developed to enable a speedy determination of rut depth intervention levels for different pavement sections in a road network. Alternatively, a neural network model can be developed to serve the same purpose.

The above steps are schematically depicted in Figure 3-4. By using either the database or the neural network approach, the analysis of the rut depth intervention level of a pavement section can be completed within an hour.

A two-layer feed-forward back-propagation network is used in the present study due to its simplicity in topology and ease in application. The architecture of the two-layer feed-forward network adopted in this study is shown in Figure 3-5, where a nonlinear hidden layer and a linear output layer work together to make predictions from the input data. The essence of this neural network is to perform space conversion on all the input vectors through a set of nonlinear activation functions in the hidden layer (Cybenko, 1989). For a given pavement surface and vehicle operating characteristics, with the

required input parameters (see Figure 3-5), the neural network will provide the skid number as the output.

3.7 Examples for Intervention Level Rut Depth Determination

3.7.1 Numerical Illustrative Examples

This section presents an analysis of an urban expressway asphalt pavement in Singapore. Based on a calibrated finite element skid resistance simulation model for the asphalt pavement, a database as well as neural network model have been developed for the skid resistance-vehicle speed relationships covering the following ranges of the key parameters:

- Range of vehicle speeds: 20 to 90 km/h (90 km/h is the dry-weather speed limit of the urban expressway)
- Range of surface water depths: 0.5 to 25 mm
- Range of SN_{40}: 25 to 60
- Range of SN_0: 40 to 80

Different scenarios are analyzed below to examine the influence of the following factors on the value of intervention level rut depth:

(i) The skid resistance value selected as the skid resistance intervention level;

(ii) The current skid resistance state of the in-service pavement section; and

(iii) The "wet-weather threshold speed" selected.

Scenario 1

Consider a case where the pavement section at its intervention level state has $(SN_0)_{IL} = 45$ and $(SN_{40})_{IL} = 30$, and a current in-service pavement skid resistance of $(SN_0)_1 = 70.0$ and $(SN_{40})_1 = 48$. With $(SN_{40})_{IL} = 30$ and $(SN_0)_{IL} = 45$, the "skid resistance intervention curve" can be ted, as shown in Figure 3-6

(a). Again from the neural network model, with $(SN_{40})_1 = 48$ and $(SN_0)_1 = 70.0$, a family of skid resistance curves can be derived for different surface water depths (i.e. ponded rut depths). Four skid resistance curves for water depths of 6, 9, 12 and 25 mm are plotted in Figure 3-6 (a), and it can be read from the plot that the "wet-weather threshold speeds" corresponding to these four water depths are 76, 69, 67, and 60 km/h, respectively.

Scenario 2

All conditions are the same as Scenario 1 except that the in-service pavement skid resistance has deteriorated to $(SN_{40})_1 = 40$ and $(SN_0)_1 = 60$, and from the neural network model the skid resistance curves corresponding to water depths of 6, 9, 12 and 25 mm are plotted in Figure 3-6 (b). The "wet-weather threshold speeds" obtained from Figure 3-6 (b) for these four water depths are 60, 55, 53, and 48 km/h, respectively.

Scenario 3

All conditions are the same as Scenario 2 except that the assigned skid resistance intervention level of $(SN_{40})_{IL}$ is lowered from 30 to 25, and $(SN_0)_{IL} = 37.5$. The new "wet-weather threshold speeds" obtained from Figure 3-6 (c) for the four water depths are 74, 68, 66, and 61 km/h, respectively.

From Figures 3-6 (a), (b) and (c), the results of the three scenarios indicate that if a "wet-weather threshold speed" of 75 km/h is chosen, the intervention level rut depths would be 6 mm, 2.9 mm (not shown in Figure 3-6 (b)), and 5.25 mm for Scenario 1, 2 and 3 respectively. If a "wet-weather threshold speed" of 65 km/h is chosen instead, the corresponding intervention rut depths would be 10 mm, 4.8 mm (not shown in Figure 3-6 (b)), and 9.5 mm.

3.7.2 Findings of Numerical Examples

The numerical examples above together with Figures 3-6 (a), (b) and (c), though limited to a specific pavement surface material, do highlight some of the relationships between the rut depth intervention level and the following key influencing factors: skid resistance intervention level $(SN_{40})_{IL}$, pavement skid resistance state (characterized by SN_0 and SN_{40}), and vehicle speeds. The observations may be summarized as follows:

- Effect of skid resistance intervention level $(SN_{40})_{IL}$ – For a given "wet-weather threshold speed", lowering the skid resistance intervention level has the effect of allowing a higher value of intervention level rut depth, and vice versa. For example, comparing the results of Scenarios 2 and 3 (see Figures 3-6 (b) and (c)), it is seen that by lowering the skid resistance intervention level $(SN_{40})_{IL}$ from 30 to 25, the intervention level rut depth is increased from 6 mm to 25 mm at a "wet-weather threshold speed" of 60 km/h.

  On the other hand, if one chooses to fix the intervention level rut depth, lowering the skid resistance intervention level has the effect of allowing a higher "wet-weather threshold speed". For example, from Figures 3-6 (b) and (c), assuming the intervention level rut depth is chosen to be 15 mm, the allowable "wet-weather threshold speed" will increase from 49 km/h to 62 km/h.

- Effect of pavement skid resistance state – As a pavement deteriorates in skid resistance with reduced values of SN_0 and SN_{40}, it will allow a lower intervention level rut depth or a lower "wet-weather threshold speed". This effect can be examined by comparing Scenarios 1 and 2

where the pavement section concerned deteriorated from (SN_0 = 48, SN_{40} =70.0) to (SN_0 = 40, SN_{40} =60), the intervention level rut depth will decrease from 25 mm to 6 mm for a "wet-weather threshold speed" of 60 km/h. If the rut depth intervention level is fixed at 15 mm, then the "wet-weather threshold speed" will reduce from 61 km/h to 49 km/h.

- Effect of vehicle speeds – The prevailing vehicle speeds of the pavement section affects the choice of "wet-weather threshold speed". For a given skid resistance state of a pavement section, raising "wet-weather threshold speed" will lead to a lower required value of rut depth intervention level. For example, in Scenario 1 (see Figure 3-6 (a)), raising "wet-weather threshold speed" from 60 km/h to 70 km/h will reduce the rut depth intervention level from 25 mm to 8 mm.

3.8 Critical Rut Depth for Pavement Structural Design

While rut depth is a control requirement for the structural design of asphalt pavements, there does not exist any mechanistically derived quantitative terminal rut depth to serve as a threshold limit to be used by the designer. It is proposed in this research that the functional critical rut depth derived mechanistically on the basis of skid resistance intervention level be used as the critical rut depth for the purpose of structural design of asphalt pavements.

The following steps can be followed to revise a standard pavement structural design procedure to incorporate the consideration of critical rut depth to satisfy the highway operation functional requirement of traffic safety:

Step 1: Determine critical rut depth – Follow the procedure in Figure 3-3 (see description in Section 3.5), determine the intervention level

rut depth and set this value as the critical rut depth for pavement structural design.

Step 2: Perform pavement structural design -- Using any suitable pavement structural design procedure, select pavement materials and thicknesses for all pavement layers to meet strength and other requirements as appropriate.

Step 3: Perform rut depth calculation of trial pavement structural design -- Using any suitable pavement structural analysis procedure to determine the terminal rut depth of the trial pavement design under the total cumulative design traffic loading for all traffic lanes.

Step 4: Check acceptability of terminal rut depth – Compare the terminal rut depth computed in Step 3 with the critical rut depth determined in Step 1. If the terminal rut depth is less than the critical rut depth, accept the design. Otherwise, repeat Step 2 to revise the structural design by using better layer materials for one or more of the pavement layers, or increasing the thickness of one or more of the pavement layers.

The above revised pavement structural design procedure with the additional critical rut depth check now provides a rational mechanistic process to integrate the structural design of asphalt pavements with the required wet-weather driving safety requirements with respect to pavement rutting.

3.9 Summary

Although pavement rutting is a load-induced structural deformation, no current pavement procedure has incorporated the functional safety consideration of pavement ruts in the structural design of asphalt pavements. To

bridge this gap, this chapter proposes to adopt the concept of skid resistance intervention level to determine the corresponding rut depth intervention level in pavement management, and equate it as the critical rut depth to be used as a design control requirement for structural design of asphalt pavements. A rational procedure for determining rut depth intervention level is proposed on the basis of the concept of skid resistance intervention level. This ensures that a consistent safety management approach is maintained in establishing the skid resistance intervention level and the rut depth intervention level for a given pavement section.

The concept and theoretical basis for the proposed approach has been presented. A finite element skid resistance simulation model is employed to evaluate the skid resistance of a ponded rut depth. Since the finite element analysis is time consuming and skill demanding, an expedient procedure is proposed by replacing the finite element analysis with either a database or a neural network model. Numerical examples are presented to illustrate that the expedient method can be a convenient and efficient analytical tool for a network level pavement management system to establish the investigatory and intervention levels for different pavement sections in a road network.

Table 3- 1 Findings of Past Studies on Critical Rut Depths

Study	Findings
1. AASHTO Task Force (1989)	• Wheel path ruts greater than 1/3 to ½ in. (8.5 to 12.7 mm) in depth are considered by many highway agencies to pose a safety hazard because of the potential for hydroplaning, wheel spray, and vehicle handling difficulties.
2. Fwa et al. (2012)	• Critical rut depth equals to 20 mm for vehicle speed of 70 km/h on a pavement surface that has acceptable skid resistance if there is no ruts.
3. Hicks et al. (2000)	• For rut depth from 7 to 12 mm, inadequate cross slope can lead to hydroplaning and wet-weather accidents; • When rut depth exceeds 13 mm, the potential for hydroplaning and wet-weather accidents is significantly increased.
4. Barksdale (1972)	• In pavements with rut depth of approximately 0.5 in. (12.7 mm), ponding is sufficient to cause automobiles traveling at speeds of 50 mi/h (80.5 km/h) or faster to hydroplane.
5. Lister and Addis (1977)	• Rut deeper than approximately 0.5 in. (12.7 mm) could result in ponding of water and cause hydroplaning or loss of skid resistance.
6. Sousa et al. (1991)	• For rut depths that exceed 0.2 in. (5.1 mm), hydroplaning is a definite threat particularly to cars.

Table 3- 2 Examples of Rut Severity Classifications Adopted in Practice

Reference	Rut Severity		
	Low	Medium	High
Walker et al. (2002)	< 25.4 mm	> 25.4 mm	> 50.8 mm
WSDOT (1999)	6.3 – 12.7 mm	12.7 – 19.1 mm	> 19.1 mm
ODOT (2006)	3.2 – 9.5 mm	9.5 – 19.1 mm	> 19.1 mm
CMRPC (2006)	6.3 – 12.7 mm	12.7 – 38.1 mm	> 38.1 mm
BC MTI (2009)	3 – 10 mm	10 – 20 mm	> 20 mm
Shahin (1994)	6.3 – 12.7 mm	12.7 – 25.4 mm	> 25.4 mm
Caltrans (2006)	Schedule corrections when rut depth > 25.4 mm		

Note: Numerical value in each cell represents rut depth.

Table 3- 3 Examples of Skid resistance Intervention Level

Reference	Skid Resistance Intervention Level			
Selected examples from survey by Henry (2000) on threshold friction level for intervention	Agency	Interstate/ Motorway	Primary Road	Secondary Road
	• Idaho • Illinois • Kentucky • New York • S Carolina • Texas	SN40S < 30 SN40R < 30 SN40R < 28 SN40R < 32 SN40R < 41 SN40R < 30	SN40S < 30 SN40R < 30 SN40R < 25 SN40R < 32 SN40R < 37 SN40R < 26	SN40S < 30 SN40R < 30 SN40R < 25 SN40R < 32 SN40R < 37 SN40R < 22
Intervention level proposed to Ohio Department of Transportation (2008)	SN40R < 32 SN40S < 23			
Intervention level proposed to Maryland Department of Transportation (2009)	SN40R < 30 for undivided highways SN40R < 25 for divided highways			
New Zealand Transport Agency (2010) (see Note (i))	Site Category	Low Skidding Crash Risk	Medium Skidding Crash Risk	High Skidding Crash Risk
	Undivided carriageway	ESC < 0.30	ESC < 0.30	ESC < 0.35
	Divided carriageway	ESC < 0.30	ESC < 0.30	ESC < 0.35
UK Design Manual (2006) (see Note (ii))	Motorway: CSC < 0.30 for low traffic CSC < 0.35 for heavy traffic			

Notes: (i) ESC is the Equilibrium SCRIM Coefficient computed as normalized (seasonally corrected) SCRIM coefficients for both within year and between year variations. SCRIM coefficient is the skid resistance measured at 50 km/h by skid testing machine SCRIM (2006). Intervention level is termed as threshold level, which is defined as a skid resistance level 0.1 ESC units below Investigatory Level or 0.30 whichever is highest. Investigatory and threshold levels for other site categories are given in Ref (NZ Transport Agency, 2010)

(ii) CSC is Characteristic SCRIM Coefficient computed form measured SCRIM coefficients corrected for the effect of seasonal variation. Investigatory levels for other road types are given in British Standard BS 7941-1:2006. Only investigatory levels are given. Wherever the CSC is at or below the assigned Investigatory Level a site investigation shall be carried out, to determine whether treatment to improve the skid resistance is required or whether some other action is required.

(iii) SN40R and SN40S are the skid numbers measured at 64 km/h (40 mph) in accordance with ASTM standard method E274 (2011) using rib tire and smooth tire respectively.

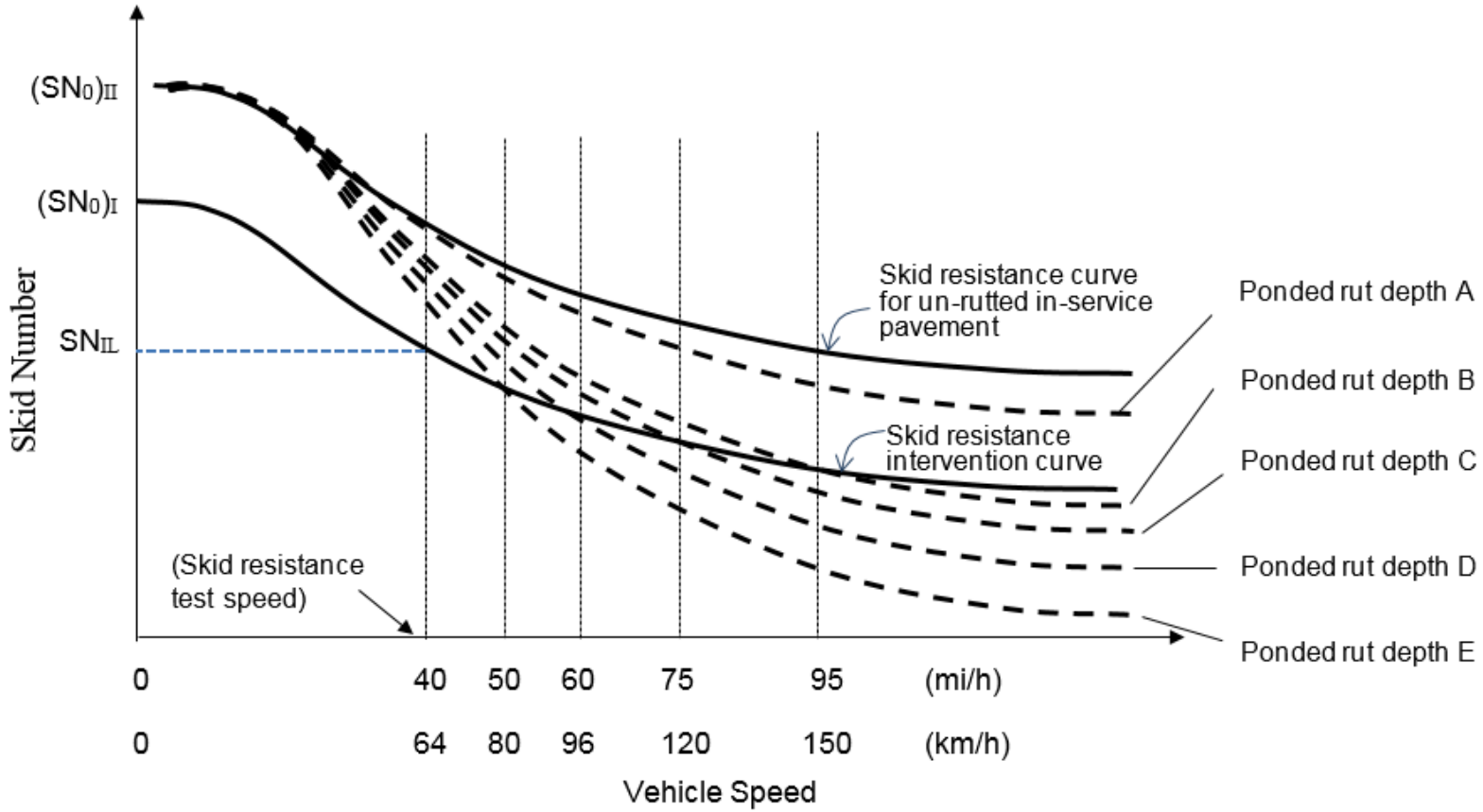

Figure 3-1 Schematic Diagram Illustrating the Concept of Rut Depth Intervention Level

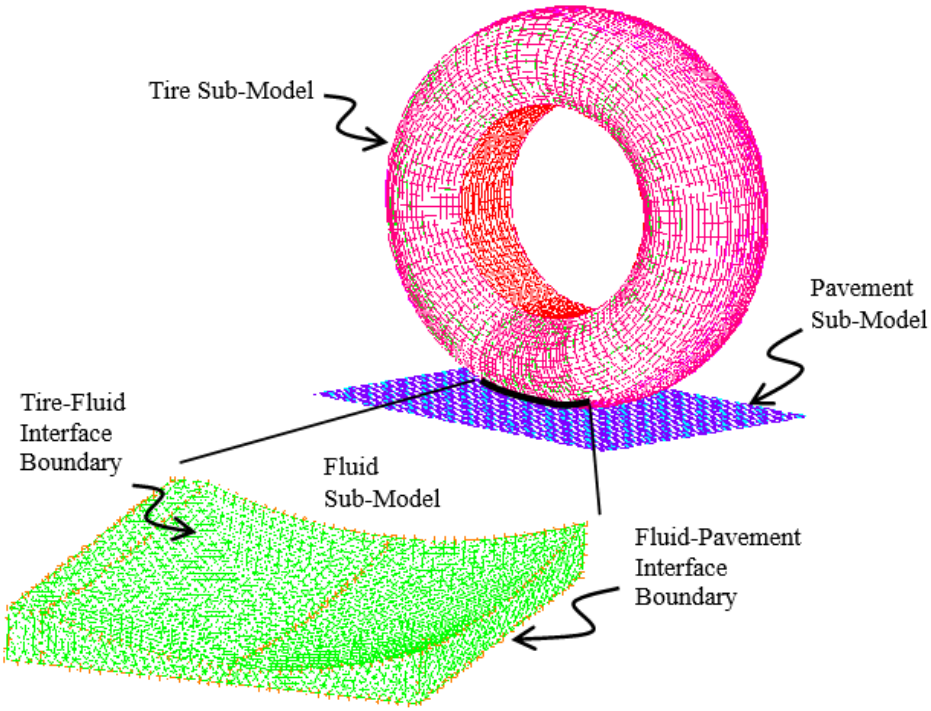

Figure 3-2 Mesh Design of Finite Element Simulation Model

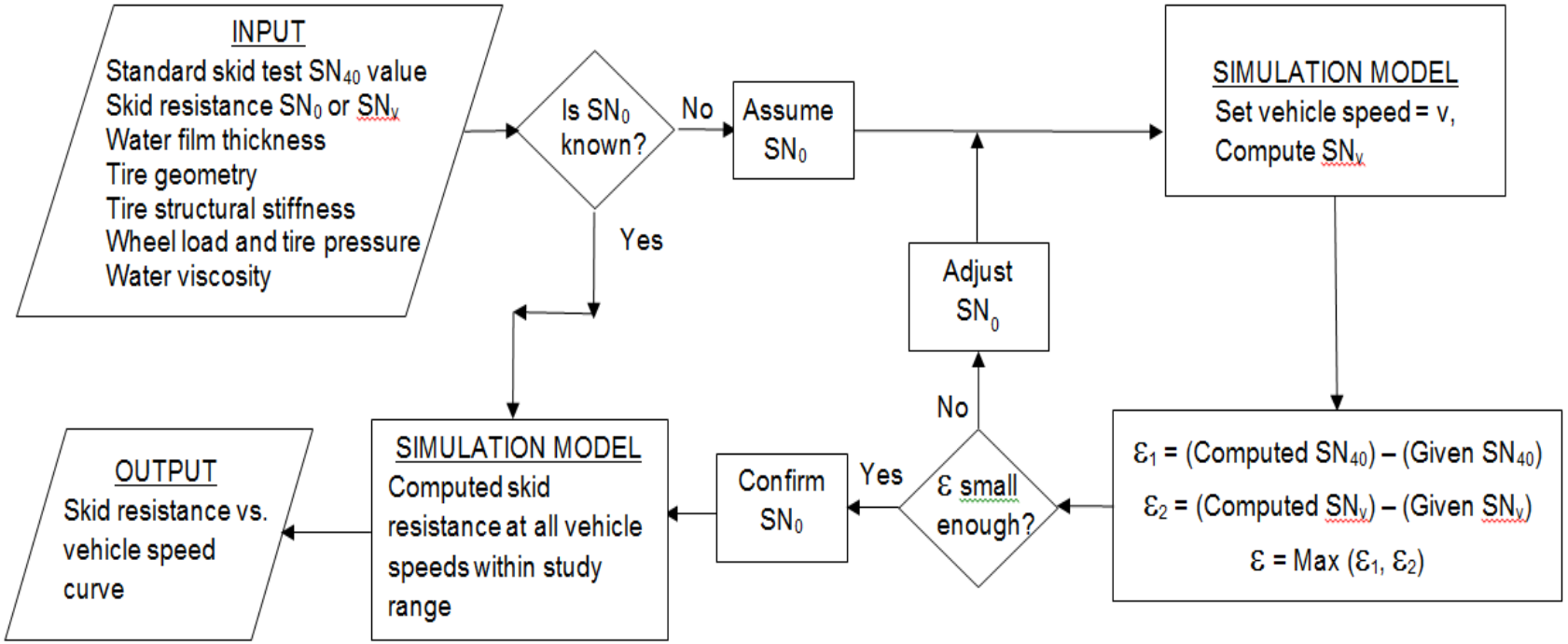

Figure 3-3 Flow Diagram for Deriving Skid Resistance-Speed Performance Curve

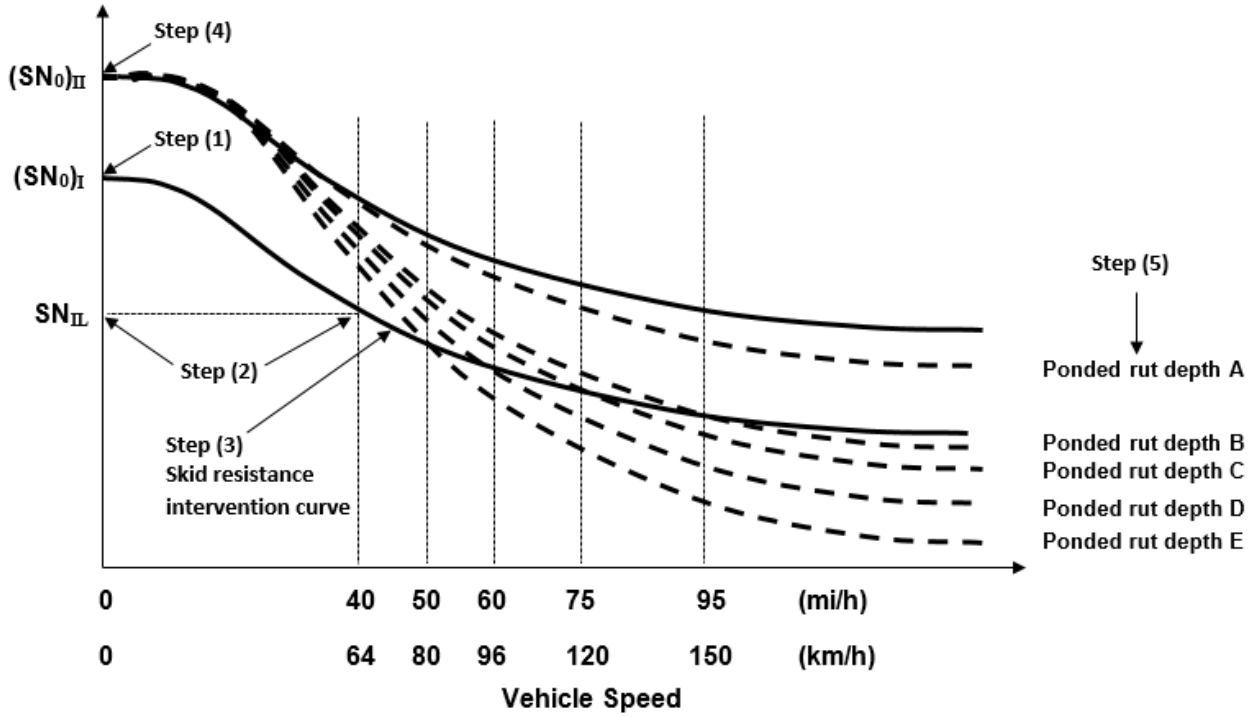

Figure 3-4 Steps in Determination of Rut Depth Intervention Level

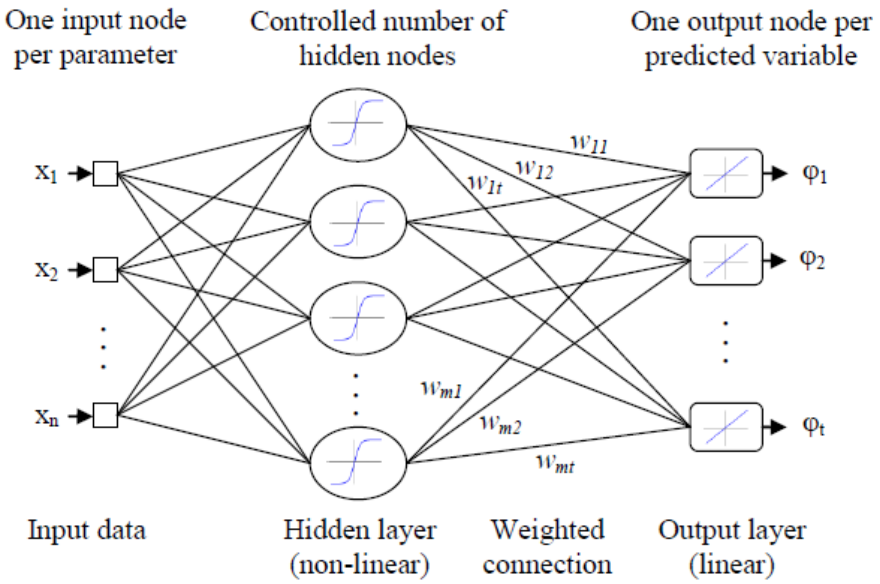

Figure 3-5 Two Layer Feedforward Network (Zhang, 2014)

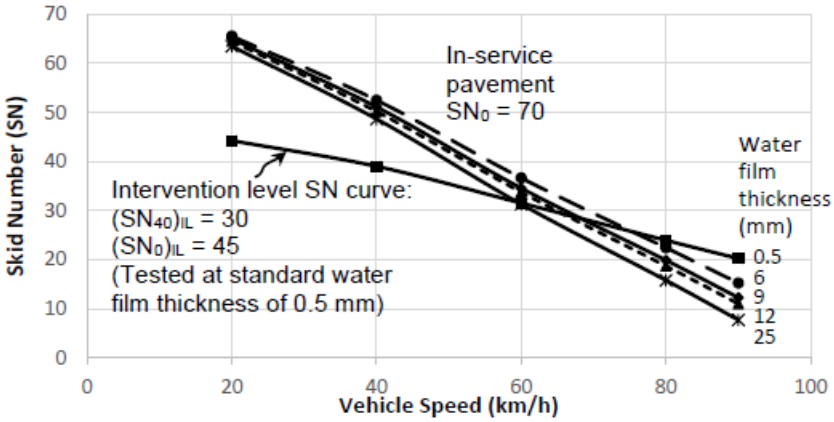

(a) Scenario 1: In-service pavement SN_0 = 70, Intervention level $(SN_{40})_{IL}$ = 30 with $(SN_0)_{IL}$ = 45

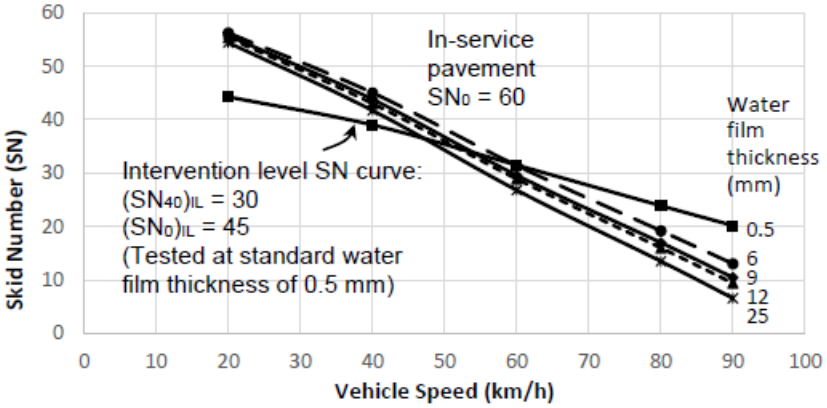

(b) Scenario 2: In-service pavement SN_0 = 60, Intervention level $(SN_{40})_{IL}$ = 30 with $(SN_0)_{IL}$ = 45

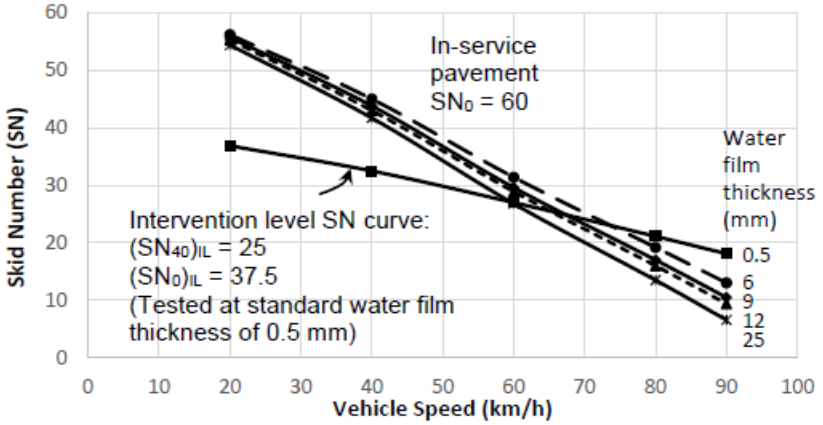

(c) Scenario 3: In-service pavement SN_0 = 60, Intervention level $(SN_{40})_{IL}$ = 25 with $(SN_0)_{IL}$ = 37.5

Note: $(SN_{40})_{IL}$ is measured at 40 mi/h (64 km/h) with smooth tire.

Figure 3-6 Numerical Examples for Determination of Rut Depth Intervention Levels

CHAPTER 4 IMPROVED ASPHALT MIX DESIGN WITH CONSIDERATION OF SKID RESISTANCE AND HYDROPLANING RISKS

4.1 Introduction

Ever since the pioneering research and development works in the 1950s and 1960s in Europe (MaClean, 1958; Road Research Laboratory, 1960) and North America (Dillard et al., 1957; Burnett et al., 1968), much progress has been made in asphalt mix design over the years in devising testing procedures and equipment for the selection of aggregates so as to produce an asphalt wearing course with adequate frictional properties for the full length of pavement service life. In a typical asphalt pavement construction project, it is required to provide aggregates and asphalt binder to produce a mix meeting the project specified requirements. Besides the standard requirements to test the required structural properties of aggregates such as crushing strength, surface hardness, and Los Angeles abrasion resistance, etc, there is also a common requirement to satisfy a minimum aggregate polishing resistance with the aim to produce an asphalt wearing course with adequate frictional properties over the entire pavement service life.

The most widely adopted laboratory method of testing the required friction properties of aggregates is by means of a polishing test followed by friction measurement using a friction measurement device. Standard procedures have been established in North America and Europe for this purpose (ASTM, 2013b; ASTM, 2013a; ASTM, 2011b; British Standard BS 812, 1989; BS EN 12697-49, 2014; ASTM, 2002; ASTM, 2009a). The results of the test are used as a basis for aggregate selection to guard against wet weather skidding accidents over the design service life of the pavement.

Guidelines have been established by highway agencies in many parts of the world for the selection of aggregates in asphalt mix design (Subedi, 2015; Feighan, 2006; Henry, 2000; Hall et al., 2009). Such aggregate selection guidelines based on laboratory friction testing of polished aggregates or asphalt mixtures provide useful criteria for pavement engineers, especially in differentiating aggregates with good, average and poor polishing resistance. However, it should be highlighted that in most cases, the results obtained from laboratory tests do not provide one with all the information required to evaluate the skid resistance available from the pavement surface under actual road operating conditions. The problem of applying the laboratory measured polished friction properties of the aggregates or mixture to assess the expected skid resistance performance of the pavement surfacing design mix under the actual road operating conditions, remains a major challenge to the pavement researcher and practitioner today.

This chapter presents a rational analytically-sound procedure as an attempt to overcome the aforementioned problem by the use of a 3-dimension finite-element skid resistance computer simulation model. Laboratory measured polished friction properties of the selected design surfacing mix are applied to calibrate the simulation model. The calibrated model is next employed to evaluate the skid resistance, hydroplaning speed, as well as braking distance under different design service conditions of the pavement surface, and check against the design safety requirements of the pavement.

4.2 Significance of Study

The incorporation of skid resistance consideration in pavement surface course mix design has significant practical implications in the following aspects:

(1) The skid resistance service life of a pavement is different from the design life defined in the structural design of the pavement. Different surface course mix designs using different materials and mix proportions will produce different skid resistance performance and different lengths of skid resistance service life, as well as different structural strength and design lives. Hence, skid resistance consideration has a major impact on the life cycle cost analysis of different pavement designs, and should be included as an integral part of the pavement design process.

(2) Different highways, or even different sections of a highway, having similar design traffic loadings and similar structural design requirements, may have different skid resistance requirements due to differences in operating speeds, geometric designs (e.g. horizontal and vertical curvatures), and rainfall characteristics, etc. These differences in skid resistance requirements can lead to different surface course mix designs, and hence different pavement design considerations.

(3) The common current practice of specifying the polishing property of coarse aggregates used in preparing asphalt mixtures only addresses pavement skid resistance performance at low vehicle speeds below 40 km/h. It does not provide an assessment of pavement skid resistance performance at the operating speeds of a highway. There is a need for a procedure to predict the expected skid resistance performance of a pavement design mix under the actual operating conditions of a highway.

4.3 Current Laboratory Procedures for Aggregate Selection

4.3.1 Review of Current Practices and Procedures

Recognizing the fact that an asphalt pavement surfacing will be subject to constant abrasive actions of vehicular traffic, and that the exposed surface aggregates will be fractured and polished during the design service life of a typical asphalt pavement, pavement researchers and engineers have been assessing the skid resistance characteristics of polished aggregates since the 1950s (MaClean et al., 1958; Road Research Laboratory, 1960; Dillard et al., 1957; Burnett et al., 1968). The significance of evaluating the skid resistance of a pavement surfacing at its polished state is that its skid resistance and hydroplaning characteristics will be at their worst when fully polished.

Once the asphalt mix design with respect to aggregate gradation and asphalt binder grade has been confirmed, the main issue left is the selection of aggregate type. With a given aggregate gradation, the choice of aggregate type is a key determinant of the skid resistance performance of asphalt pavement surfacing because the latter affects the speed-dependent friction properties of exposed polished aggregates in an in-service pavement. Therefore, to design an asphalt surfacing mixture for safe traffic operation, testing of the friction properties of polished aggregates or asphalt mixture has become a central focus in the selection of aggregates for the design and production of asphalt mixtures.

One of the earliest and widely adopted standardized procedures for evaluating the polished friction properties of an aggregate type is by measuring its polished stone value (PSV) (see Section 2.5.1.2). Table 4-1 shows examples of PSV-based aggregates selection guidelines used in practice. A major drawback of the PSV-based approach is that PSV represents only the micro-texture property of the coarse aggregates. It alone does not allow one to

calculate the skid resistance actually available on an in-service pavement. This consideration has led to development of laboratory tests that polish the surface of an asphalt mixture fabricated using the aggregates to be examined. Examples of such tests include the ASTM standard tests E660 (ASTM, 2011b) and E1911 (ASTM, 2009a), and the latest European standard test EN 12697-49 (BS EN 12697-49, 2014). The intention of these laboratory tests is to simulate the effects of vehicular traffic action on the surface material of asphalt pavement wearing course. The vehicular traffic introduces compacting and abrasive effects on the wearing course materials that may cause realignment, fracturing and rounding off of edges, wear and tear, and polishing of the exposed coarse aggregates. It is the aim of the polishing tests to produce a polished asphalt mixture surface that represents as closely as possible the state of micro-texture and macro-texture of a polished pavement surfacing of the same mix design (Subedi, Y. P., 2015; Hall et al., 2009).

A number of laboratory friction testing devices has been developed to measure the skid resistance of polished asphalt mixture specimens. Among them are the British Pendulum Tester (ASTM, 2013b), Dynamic Friction Tester (ASTM, 2009a), and the North Carolina State University Variable-Speed Friction Tester (ASTM, 2002). The laboratory measured skid resistance data of the polished specimens are then converted to field skid resistance properties of in-service pavements by means of some empirical or correlation relationships. As shown in Table 4-2(a), researchers have established such relationships for different asphalt mixtures. Typically, laboratory measured skid resistance data are converted to standard field skid resistance measurements such as SN64R or SN64S which are commonly used for reporting field skid resistance and for skid resistance management of in-service pavements. SN64R and SN64S are the skid

numbers measured at 64 km/h (40 mph) in accordance with ASTM standard method E274 (ASTM, 2011a) using rib tire and smooth tire respectively.

The predicted polished SN64R or SN64S values are then compared with the required minimum in-service pavement skid resistance level to determine if the selected aggregates are satisfactory for the design mixture. Minimum in-service pavement skid resistance levels are adopted in many highway agencies to ensure safe wet-weather operations of roads. Examples of minimum skid resistance levels adopted by different highway agencies are found in Table 3-3.

4.3.2 Recent Development Trends and Challenges

The inadequacy of selecting pavement aggregates based on the sole requirement of minimum skid resistance is well recognized because it is only a point control of skid resistance at the specified standard test speed and water film thickness. The skid resistance performance at other speeds and water film thickness remains unknown. This has given rise to a practice of specifying 2-parameter controls by establishing values of minimum acceptability for both a skid resistance parameter and a measurement of macro-texture (Feighan, 2006; Henry, 2000; Hall et al., 2009). The aim is to cover the expected skid resistance performance of the design asphalt pavement mixture over the full spectrum of vehicle operating conditions, addressing particularly the effects of different vehicles speeds.

Table 4-2(b) lists several recent studies to highlight the current research directions in achieving the above aim. It is apparent that a common focus of the research efforts is to predict the expected field skid resistance at a desired standard slip speed from laboratory skid resistance and surface macrotexture measurements. A key requirement of the laboratory test procedure is the ability to polish the asphalt mixture surface with exposed aggregates to a state of

terminal friction characteristics (Hall et al., 2009; Voller, 2006; Liang, 2013). There is also the need to polish a sufficiently large surface area of the test specimen to enable skid resistance and surface texture measurements to be made. Typically slab specimens of the design asphalt mixture will have to be specially prepared for this purpose.

With the measurement of skid resistance and macrotexture made on the laboratory specimens of design asphalt mixture, a sound basis can be developed based on pre-established in-service pavement safety requirements to select suitable aggregates having good polishing resistance and with a gradation that would provide good macrotexture to control skid resistance loss with slip speed.

Equipped with the above described capability of laboratory testing and field skid resistance prediction, a remaining challenge in aggregate selection for asphalt mixture design is how to effectively apply the available data to predict field skid resistance performance, and to assess if the selected aggregates and the mix design are adequate in meeting specific pavement safety design requirements. Such safety requirements include braking distance and minimum skid resistance under different vehicle operating and weather conditions, and hydroplaning risk with respect to vehicle travel speeds in wet weather. It is apparent that none of the procedures or models reviewed in this chapter (Table 4-2 (a) and Table 4-2 (b)) could provide a satisfactory answer to these challenges.

4.4 Proposed Enhanced Skid Resistance-Based Procedure for Aggregates Selection

4.4.1 Overview of Proposed Procedure

An improved skid resistance-based procedure to select aggregates for an asphalt pavement wearing course is presented in this section. The proposed procedure consists of two main components:

Phase (A) -- A laboratory test component that polishes the surface of design mix prepared using the aggregates to be evaluated, and measures the frictional resistance of the polished surface at two selected test speeds; and

Phase (B) -- An evaluation phase that applies laboratory measured data to estimate filed skid numbers at the desired speeds, and calibrates a three-dimensional finite-element skid resistance simulation model, for the purpose of predicting in-service field skid resistance performance of the polished mixture.

The intended improvements to be achieved by the proposed procedures are to fulfill the requirements highlighted in the challenges described in the preceding section. That is to enable the prediction of field skid resistance performance so as to assess if the selected aggregates and the mix design are adequate in meeting specific pavement safety design requirements. The specific requirements include the following:

i. Calculation of braking distances for road segments of different design speeds, and under various weather conditions, and check if they meet the corresponding minimum braking distance requirements;

ii. Estimation of skid resistance available on road segments of different design speeds, and under different weather conditions, and check if they meet the corresponding minimum skid resistance requirements; and

iii. Estimation of the hydroplaning speeds on road segments of different design speeds, and under different weather conditions, and evaluation of hydroplaning risk with respect to vehicle travel speeds in wet weather.

4.4.2 Input Parameters and Key Features of Proposed Procedure

The proposed enhancements of the proposed procedure derive mainly from its second phase, i.e. Phase (B) -- the evaluation phase in which useful information is generated from the calibrated simulation model. However, the key input parameters related to the friction characteristics of the asphalt mixtures have to be generated from the laboratory tests in Phase (A).

The skid resistance simulation model employed in this section is a three-dimensional finite-element computer simulation model developed by Ong et al. (2007) and Fwa et al. (2008) which has been introduced in Chapter 3 (Section 3.4.1). With the two skid numbers obtained at two different speeds, the skid resistance simulation model can be calibrated to identify the zero-speed skid number SN_0, and the skid resistance-vehicle speed curve of the in-service pavement section covering the full speed range of interest. Typically the two skid numbers required to input to the simulation model involves SN_{64} value measured at the standard speed of 64 km/hr (40mi/hr) and a second skid number at another speed, although theoretically any two test speeds could be chosen. The detailed calibration procedure, also known as back-calculation procedure, has also been discussed in Chapter 3 (Section 3.4.2).

Instead of determining skid numbers at two slip speeds, an alternative method is to determine one skid number SN_V at a slip speed V, and estimate the

zero-speed skid number SN_0 using a low speed friction tester such as the British Pendulum Tester (BPT) (ASTM, 2013b). The BPT measures the skid resistance of a test surface at a low speed of approximately 10 km/h, and reports the test results in British Pendulum Number, BPN. BPN is known to be essentially a function of the micro-texture of the test surface, and is commonly adopted as a surrogate measure of pavement surface micro-texture. Hence, it is possible to measure BPN of a polished specimen and estimate its zero-speed skid number, SN_0. For example, the following experimental relationship of high correlation was obtained in research at the Pennsylvania State University and used by researchers (Henry, 2000; Henry, 1986; Henry et al., 1978) for the estimation of SN_0,

$$SN_0 = 1.32BPN - 34.9 \qquad R^2 = 0.90 \qquad (4\text{-}1)$$

With the knowledge of SN_0 and another SN_V at slip speed V, the calibration of the simulation model can proceed using the back-calculation procedure. The calibration process basically defines the micro-texture property (represented by SN_0 of the skid resistance-speed curve), and the macro-texture property (represented by the rate of deterioration of skid resistance with vehicle speed) of the SN-speed performance curve of the pavement surface mixture. It is of significance to note that the simulation model calibrated for the E274 test condition (ASTM, 2011a) can be used to obtain the following additional information:

(i) Calculate the skid resistance of the test surface under the test tire (E524 tire in the present case) for any water film thickness. This means that the SN-speed performance curve of the test mixture at any water film thickness can be generated and studied.

(ii) Since calibrated simulation model can generate the SN-speed performance relationship for any given water film thickness, the braking distance for any vehicle speed on the test surface with any depth of surface water can be calculated. The computation process of braking distance is described in the next sub-section (4.3.3).

(iii) The hydroplaning speed at any water film thickness can be calculated. This is done by increasing the slip speed in the simulation analysis until hydroplaning occurs. Hydroplaning is defined to occur when the computed hydrodynamic uplift force is equal to the tire load, and the associated slip speed is the hydroplaning speed.

For the problem dealt with in this chapter, the skid resistance simulation model has to be calibrated using the laboratory measured skid resistance properties of the laboratory specimens prepared using the mix design and aggregates selected. It requires laboratory skid resistance measurements of the test specimens at two different speeds at a known water film thickness, followed by converting the two laboratory skid resistance measurements to their equivalent field skid number values for the purpose of calibrating the skid resistance simulation model.

4.4.3 Checking of Pavement Safety Design Requirements

Of the three pavement safety design requirements, namely the maximum braking distance allowed, the minimum skid resistance, and an acceptable hydroplaning risk, the checking procedures for the latter two requirements are the same as those described in Chapter 3 for flooded rutted pavements. This section explains the calculation of braking distances and the checking against the maximum braking distance allowed.

The highway project in question may have road segments of different design speeds and different geometric features (e.g. straight sections and sections of horizontal curves of different radii). The maximum braking distances allowed for different road segments may be different. These braking distance requirements must be checked for the trial design mix for the respective appropriate design speeds and wet-weather driving conditions (i.e. water film thickness).

On a wet pavement, the tire-pavement friction coefficient varies with vehicle speed in a nonlinear manner. Hence, the braking distance D_B must be calculated from the following expressions taking into account the changes of vehicle speed V and tire-pavement friction coefficient with time during vehicle braking:

$$D_B = \int_0^T V(t)\, dt \tag{4-2}$$

$$V(t) = V_0 - \int_0^T \left[\mu(t) + G\right] g\, dt \tag{4-3}$$

where V(t) is the vehicle speed at any time t, $0 \leq t \leq T$, T is the total duration of braking time taken by the vehicle to come to a complete stop, V_0 is the initial vehicle speed at time zero when the brake is applied, $\mu(t)$ is the tire-pavement friction coefficient at time t when the vehicle speed is v(t), G is roadway grade expressed as a positive decimal value for upslope and negative for downslope, and g is the gravitational acceleration equal to 9.81 m/s^2.

The calculation of braking distance D_B requires the establishment of the relationship between μ and vehicle speed V. The tire-pavement friction coefficient μ at any vehicle speed V for a given water film thickness can be calculated using the finite element simulation model. This information is required for calculating the decrease of vehicle speed with time, and the

calculation of the total braking distance. The technique of numerical integration is adopted for the computation, as illustrated in Figure 4-1.

The braking distance check must be performed for different representative segments of the highway project concerned with their respective design or operating conditions as specified by the highway agency responsible. The operating conditions to be considered for each representative segment refers to its worst design conditions for braking distance represented by specified design vehicle speed and water film thickness, and the applicable maximum braking distance allowed.

4.5 Steps of Proposed Aggregates Selection Procedure

There are four main steps involved in the proposed procedure for aggregates selection for the objective of designing an asphalt mixture that is able to maintain a sufficient high skid resistance above the required minimum safe level even after it has been fully polished. The following gives the details of the four steps:

(1) Laboratory polishing treatment – A laboratory polishing treatment is to be performed on the specimens of design mixture prepared using the aggregates to be examined so as to produce a polished pavement surface representative of the terminal polished state of the simulated in-service pavement surface. This is to present the specimens for subsequent testing in their worst possible state of skid resistance performance.

(2) Laboratory skid resistance test – A laboratory skid resistance test is to be performed on the polished test specimens at two selected test speeds (V1 and V2) and a pre-determined water film thickness. Next, a correlation relationship is to be established to convert the laboratory skid

resistance measurements to in-service pavement skid numbers at the two corresponding speeds.

(3) Calibration of skid resistance simulation model - Perform the calibration of the skid resistance simulation model in two phases: tire calibration and skid-resistance characteristics calibration. Tire calibration for the present study is performed for ASTM E274 test (ASTM, 2011a) using E524 smooth tire. The skid-resistance characteristics calibration is performed using SN (V_1)S and SN (V_2)S as input as described earlier in this chapter.

(4) Skid resistance and hydroplaning analysis - Analyses using the calibrated skid resistance simulation model are performed: (i) to calculate skid numbers at selected speeds as specified for road safety or pavement friction maintenance requirements; (ii) to calculate braking distances at selected speeds and water film thickness as considered in road geometric design; and (iii) to calculate hydroplaning speeds at selected water film thickness as appropriate for hydroplaning risk assessment.

The laboratory polishing treatment in Step (1) can be performed by using an appropriate polishing device that is able to polish a laboratory fabricated asphalt mixture specimen to a state that is representative of the advanced state of polished in-service pavement wearing surface. The polished surface area must be large enough for laboratory skid resistance tests at two different speeds. Currently, the Dynamic Friction Tester (DFT) specified in ASTM E1911 (2009) appears to be the most ideal skid resistance test device for the procedure proposed in this chapter. A review of literature suggests that the NCAT accelerated polishing machine (Vollor and Hanson, 2006), a machine

called “The Polisher” developed for Ohio Department of Transportation (Liang, 2013), and the Auckland Accelerated Polishing Machine (Wilson D. J., 2013; Wilson et al., 2005) are examples of suitable laboratory devices for the purpose of the proposed procedure.

Establishing a correlation relationship between the laboratory measured DFT skid resistance values and in-service pavement skid numbers is another key requirement of the proposed procedure. Recent studies as summarized in Table 4-2 show that such relationships exist and they usually are statistically highly significant. These studies can be classified into two groups: one-parameter regression models shown in Table 4-2 (a) and two-parameter regression models presented in Table 4-2 (b). In the two-parameter control methods, besides the laboratory measured DFT skid resistance measurements, the mean profile depth (MPD) of the polished specimen surface is the other parameter which can be measured by means of the Circular Track Meter (ASTM, 2015b).

Once the skid resistance simulation model has been calibrated, and the skid resistance-slip speed performance curve derived, the computation of braking distance for any given initial vehicle speed according to the procedure of Figure 4-1 is computationally straight-forward. Its computation time using computer program is a matter of a few seconds. In contrast, the performing of skid resistance and hydroplaning analysis using the finite element simulation model is skills and experience demanding, particularly in the design of finite element mesh and checking of convergence. In addition, each skid resistance analysis may require several CPU hour. This is an issue of concern if the proposed procedure is to be used as a laboratory working procedure of selecting aggregates for asphalt mix design.

These two problems identified above can be overcome by employing either a database or an artificial neural network (ANN) approach (Beale et al., 2015). A database of solutions for skid resistance and hydroplaning speeds can be developed for typical ranges of the input parameters. Alternatively, an artificial neural network approach can be employed to develop a prediction model for both skid resistance and hydroplaning speed. For the purpose of the present study, an artificial neural network (ANN) model (Beale et al., 2015) for computing the skid number and hydroplaning speed respectively for the case of E524 smooth tire has been developed.

The ANN model for predicting skid number requires SN_0, SN64S, slip speed V, and water film thickness as input. It can compute the skid numbers at different slip speeds under the E274 test conditions to generate the SN-V performance curve for the standard test water film thickness of 0.5 mm (Henry, 2000; Kubiak et al., 1972). Next, by setting the water film thickness and slip speed at the desired values, the skid number at any water film thickness at any slip speed using the same ANN model can be obtained. For the case of hydroplaning speed prediction, only SN_0, SN64S, and water film thickness are required as input. This ANN model can be used to compute the hydroplaning speed for any water film thickness.

4.6 Adjustment of Design Mix to Meet Functional Safety Requirements

Adjustments to the trial design mix are required if the terminal skid resistance and hydroplaning properties of the mix fail to meet the three functional requirements described in the preceding sub-sections. There are the following two main options available to the design engineer to improve the mix design: (1) Change the type of aggregates to improve the microtexture of the mixture; and (2) Change the aggregate gradation and binder content to either

increase the surface macrotexture of the mixture, or increase the porosity to improve the drainage properties of the mix, or both.

When a design mix fails to provide sufficient terminal skid resistance and/or braking distance, options (1) or (2) above, or both, may be employed to improve the mix. If a design mix does not provide a sufficiently hydroplaning speed, option (2) appears to be the more relevant strategy to overcome the problem. Past studies have shown that, compared to macrotexture, the microtexture of a pavement surface material has relatively little influence on the magnitude of hydroplaning speed (Gallaway et al., 1979; Ong et al., 2005).

There might be situations where changing of mix design to meet one or more of the three functional safety requirements for certain road segments may not be cost effective or practical. Under such situations, other measures such as laying of special surface treatments, modifying of geometric design, or changing of design speed, could be applied.

4.7 Numerical Illustrative Examples

This section considers a set of possible functional safety requirements of a highway, and presents a numerical example to illustrate the application of the proposed procedure. The three functional safety requirements are:

1. An intervention skid resistance level of SN64S = 30 is set as the minimum safe skid resistance. SN64S refers to the skid number measured at 64 km/h (40 mph) in accordance with ASTM standard method E274 (ASTM, 2011a) using smooth tire.
2. For the wet-weather braking distance requirement, a choice of wet-weather speed and water film thickness is required. Traffic speed reduction caused by rainfall has been a topic of interest in wet-weather driving studies (Hall et al., 2009, Kyte et al., 2001). Higher speed

reductions are observed during the peak of a rainfall, and lower at the beginning or toward the end of the rain. A study by Kyte et al. (2001) showed an average speed reduction of 9.5 km/h during rainfall. Ibrahim and Hall (1994) gave a reduction range of 1.9 to 16.1 km/h, and Smith et al. (1995) reported 3 to 5% reduction in traffic speeds. For illustration purpose, considering an urban expressway in Singapore with a dry-weather speed limit of 90 km/h, this example adopts a water film thickness of 1.0 mm and a vehicle speed of 80 km/h for the analysis. Consider a case of zero percent roadway grade, the maximum braking distance allowed for a vehicle speed of 80 km/h is computed to be 74.8 m based on the requirements recommended by AASHTO (2011).

3. The minimum hydroplaning speed is considered for the same wet-weather driving condition stated above, i.e. water film thickness = 1.0 mm and vehicle speed = 80 km/h. It is appropriate to set the minimum hydroplaning speed as, say, 85 km/h.

The illustration of the proposed procedure is made by analyzing the adequacy of two trial design asphalt mixes having identical aggregate gradation but using aggregates of different mineral and chemical compositions. The terminal polished skid resistance performance curves for the two trial design mixes, designated as Mix Design A and B, are shown in Figure 4-2 as the two curves with water film thickness equal to 0.5 mm (i.e. the standard ASTM E274 test condition). It should be noted that these performance curves are derived from the finite element skid resistance simulation analysis based on laboratory accelerated polishing test. Because of their different resistance to polishing, Mix Design A has $SN_0 = 60$, and Mix Design B has $SN_0 = 45$.

Minimum Terminal Skid Resistance Check

The required minimum safe skid resistance is specified to be SN64S = 30. Since the two mix designs have SN64S greater than 30, both trial mix designs meet the requirement for the minimum terminal skid resistance.

Braking Distance Check

For the wet-weather operating conditions considered (i.e. water film thickness = 1.0 mm and vehicle = 80 km/h), the skid resistance performance curves for Mix Design A and B are derived using the finite element simulation model and plotted in Figure 4-2. These two skid resistance performance curves are calculated based on the ASTM E274 test condition, but with a water film thickness of 1.0 mm. With the knowledge of the performance curves, the respective braking distances for the two design mixes are calculated according to the procedure in Figure 4-1. The calculated braking distances for Mix Design A and B are found to be 63.4 m and 83.7 m respectively. Since the maximum braking distance allowed is 74.8 m, Mix Design A is able to meet the requirement, but Mix Design B fails to do so.

Minimum Hydroplaning Speed Check

The only major difference between Mix Design A and B is aggregate microtexture due to the differences in their mineralogical structure. There are negligible differences in the surface macrotexture of the two mixes. Analysis using the finite-element simulation model shows that at the water film thickness of 1.0 mm, both mix designs give the same predicted hydroplaning speed of 88.1 km/h. Hence, both Design Mix A and B are able to satisfy the requirement of minimum hydroplaning speed which is 85 km/h.

In summary, Mix Design A meets all the three functional safety requirements and offers an acceptable surface course material for the proposed

highway pavement. On the other hand, while Mix Design B is able to satisfy the requirements for minimum terminal skid resistance and minimum hydroplaning speed, it fails because it produces a braking distance exceeding the maximum allowed.

4.8 Summary

This chapter has examined the recent developments in laboratory techniques to test the skid resistance properties of asphalt mixture for the selection of aggregates to meet the skid resistance requirements of in-service pavements. This is an improvement over the traditional approach of testing the polished stone value of aggregates. It is proposed in this chapter that with the enhanced capability of laboratory testing, a more elaborate and improved basis of aggregates selection can be developed.

The proposed procedure makes use of a finite-element skid resistance simulation model to mechanistically predict friction related properties of the asphalt mixture prepared using the aggregates selected. The information includes SN-slip speed performance curves of the polished test surface at different water film thickness, its hydroplaning speeds for different water film thickness, and braking distance for any vehicle speed and water film thickness. The proposed procedure requires two skid resistance measurements of the laboratory polished specimens, which is now possible with the ASTM standard test method E1191 using the Dynamic Friction Tester. Alternatively, with only one skid resistance measurement at a test speed, the additional skid resistance data can be estimated from BPN and MPD measurements as illustrated in the numerical example presented. The laboratory measured data are used as input to calibrate the finite element simulation model, which in turn is used to generate the skid resistance, hydroplaning speed and braking distance

information. The information generated provides a rather comprehensive basis for assessing the suitability of the aggregates and the mix design chosen by checking against the in-service pavement design requirements of skid resistance, hydroplaning risk level, and braking distance control.

Table 4-1 Examples of PSV-based Aggregates Selection Guidelines

Highway Agency	PSV Requirements
Louisiana Department of Transportation (Subedi, 2015; DOTD, 2006)	Friction rating I: PSV > 37 (aggregates for all asphalt mixtures, including wearing courses) Friction rating II: 35 ≤ PSV ≤ 37 (aggregates for all asphalt mixtures, including wearing courses) Friction rating III: 30 ≤ PSV ≤ 34 (aggregates for all asphalt mixtures, except travel lane wearing courses with average daily traffic greater than 7,000) Friction rating IV: 20 ≤ PSV ≤ 29 (aggregates for all asphalt mixtures, travel lane wearing courses)
New Zealand Transport Agency (NZTA, 2010)	PSV ≥ 100 x SR + 0.00663 x CVD + PSF SR = Investigatory level skid resistance value for the site CVD = Commercial vehicles per lane per day PSF = Polishing stress factor equal to a whole number between 3 and 9 assigned according to friction demand of the site
UK Design Manual (Highways England, 2006)	For site category A1 – Motorways where traffic is generally free-flowing on a relatively straight line with investigatory level of SCRIM skid resistance equal to 0.30: PSV ≥ 50 for CVD ≤ 2000 PSV ≥ 55 for 2001 ≤ CVD ≤ 4000 PSV ≥ 60 for 4001 ≤ CVD ≤ 5000 PSV ≥ 65 for CVD > 5000 CVD = Commercial vehicles per lane per day PSV are available for nine other site categories, see (NZTA, 2010)

Table 4-2 Relationships between Laboratory Measured Friction Properties and Field Skid Resistance Measurements for Asphalt Mixtures

(a) One-parameter regression models

Study	Regression Model	Laboratory Polishing Machine Used
Khanawneh (2008)	SN64R = 30.581+37.92(DFT20) R^2=0.333 SN64R = -14.492+139.42(DFT64) R^2=0.70	Specially fabricated polishing machine for project.
Erukulla (2011)	SN64R = -19.43+136(DFT60) R^2=0.95	NCAT polishing machine (Voller et al., 2006).
Subedi (2015)	SN64R = 16.036+96.986(DFT20) R^2=0.69	NCAT polishing machine (Voller et al., 2006).

(b) Two-parameter regression models

Study	Regression Model	Laboratory Polishing Machine Used
Khanawneh (2008)	SN64R = 26.066+2.761(MPD)+40.0(DFT20) R^2=0.59 SN64R = 12.600+3.391(MPD)+70.8(DFT64) R^2=0.75	Specially fabricated polishing machine for project.
Rozaei at al. (2011)	SN50S = 5.135+128.486(IFI-0.045)$e^{-20/Sp}$ IFI = 0.081+0.732(DFT20)$e^{-40/Sp}$ Sp = 14.2+89.7(MPD)	NCAT polishing machine (Voller et al., 2006).
Subedi (2015)	SN64S = 215(DFT20)$e^{-0.54/MPD}$ R^2=0.73	NCAT polishing machine (Voller et al., 2006).

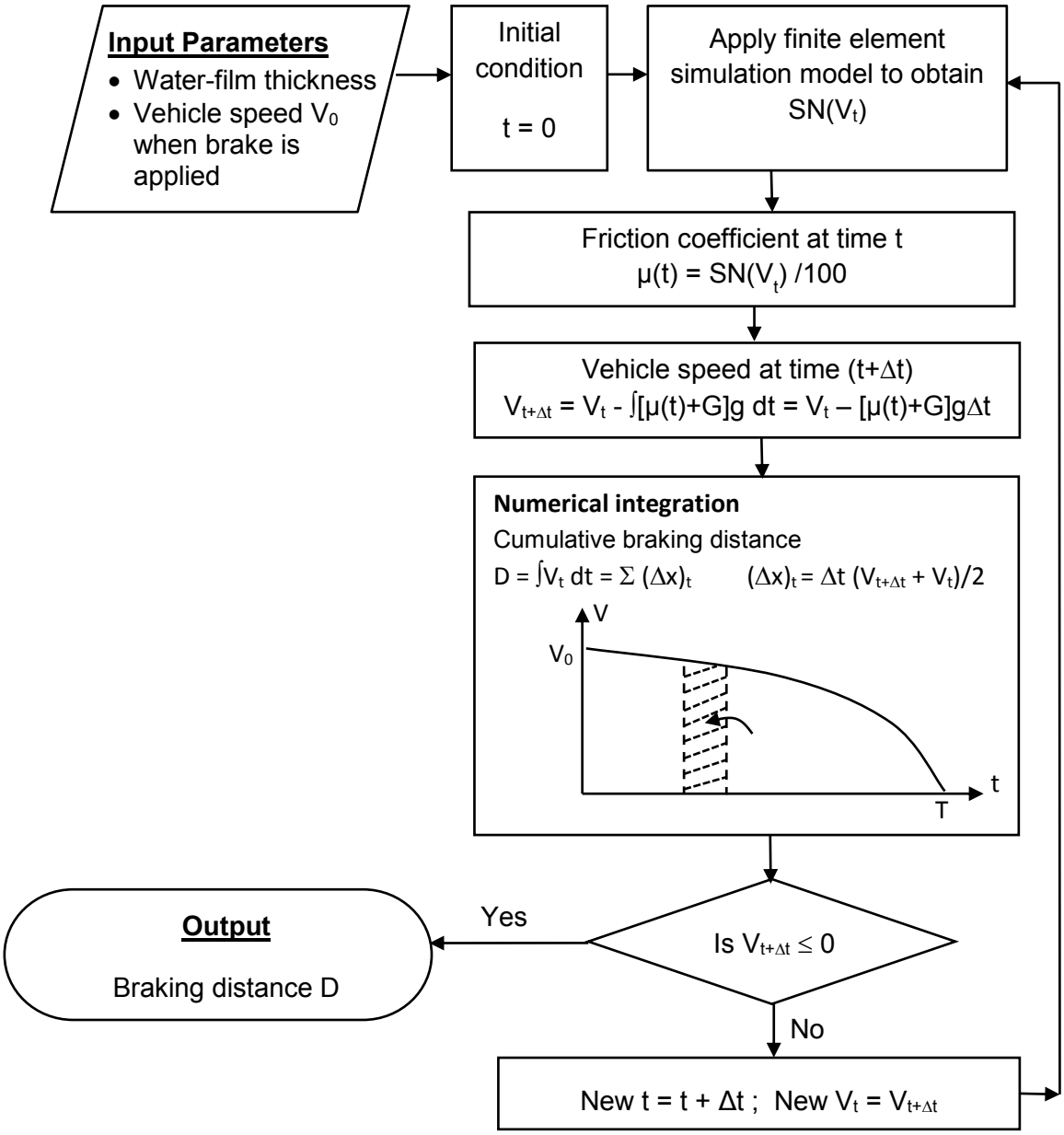

Figure 4-1 Procedure for Calculating Braking Distance

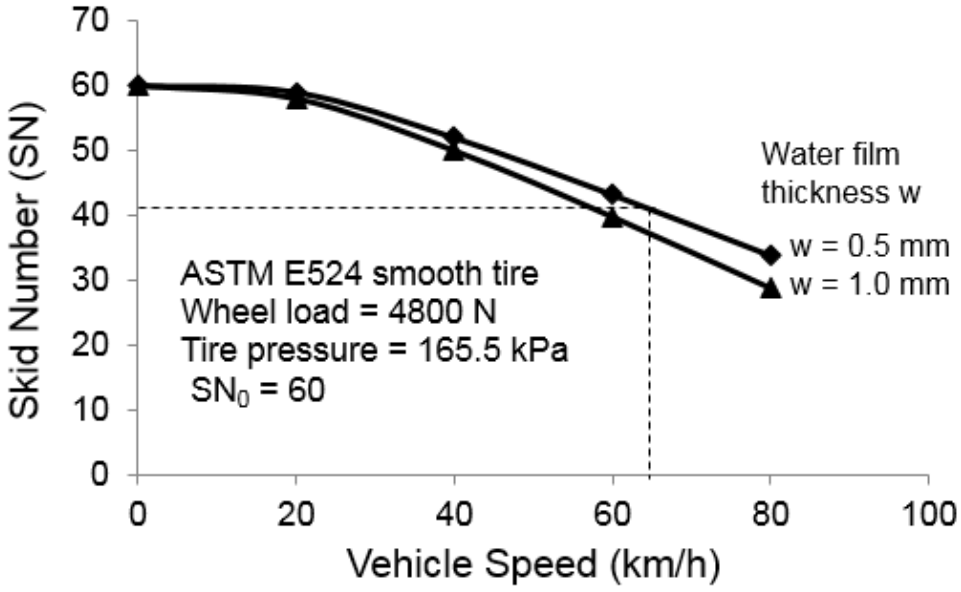

(a) Skid resistance performance curves for Mix Design A

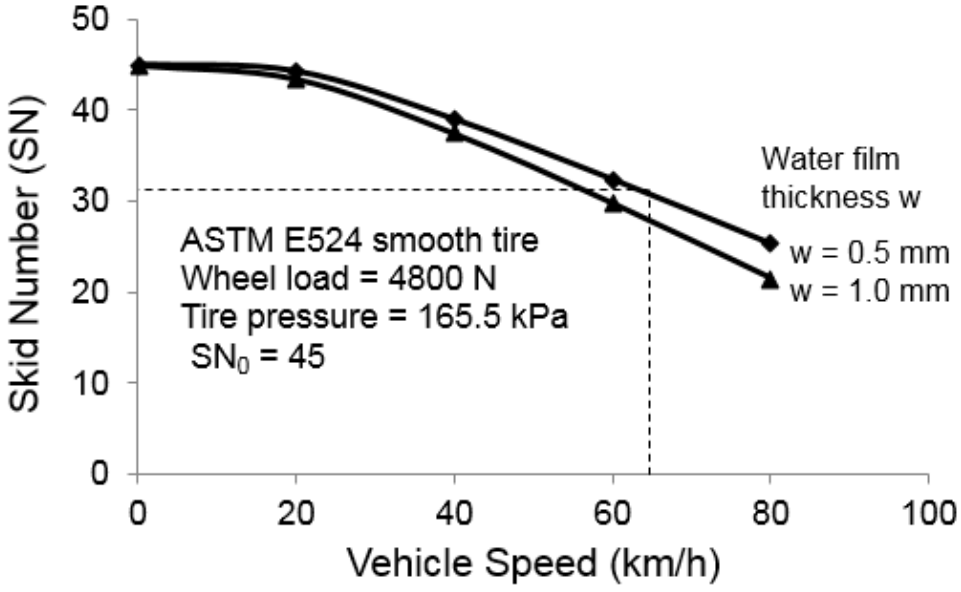

(b) Skid resistance performance curves for Mix Design B

Figure 4-2 Skid Resistance Performance Curves for Mix Design A and B

CHAPTER 5 IMPROVED PROCEDURE FOR DETERMINING RAIN-RELATED WET-WEATHER SPEED LIMITS BASED ON DRIVING SAFETY CONSIDERATIONS

5.1 Introduction

Posted speed limits are legal speed limits imposed by highway agencies to control vehicle speeds for various reasons, such as safety (e.g. school zone and accident-prone road section), security, and traffic noise reduction, etc. For most public roads, a maximum posted speed limit is specified and it is commonly set at the 85th percentile operating speed or at a certain value below this speed (AASHTO, 2011; Fitzpatrick, 2003). The main purpose is to inform drivers of the maximum acceptable and safe speed for normal free flow travel conditions.

Numerous studies (Katz, 2012; Han et al., 2009; Goodwin, 2003; Jonkers et al., 2008) have highlighted the fact that for some road sections under certain operating conditions such as during wet weather, the maximum posted speed limit may exceed the maximum safe speed determined based on either the stopping sight distance of the road section considered, or the minimum skid resistance set by highway agency concerned. Wet weather conditions that can adversely affect highway operations and driving include those caused by rain, fog, snow, ice, wind, and flood, etc. For instance, rain and fog can cause reduce visibility and it may not be safe for drivers to continue driving at or close to the posted speed limit. Rain also wets the pavement and the presence of rainwater on pavement surface reduces tire-pavement friction, which requires drivers to slow down to avoid possible safety hazards such as skidding and hydroplaning (Henry, 2000; Horne et al., 1963).

Various attempts have been made by highway agencies to avoid the undesirable situation of having drivers, who either under-estimate or are unaware of the unfavorable driving conditions brought about by wet weather, driving at speeds above the wet-weather safe speed which is lower than the posted speed limit. A practice that is being adopted by more and more highway agencies in recent years is the variable speed limit (VSL) systems that impose reduced posted speed limits during wet weather so as to improve wet-weather driving safety (Katz, 2012; Han et al., 2009; Jonkers et al., 2008; Al-Kaisy et al., 2012).

This chapter focuses on the pavement-related effect of rainfall on vehicle speed limit. It examines the effect of pavement surface runoff on tire-pavement friction and vehicle braking distance, and the safe driving speed. It is noted that both tire-pavement friction and vehicle braking distance are functions of vehicle speed as well as the water film thickness on the pavement surface. The knowledge of these relationships will be useful to serve as guidelines for highway authorities to establish rain-related wet-weather speed limits. An analytical procedure is proposed in this chapter to determine the maximum safe speeds based on the considerations of skid resistance and vehicle braking distance. The proposed procedure makes use of a finite-element skid resistance simulation software to determine both the available skid resistance values and vehicle braking distances at different vehicle speeds under specified wet-weather conditions for a given road section.

5.2 Current Development of Rain-Related Wet-Weather Speed Limits Systems

A posted maximum speed limit indicates to drivers the speed they should not exceed on the road section concerned. It is usually set based on a statutory speed limit, or it can be set at the 85th percentile operating speed or at

a certain value below this speed. However, drivers are responsible for selecting an appropriate speed not exceeding the post speed, giving consideration to the roadway and environmental conditions, and potential hazards (AASHTO, 2011; Han et al., 2009; Goodwin, 2003; ITE, 2009). This means that the driver has the primary responsibility of adjusting vehicle speed in response to adverse driving conditions such as rain-related wet weather.

Katz et al. (2012) noted that driver behavior varies during adverse weather events based on experience and risk tolerance, and that some drivers may slow down when they encounter wet weather, but others may maintain or even increase their speeds. This results in a significant speed differential which tends to increase the potential for crashes. The idea of leaving the driver to select driving speed in rain-related wet weather may not be ideal for locations where reductions in pavement skid resistance may not be fully realized by most drivers. For example, a study was made by the Florida Department of Transportation on the effect of an automated motorist warning system installed at an exit ramp of the Florida Turnpike/Interstate 595 interchange that had a wet-pavement crash rate three times higher than the national average and nearly four times greater than the statewide average (Goodwin, 2003). When wet pavement was detected by embedded sensors, flashing beacons were activated to alert motorists that speeds should not exceed the posted limit of 35 mi/h (56.3 km/h). It was found that the warning system reduced the 85th percentile speed from 49 to 45 mi/h (78.8 to 72.4 km/h) in light rain conditions, and from 49 to 39 mi/h (78.8 to 62.7 km/h) in heavy rain conditions. There were no reported crashes during a nine-week evaluation period.

There are similar positive experiences with the use of rain-related wet-weather warning systems or variable speed limit (VSL) systems in reducing

crash risk, as reported in Ref (Katz et al., 2012), (Han et al., 2009), (Goodwin, 2003) and (Al-Kaisy et al., 2012). In general, for the rain-related wet-weather VSL systems in use today, the posted speed limits are declared in the following two formats:

(a) Pre-determined fixed speed limit for the duration of wet-weather– A fixed speed limit lower than the dry-weather speed limit is posted for the duration of rain-affected period, regardless of the rainfall intensity and the actual condition of the wet pavement.

(b) Variable speed limits for the duration of wet-weather condition – The posted speed limit during wet weather is changed according to the condition of the wet pavement. Most commonly, the state of pavement condition is represented by the thickness of water film on the pavement surface.

Table 5-1 shows selected examples of Format (a) and (b) rain-related wet-weather VSL systems adopted in practice. Format (a) is easier to implement but has the limitation that it does not differentiate the different safe speed limits under different rainfall conditions and the state of the wet pavement. Format (b) is an improvement of Format (a) but requires the installation of pavement moisture or rainfall intensity sensors, and an associated speed limit activation system. Format (b) also requires some knowledge of the relationship between wet pavement conditions and the skid resistance available. As shown in Table 5-1, the current systems that adopt Format (b) typically assign rain-related wet weather speed limits based on empirical relationships, actual site experience and engineering judgement, or case studies of similar VSL systems elsewhere (Katz et al., 2012; Han et al., 2009; Goodwin, 2003; Jonkers et al., 2008; Al-Kaisy et al., 2012).

Katz et al. (2012) stressed the importance for a VSL system to display a speed limit that is representative of the less than ideal weather conditions, and suggested that the speed limit displayed should be the maximum safe speed limit based on real-time conditions, using information from traffic, pavement, and weather sensors. They went on to propose, for informational purpose, a weather responsive algorithm for determining rain-related wet-weather speed limits based on sight distance (or braking distance) consideration. Figure 5-1 summarizes the main steps of the algorithm proposed by Katz et al. (2012).

The algorithm in Figure 5-1 assumes that the coefficient of cohesion μ for the current weather condition can be measured in real-time. Unfortunately, this is practically not achievable with the pavement friction measuring devices available today. It is impractical to station a friction tester on-site for real time measurement of μ as the water film thickness on the pavement surface varies. Another aspect where improvement can be made is the computation of speed V using the formula below:

$$V = \frac{-3.67 + \sqrt{13.47 + \frac{0.12S}{\mu + G}}}{\frac{0.06}{\mu + G}} \tag{5-1}$$

where S is sight distance in ft, μ is coefficient of pavement cohesion, and G is roadway grade expressed as a positive decimal value for upslope and negative for downslope. Eq. (5-1) actually assumes that μ is independent of V. In reality, μ varies with vehicle speed of travel and the thickness of water film. μ is typically measured at a standard speed which would not be the same as the unknown variable V. In addition, during the braking process, vehicle speed will decrease from V to zero, hence the value of μ would also vary (increase as V

decreases). Hence, a modification to Eq. (5-1) is necessary to account for the interdependency of V and μ. Although one may suggest that μ in Eq. (5-1) is the mean coefficient of cohesion. This would also not work as it introduces approximation or error in estimating the average μ and would complicate the interpretation of friction measurements.

The above review suggests that the following possible improvements can be made to the current methods of determining rain-related wet-weather speed limits:

- Improved procedure of predicting wet-weather pavement friction performance from measured pavement friction properties;
- Computation of braking distance taking into consideration the nonlinear dependency of pavement friction coefficient on vehicle speed.

5.3 Consideration and Concept of Proposed Procedure

5.3.1 Main Consideration for Proposed Approach

The proposed approach applies two pavement-related safety considerations in the calculation of safe speed limits on wet pavements. Besides the sight distance and stopping distance consideration commonly adopted in past studies (Katz et al., 2012; Han et al., 2009; Goodwin, 2003; Jonkers et al., 2008; Al-Kaisy et al., 2012), this chapter also applies the minimum safe skid resistance in the computation of wet-weather speed limits. These two considerations address two different safety aspects of vehicle operations on highways.

Braking distance consideration is a must to ensure that a vehicle will be able to stop within a safe distance when required (e.g. in front of a stop sign or railroad crossing) or in times of emergence (e.g. unexpected obstacles or sudden

lane intrusions by other vehicles or objects). Minimum safe skid resistance is usually specified by highway agencies to guard against skidding accidents on wet pavements. When skid resistance is too low, skidding can occur during cornering or overtaking maneuver of vehicles, or during braking (Goodwin, 2003; Henry, 2000; Hall et al., 2009). While the sight distance and braking distance is a key consideration in situations where sight distances are restricted (such as locations of horizontal and/or vertical curves), safe minimum skid resistance may be the governing factor in locations where sight distance is not an issue. Therefore, a rain-related wet-weather speed limit must meet the requirements for both sight distance and minimum skid resistance.

5.3.2 Determination of Stopping Distance in Proposed Approach

For a given site, the sight distance S can be determined from a field study and the maximum speed limit V can be set such that a vehicle traveling at speed V will have a stopping distance D less than or equal to S. D is usually calculated in practice as the sum of reaction distance D_R and braking distance D_B (AASHTO, 2011). D_R is the distance the vehicle travels during the driver's brake reaction time, and D_B is the distance that the braking action takes to bring the vehicle to a complete stop. Following the recommendation by AASHTO (2011), taking the reaction time as 2.5 s, the following equation is obtained for the stopping distance D:

$$D = D_R + D_B = 0.694V + 0.039\left[\frac{V^2}{d + Gg}\right] \tag{5-2}$$

where D, D_R and D_B are stopping distance, reaction distance and braking distance respectively in m, V is vehicle speed in km/h, d is vehicle deceleration in m/s, G is roadway grade expressed as a positive decimal value for upslope and negative for downslope, and g is gravitational acceleration equal to 9.81

m/s^2. AASHTO (2011) applies a value of 3.4 m/s^2 for deceleration d in roadway geometric design. For the purpose of variable speed limit determination, the actual deceleration that can be provided by the wet pavement, i.e. the tire-pavement friction coefficient μ, must be determined, and the following revised expression should be used:

$$D = D_R + D_B = 0.694V + 0.039\left[\frac{V^2}{(\mu + G)g}\right] \tag{5-3}$$

The term μg represents the actual deceleration force available to the vehicle from the wet pavement. It should be noted that Eq. (5-3) is valid only for the case of constant tire-pavement friction coefficient μ when the vehicle speed decreases from the initial speed V to zero when the vehicle comes to a complete stop. Unfortunately, this is not the case on a wet pavement. The tire-pavement friction coefficient μ on a wet pavement varies with vehicle speed. Hence, instead of Eq. (5-3) or Eq. (5-2), the stopping distance D must be calculated from the following expressions taking into account the changes of vehicle speed V and tire-pavement friction coefficient μ with time during vehicle braking:

$$D = D_R + D_B = 0.694V_0 + \int_0^T V(t)dt \tag{5-4}$$

$$V(t) = V_0 - \int_0^T \left[\mu(t) + G\right]gd(t) \tag{5-5}$$

where V_0 is the initial vehicle speed at time zero when the brake is applied, T is the total duration of braking time taken by the vehicle to come to a complete stop, V(t) is the vehicle speed at any time t, $0 \le t \le T$, μ(t) is the tire-pavement friction coefficient at time t when the vehicle speed is v(t). Therefore, the calculation of stopping distance D requires the establishment of the relationship

between μ and vehicle speed V. This relationship is a key aspect of the proposed procedure and will be described in a subsequent section of this chapter.

5.3.3 Minimum Skid Resistance Threshold and Available Skid Resistance

Past studies of road accidents have provided statistically significant evidence of the general trend that the number of wet crashes increases as pavement friction decreases (Goodwin, 2003; Henry, 2000; Hall et al., 2009). To improve wet-weather driving safety, more and more highway agencies are establishing minimum acceptable skid resistance level by specifying either investigatory or intervention levels, or both, for skid resistance. Table 3-3 shows examples of such practices by selected highway agencies. When the available skid resistance of a road section reaches or falls below the assigned investigatory level, the need for warning or remedial action must be investigated. When the intervention level is violated, an appropriate remedial treatment must be activated (Hall et al., 2009). It is reasonable to implement wet-weather variable speed limit when the investigatory level is reached, although some may choose to activate it only when the intervention level is reached.

It should be noted that, as apparent from Table 3-2, the minimum skid resistance threshold is typically reported as a measurement made using a standard test procedure such as the ASTM E274 locked wheel method (2011). The standard test conditions are fixed and would not be the same as the actual operating conditions. Hence, a procedure must be established to enable a comparison to be made between the actual available skid resistance and the skid resistance threshold. Figure 5-2 shows the procedure proposed in this chapter.

The proposed procedure first establishes the “skid resistance threshold curve” as shown in Figure 5-2. This curve represents the skid resistance state of the pavement when its skid resistance has deteriorated to the minimum

threshold level (i.e. the investigatory or the intervention level as appropriate). At this state, the pavement's zero-speed skid resistance has deteriorated to $(SN_0)_T$ and its skid resistance SN_{64} measured at the standard test speed of 64 km/h (40 mi/h) is $(SN_{64})_T$, which is the skid resistance threshold level. This "skid resistance threshold curve" gives the skid resistance of the pavement section at the threshold state tested different speeds by the standard test device at the standard water film thickness of 0.5 mm.

Figure 5-2 also shows another skid resistance curve A which is the actual available skid resistance curve of the in-service pavement for the actual weather condition with a water film thickness of $w > 0.5$ mm. The in-service pavement, which has not deteriorated to the threshold state, has a zero-speed skid resistance $(SN_0)_A > (SN_0)_T$, and a $(SN_{64})_A > (SN_{64})_T$. Because of its higher water film thickness, the skid resistance curve A suffers a higher deterioration rate, and intersects the "skid resistance threshold curve" at 70 km/h. This means that, based on the minimum skid resistance consideration alone, the wet-weather speed limit should be set at 70 km/h.

The main challenge in implementing a wet-weather variable speed limit system based on the minimum skid resistance threshold is to determine the available skid resistance for the actual site and operating conditions. The central issue of this challenge is the establishment of the skid resistance curves, i.e. the relationship between tire-pavement skid resistance and vehicle speed for different wet weather conditions. This relationship is also a key input requirement for the calculation of stopping distance, as mentioned in the preceding section.

5.3.4 Establishment of Relationship between Skid Resistance and Vehicle Speed

To determine the tire-pavement skid resistance available on a wet pavement, the relationship between skid resistance and vehicle speed for the road section must first be established. This is achieved in this chapter by employing a finite-element skid resistance simulation computer program developed by Ong and Fwa (2007, 2008). The validity of this simulation program has been tested and confirmed using measured skid resistance values from experimental and field measured data of studies by different researchers. The theoretical formulation of the simulation model and the detailed finite element modeling are found in the earlier works of the Ong and Fwa (2007, 2008). Figure 5-3 shows the main steps involved in the calibration of the skid resistance simulation model and derivation of skid resistance curve. This simulation program can be calibrated to generate the skid resistance curve of a pavement with the following input data:

- Skid numbers of the pavement at any two different speeds, say one at 64 km/h and another at speed v
- Water film thickness
- Tire type (either ASTM E501 rib tire (2008a) or E524 smooth tire (2008b))
- Tire width and diameter
- Tire structural stiffness
- Wheel load and tire inflation pressure of ASTM E274 test procedure
- Water viscosity

As shown in Figure 5-3, the calibration of the skid resistance simulation model requires the skid numbers of the pavement in question at two different speeds to be measured. That is, besides the usual SN_{40} from routine skid resistance survey, the skid number at another speed is needed. With these two skid numbers, the skid resistance simulation model can be calibrated to determine the zero-speed skid number SN_0 and the skid resistance-vehicle speed curve of the in-service pavement section. The detailed calibration procedure, also known as back-calculation procedure, is found in reference by Fwa and Ong (2008). Once calibrated, the simulation model can be applied to derive the skid resistance curve of the pavement for any water film thickness.

5.4 Procedure of Proposed Method of Speed Limit Determination

The proposed variable speed limit determination procedure consists of the following four main components: (i) Determination of input parameters, (ii) Calibration of the skid resistance simulation model, (iii) Determination of speed limit based on stopping distance, and (iv) Determination of speed limit based on minimum skid resistance. The final speed limit selected is the lower of the two computed speed limits of (iii) and (iv). Figure 5-4 presents a flow chart that highlights the steps involved. The calibration procedure of the skid resistance model, i.e. component (ii), has been presented in the preceding section (see Figure 5-3). This section will describe components (i), (iii) and (iv) of the process.

5.4.1 Determination of Input Data

The following four groups of input data are required for the determination of rain-related wet-weather speed limits for a given pavement section:

- Input data for calibration of skid resistance simulation model for the in-service pavement;
- Input data for calibration of skid resistance simulation model for the pavement at the minimum skid resistance threshold state;
- Input data for determination of speed limit based on stopping distance;
- Input data for determination of speed limit based on minimum skid resistance; and
- Input data for determination of water film thickness on pavement surface.

The detailed data requirements for the four groups above are summarized in Table 5-2.

Data for Calibration of Skid Resistance Simulation Model

As explained in an earlier section, the calibration of skid resistance simulation model for the in-service pavement requires two inputs of skid numbers measured at two different speeds. These measurements can be made as part of the routine or specially scheduled skid resistance surveys conducted for the pavement section in question. As illustrated in Figure 5-3, the calibrated model can generate skid resistance curves for different water film thickness on the in-service pavement. A database of skid resistance curves for different water film thickness can thus be prepared for speedy determination of variable speed limits at different water film thickness.

The skid resistance curve for the pavement at the minimum skid resistance threshold state is required for the determination of speed limit based on minimum skid resistance consideration. This requires a separate calibration of the skid resistance simulation model because the skid resistance characteristics (i.e. microtexture and macrotexture) of the pavement at the threshold state are different from those of the in-service pavement. The required

skid resistance characteristics (i.e. skid numbers at two different speeds) can be estimated from one of the following two methods: (i) past records or measurements of pavement wearing courses of the same mix design; or (ii) laboratory skid resistance measurements of accelerated polished specimens simulating the threshold state of the pavement surface mixture. Such laboratory polishing treatment and skid resistance measurements using Dynamic Friction Tester (ASTM, 2009a) have been used in a number of studies (Hall et al., 2009; Liang, 2013; Wilson et al., 2005; Rozaei et al., 2011).

Data for Speed Limit Based on Stopping Distance

In the determination of speed limit based on stopping distance, besides the in-service pavement skid resistance curves for different water film thickness to be generated from the calibrated skid resistance model, the following inputs are also required: the sight distance, the 85th percentile operating speed, and the design speed of the pavement section.

Data for Speed Limit Based on Minimum Skid Resistance

The speed limit based on the minimum required skid resistance is determined from the skid resistance curves of the in-service pavement, and that of the pavement at the threshold skid state. The minimum threshold level of skid resistance for the pavement section is a required input.

Data for Determination of Water Film Thickness

The speed limit to be posted during a rainfall is dependent on the water film thickness present on the pavement surface. The ability to generate real-time information of water film thickness is key to fulfilling the very objective of a variable speed limit system. On-site water-depth sensors can be installed to provide real-time measurements of water film thickness (Goodwin, 2003; Pilli-

Sihvola et al., 1997). Alternatively, instead of making direct measurements, water film thickness can be estimated from measured rainfall intensity by means of an appropriate computer program such as PAVDRN (Anderson et al., 1998). Input data requirements for PAVDRN include rainfall intensity, pavement surface material Manning coefficient, roadway grade and cross slope.

5.4.2 Determination of Speed Limits

As indicated in Figure 5-4, the posted speed limit for the pavement section at a given water film thickness is derived by first calculating two speed limits, one based on stopping distance and the other based on minimum skid resistance.

The numerical integration algorithm for stopping distance calculation, as outlined in Figure 5-4, is based on the relationships of Eq. (5-4) and (5-5). For each water film thickness, the algorithm searches for the vehicle speed limit V_0 that can satisfy the sight distance requirement. V_0 is next compared with the 85th percentile operating speed as well as the design speed, and the smallest of the three values is designated as the speed limit V_B for the given water film thickness based on stopping distance consideration.

For each water film thickness, the speed limit V_A based on minimum skid resistance is obtained as the speed given by the intersection of the two skid resistance curves shown in Figure 5-4 (see also Figure 5-2). The lower of the two speed limits V_A and V_B calculated is taken as the posted speed limit for the water film thickness. This process is repeated for other water film thickness to obtain the speed limits for the full range of water film thickness as required.

5.5 Numerical Illustrative Example

Consider a pavement section with an 85^{th} percentile operating speed of 100 km/h and a design speed of 120 km/h. The roadway grade is 0% and the

sight distance is 145 m. Figure 5-5 shows the pre-determined ready plots of two sets of skid resistance curves of the pavement section: a family of skid resistance curves for the current in-service pavement at five water film thickness (1, 3, 6, 9 and 15 mm), and the skid resistance curve of the pavement section at the threshold state set by the highway agency concerned. The threshold state is set at smooth tire $SN_{64} = 30$, and the zero-speed SN_0 is 45. The in-service pavement section has not deteriorated to the threshold state, and its SN_0 is 60. The intersections of the skid resistance curves give the minimum skid resistance based speed limits V_A at different water film thickness w, given as follows:

100 km/h for w = 1 mm (speed limit governed by 85th percentile operating speed),

76 km/h for w = 3 mm,

60 km/h for w = 6 mm,

54 km/h for w = 9 mm, and

51 km/h for w = 15 mm.

Using the family of skid resistance curves, the braking distances and stopping distance and hence the speed limit V_B can be calculated iteratively for each water film thickness as indicated in the flow diagram of Figure 5-4. The following stopping distance based speed limits V_B are obtained:

80.6 km/h for w = 1 mm,

73.4 km/h for w = 3 mm,

72.1 km/h for w = 6 mm,

71.3 km/h for w = 9 mm, and

70.4 km/h for w = 15 mm.

Taking the smaller value of V_A and V_B as the posted speed limit for each water film thickness w, the selected scheme of speed limits (rounded down to whole numbers) are:

80 km/h for w = 1 mm,

73 km/h for w = 3 mm,

60 km/h for w = 6 mm,

54 km/h for w = 9 mm, and

51 km/h for w = 15 mm.

It is noted that in this example, the consideration of stopping distance and sight distance governs the speed limit at lower water film thickness, while the consideration of minimum skid resistance governs at higher water film thickness.

5.6 Remarks on Application of Proposed Procedure

Water film thickness or rainfall intensity is the only real-time data required for the application of the proposed approach for variable speed limits determination. All other required input data are pre-computed and stored in a database for ready computation of speed limits when the water film thickness data is available. Both the skid resistance curve for the threshold state of the pavement section for standard water film thickness of 0.5 mm, and the skid resistance curves for the in-service state of the pavement section for different water film thickness are pre-determined and stored for ready application.

For applications in practice, instead of displaying a speed limit that continuously changes with water film thickness, it is more practical to change speed limit in steps according to pre-set ranges of water film thickness w. For instance, for the illustrative numerical example presented, the following steps of speed limit can be set:

Speed limit = 80 km/h when $w \leq 1$ mm,

Speed limit = 73 km/h when $1 < w \leq 3$ mm,

Speed limit = 60 km/h when $3 < w \leq 6$ mm,

Speed limit = 54 km/h when $6 < w \leq 9$ mm, and

Speed limit = 51 km/h when $9 < w \leq 15$ mm.

5.7 Summary

This chapter has presented a proposed procedure for determination of rain-related variable speed limits as a function of water film thickness based on two criteria, namely a stopping distance criterion and a minimum skid resistance criterion. The proposed speed limit determination procedure based on stopping distance is an improvement to existing methods by incorporating the skid resistance-speed relationship (i.e. skid resistance curve) into the computation process. The proposed speed limit determination procedure based on a minimum skid resistance threshold level is consistent with the current practice of investigatory and intervention skid resistance levels being adopted by more and more highway agencies.

The proposed procedure makes use of analysis techniques, computational algorithms, and test devices that are currently available. Compared to the existing procedures for determining rain-related wet-weather variable speed limit system, it offers a more complete and conceptually sound basis for the formulation of the speed limit scheme.

Table 5-1 Examples of Rain-Related Wet-Weather Variable Speed Limit Systems

<table>
<tr><th>Format of Variable Speed Limit System</th><th>Examples</th></tr>
<tr><td>Format (A): Single wet-weather speed limit</td><td>(a) Along a 2-mile (3.2-km) rural roadway in South Carolina (Katz et al., 2012), non-ideal pavement condition is detected based on precipitation data from a weather station installed nearby, and activates a speed limit reduction from 55 to 45 mi/h (88 to 72 km/h)

(b) In a project to reduce wet-weather accident risks in Finland, the speed limit of a highway section was reduced from 120 km/h to 100 km/h based on aquaplaning concern, and another section from 100 km/h to 80 km/h due to slippery road conditions consideration (Pilli-Sihvola et al., 1997).

(c) At an interchange ramp of Interstate 595 in Florida (Goodwin, 2003), rain is detected by in-pavement moisture sensor and verified by precipitation sensor nearby, with flashing beacons activated on speed limit signs to alert drivers of the speed limit of 35 mi/h (56 km/h).</td></tr>
<tr><td>Format (B): Multiple wet-weather speed limits</td><td>(a) A variable speed limit system in the Netherlands imposes speed limits based on rainfall intensity (Jonkers et al., 2008):

<table><tr><th>Water on Road Surface</th><th>Rain Intensity</th><th>Speed Limit</th></tr><tr><td>0.0 mm</td><td>0.0 mm/h</td><td>75 km/h</td></tr><tr><td>0.2 to 0.6 mm</td><td>0.0 to 2.5 mm/h</td><td>75 km/h (No change)</td></tr><tr><td>0.6 to 2.0 mm</td><td>2.5 to 6.0 mm/h</td><td>60 km/h</td></tr><tr><td>0.6 to 2.0 mm</td><td>6.0 to 30.0 mm/h</td><td>50 km/h</td></tr></table>
(b) Speed management control strategies implemented by Washington State Department of Transportation (Katz et al., 2012):
• Light to moderate rain, visibility distance greater than 0.5 mi. (0.80 km) -- No change in speed limit: 65 mi/h (105 km/h).
• Heavy rain and fog, visibility distance less than 0.2 mi (0.32 km) – Speed limit reduced to 55 km/h (88 km/h). Traction tires advised.
• Heavy rain or blowing snow, visibility distance less than 0.1 mi (0.16 km), with shallow standing water or compacted snow on pavement surface – speed limit reduced to 45 mi/h (72 km/h). Traction tires required.
• Heavy rain or blowing snow or freezing snow, visibility distance less than 0.1 mi (0.16 km), with deep standing water or deep snow/slush on pavement surface – speed limit reduced to 35 mi/h (56 km/h). Tire chains required.</td></tr>
</table>

Table 5- 2 Input Parameters for Proposed Procedure of Variable Speed Limit Determination

Input Category	Input Parameters
Data for calibration of skid resistance simulation model for in-service pavement	• ASTM standard skid resistance test E274 (2011) test parameters: wheel load (4,800 N), tire pressure (165.5 kPa), water film thickness (0.5 mm), rib or smooth tire, tire width and diameter, tire structural stiffness. • Two SN values of pavement section measured at different speeds: SN64 at 64 km/h, and SN_v at speed v.
Data for calibration of skid resistance simulation model for pavement at threshold state	• Minimum skid resistance threshold level for the pavement section. • Laboratory polishing test of pavement wearing course asphalt mixture to estimate field threshold state skid numbers at two different speeds. • ASTM standard skid resistance test E274 (2011) test parameters: wheel load (4,800 N), tire pressure (165.5 kPa), water film thickness (0.5 mm), rib or smooth tire, tire width and diameter, tire structural stiffness.
Data for speed limit determination based on stopping distance for in-service pavement	• Sight distance of in-service pavement section. • 85^{th} percentile operating speed and design speed of in-service pavement. • Skid resistance curves at different water film thickness generated from calibrated skid resistance model for in-service pavement section. • Real-time water film thickness or rainfall intensity. • Roadway grade and cross slope, pavement surface flow Manning coefficient.
Data for speed limit determination based on minimum skid resistance for in-service pavement	• Minimum skid resistance threshold value for in-service pavement section. • Skid resistance curves at different water film thickness generated from calibrated skid resistance model for in-service pavement section. • Skid resistance curve at 0.5 mm water film thickness generated from calibrated skid resistance model for pavement section at threshold skid resistance state. • Real-time water film thickness or rainfall intensity. • Roadway grade and cross slope, pavement surface flow Manning coefficient.

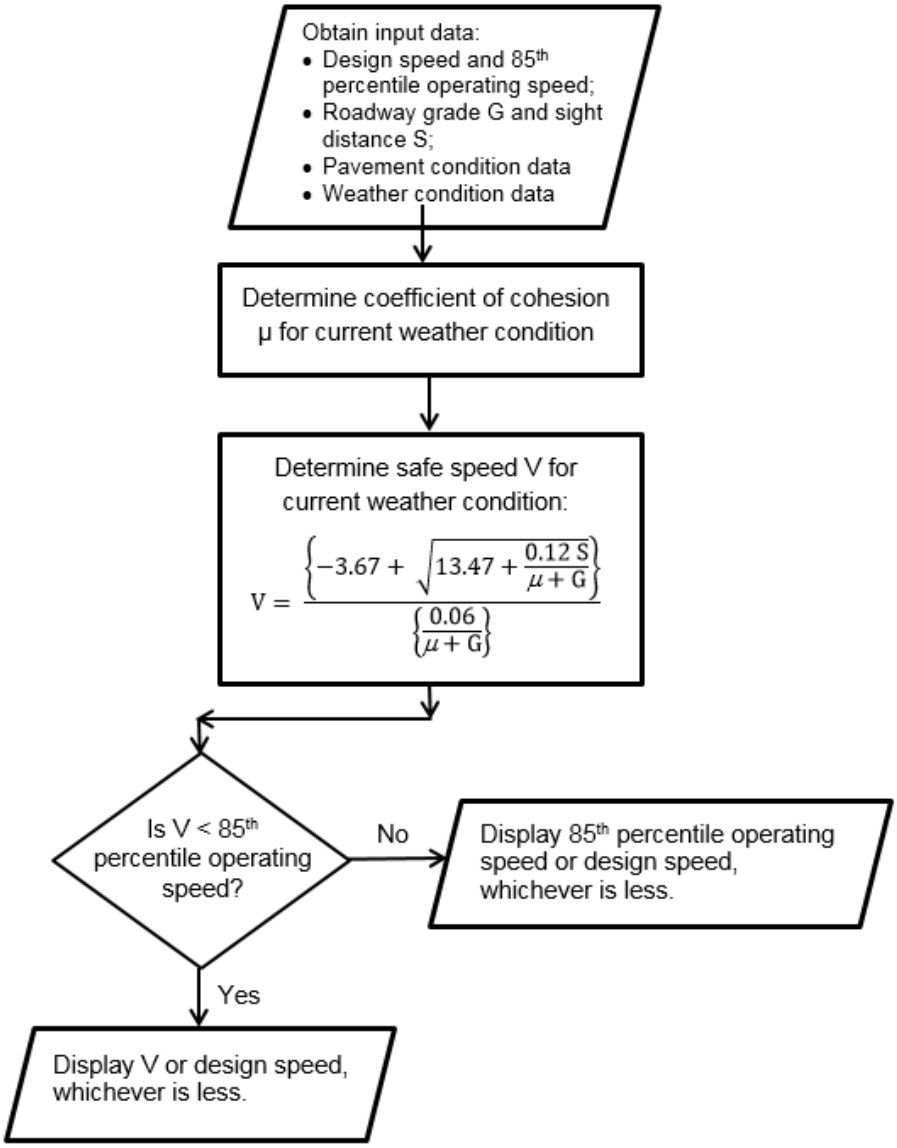

Figure 5-1 Summary of Weather Responsive Algorithm for Determining Rain-Related Wet-Weather Speed Limits Proposed by Katz et al. (2012)

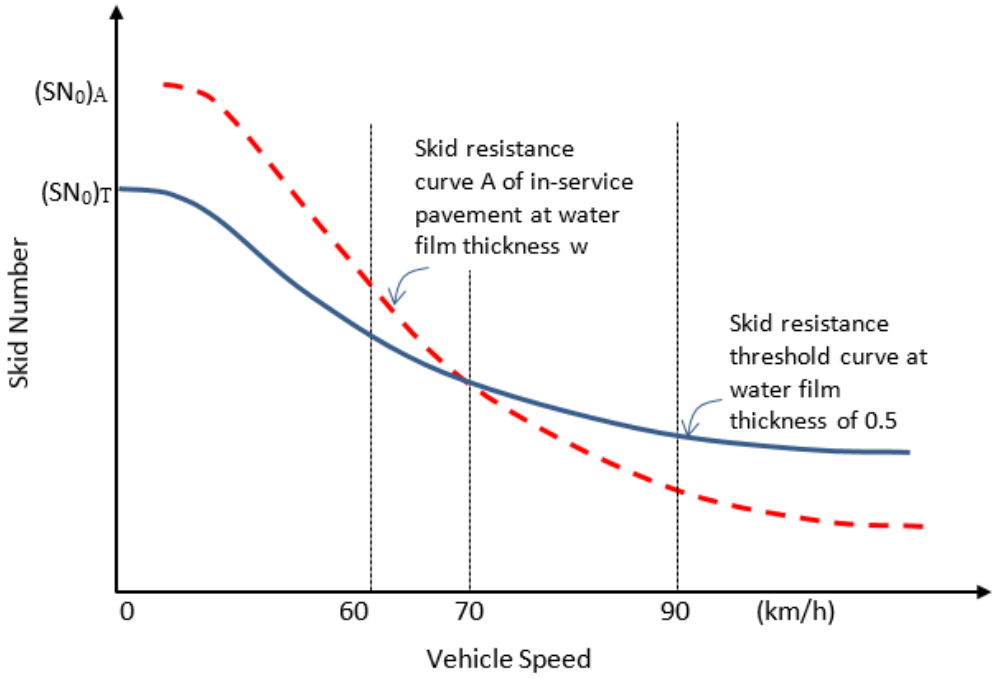

Figure 5-2 Schematic Diagram Illustrating the Concept of Minimum Skid Resistance Threshold Curve and In-Service Pavement Skid Resistance Curve

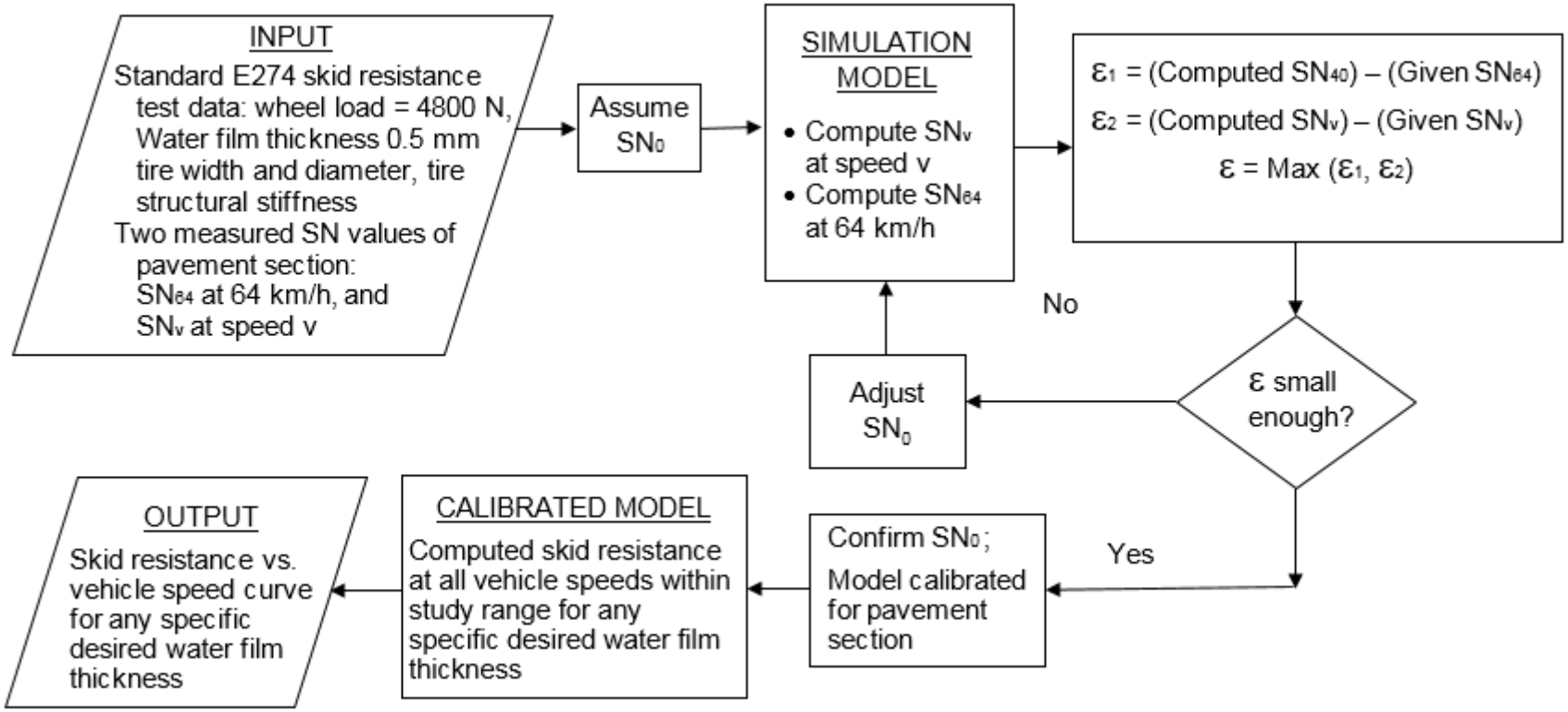

Figure 5-3 Flow Diagram for Calibrating Skid Resistance Simulation Model and Deriving Skid Resistance Curve

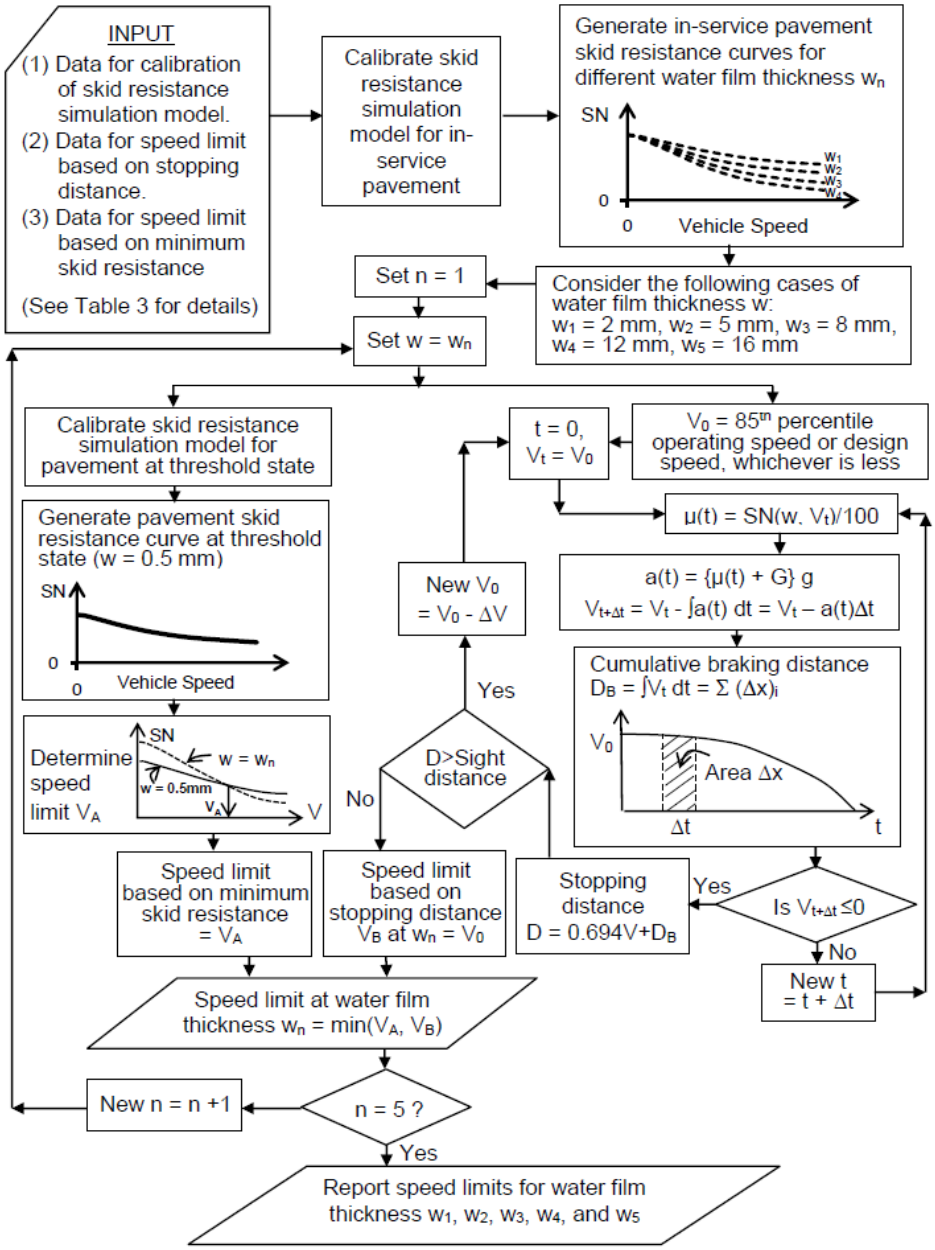

Figure 5-4 Flow Chart for Procedure of Proposed Variable Speed Limits Determination

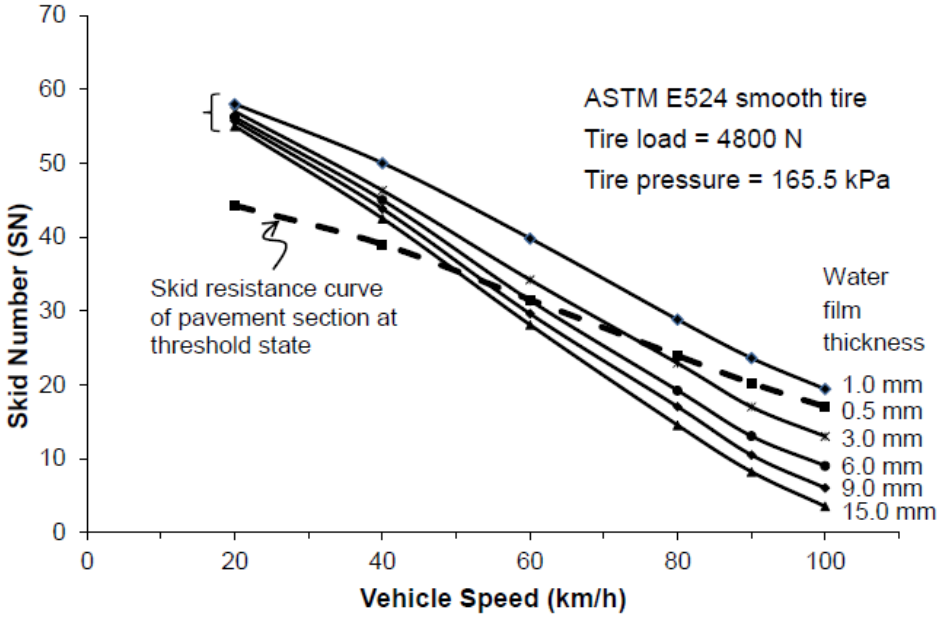

Figure 5-5 Determination of Speed Limits Based on Minimum Skid Resistance

CHAPTER 6 FUNCTIONAL APPROACH FOR DETERMINING TERMINAL SERVICE STATE OF POROUS PAVEMENT

6.1 Introduction

Traditionally, a porous pavement is constructed with a porous surface layer overlying a dense-graded asphalt layer or a Portland cement slab. The porous layer may become partially or totally clogged and loses much of its beneficial properties to fulfil the intended functions of a porous pavement. At this stage, either a maintenance treatment should be activated to de-clog the pavement, or a rehabilitation be performed to replace the affected porous materials with a new layer. A practically relevant and important question to ask is how this threshold stage for maintenance or rehabilitation can be determined in practice.

The current pavement condition survey practice follows basically the procedure that focuses on distresses related to conventional non-porous pavements. While the data collected may address the normal pavement distresses such as raveling, potholes and cracks, they do not provide pavement engineers with the necessary information to evaluate and monitor some important service performance of porous pavements, such as the loss of functional properties caused by clogging. To overcome this limitation, this chapter presents a rational engineering procedure based on the consideration of wet-weather driving safety requirement to determine the terminal service state of a porous pavement affected by clogging. The procedure analyses the wet-weather skid resistance of a clogged porous pavement under the design critical rainfall condition of the pavement section, and identifies the degree of clogging that would produce an unacceptably low skid resistance for safe traffic operations.

The concept of a theoretically sound analytical procedure for calculating wet-weathering skid resistance of porous pavement is presented in this chapter. In addition, since it is not possible or practical to measure the in-situ degree of clogging on site, a permeability measurement is proposed in this study for practical implementation of the proposed procedure.

6.2 Setting of Threshold State for Maintenance of Porous Pavement

Setting of the threshold state for maintenance of a pavement is an important requirement of a pavement management system. Knowing the maintenance threshold state, together with regular pavement condition evaluation and monitoring, timely maintenance can be planned and scheduled ahead of time. This is one of the main intended functions of pavement management systems that help to maintain a pavement at a sufficiently high level of service, and avoid premature development of severe distresses or failure, thus extending the useful service life span of the pavement (AASHTO 2012, FHWA, 2010b).

The distresses occurring in porous pavements range from the two most common porous pavement distresses, clogging and raveling, to other distresses commonly found in normal dense-graded hot-mix asphalt pavements such as potholes, rutting, and cracking, etc. While raveling and other distresses similar to those of normal hot-mix asphalt pavements can be detected by the conventional routine pavement condition surveys, this is not the case for clogging in porous pavements. In other words, although the current practice of pavement condition survey can address the maintenance needs for normal distresses in porous pavements, it does not furnish clogging related data for maintenance planning of porous pavements.

Besides the lack of suitable condition survey technique to detect clogging in porous pavements, there is also no sound engineering basis or guidelines available today to guide highway agencies to determine the state of clogged condition at which a major maintenance or rehabilitation must be carried out. This is a serious limitation because clogging can be said to be the single most critical distress form in a porous pavement. Clogging reduces the porosity and drainage capacity of a porous pavement. This in turn adversely affects the capability of the porous pavement to maintain good skid resistance for wet-weather driving, and its tire-pavement noise reduction effect in dry weather.

The importance of clogging in porous pavement and the need to set a threshold state for its maintenance are well recognized by pavement engineers and highway agencies. Several recommendations have been made by researchers and institutions. Sandberg and Ejsmont (2002) and Liu and Cao (2009) recommended that 15% void content be taken as the lower limiting state for a porous pavement. Izevbekhai and Maloney (2011) indicated that the porosity of porous pavements should be kept at around 18-22%. Some highway agencies have specified that the surface permeability of porous pavement should be at least 8 inches per hour (203 mm/h) (DCCD, 2012).

Unfortunately, none of the recommended conditions in the preceding paragraph could be easily measured in-situ and implemented in practice. As a result, most highway agencies rely on visual inspection for signs of clogging, such as ponding of water after rainfall or flooding during rainfall. This is unsatisfactory because when such signs of clogging are visible, the porous pavement would have already been clogged and lost most of its drainage capacity and beneficial functions of a porous pavement. Ideally, it would be

desirable to develop the capability to set a threshold state for maintenance of porous pavements, as well as to track and monitor the development of clogging and the associated deterioration of permeability of the porous material.

6.3 Methodology of Proposed Procedure

6.3.1 Terminal Service State Based on Skid Resistance Intervention Level

The proposed procedure presented in this chapter aims to develop a rational engineering procedure to determine the terminal service state of a porous pavement affected by clogging, as well as a method for measuring in the field the in-situ permeability of the clogged porous pavement. Since an important key function of porous pavements is to improve wet-weather driving safety, it is logical and practical from safety point of consideration to set the terminal service state of a clogged porous pavement based on skid resistance requirement for wet-weather driving safety. Once the terminal service state has been determined, the threshold state for maintenance can be set to give sufficient time allowance for maintenance planning and safe wet-weather driving (see details in 3.3.2).

The skid resistance based terminal service state caused by clogging of a porous pavement is defined in this chapter to be the state at which the skid resistance of the clogged porous pavement is equal to the skid resistance intervention level. According to the recommendations of the Federal Highway Administration (FHWA, 2010a) and the American Association of State Highway and Transportation Officials (AASHTO, 2008b), for pavement sections with friction values at or below the intervention level, some form of remedial action is required to correct the deficiency. This concept of skid resistance intervention level has been adopted for pavement friction

management by highway agencies in different parts of the world (Hall et al. 2009, NZTA 2010, Highways England 2006).

Table 3-3 has already listed some examples of skid resistance intervention level adopted by different highway agencies. The differences in the skid resistance intervention level values are due to the complex factors and the number of possible situations involved in wet-weather traffic accidents, as well as differences in the choices of acceptable accident rate adopted by different highway agencies (Hall et al. 2009, Henry 2000).

6.3.2 Procedure for Determination of Terminal Service State

The determination of the terminal service state of a clogged porous pavement involves the evaluation of its skid resistance performance as a function of the degree of clogging. However, it is impractical to measure and monitor the degree of clogging of a porous pavement because there is currently no standard or practical method to evaluate this property on site. In the current proposed procedure, instead of degree of clogging, the permeability of a clogged porous pavement is measured. The measured permeability is next used as an input for skid resistance assessment using a skid resistance computer simulation program.

The proposed procedure of determining the terminal service state of a clogged porous pavement consists of the following three main steps:

(1) Step 1 -- Determination of analysis and input parameters.

(a) Determine the following pavement properties: Number of traffic lanes, lane width, cross slope, thickness of porous surface layer, and the range of permeability of the porous surface layer from the initial unclogged state to the fully clogged state.

(b) Select the desired analysis rainfall intensity. The analysis rainfall intensity can be the design value used in the design of the roadway, or an appropriate value selected by the highway agency concerned.

(c) Select the analysis vehicle speed. A reasonable choice of this analysis speed can be the 85th percentile wet-weather traffic speed, or even a higher percentile speed if deemed appropriate by the highway agency concerned.

(d) Perform skid resistance test on the pavement section, or obtain the skid resistance from a recently conducted pavement friction survey.

(e) Identify skid resistance intervention level adopted by the highway agency concerned (see Table 3-3 for examples of skid resistance intervention levels).

(f) Select a suitable skid resistance simulation model to predict skid resistance of wet pavements.

(2) Step 2 -- Skid resistance analysis of porous pavement.

(a) For the given analysis rainfall intensity, calculate water film thickness for permeability values at suitable interval within the permeability range identified in Step 1(a).

(b) With the calculated water film thickness, the selected vehicle speed and the field measured skid resistance as inputs, apply porous pavement skid resistance simulation model to derive the relationship between skid resistance and porous pavement permeability, and obtain a skid resistance-permeability plot.

(c) With the identified skid resistance intervention level in Step 1(e), apply pavement skid resistance simulation model to derive the corresponding skid resistance intervention curve.

(3) Step 3 -- Determination of terminal service state of porous pavement.

(a) From the skid resistance intervention curve derived in Step 2(c), obtain the intervention skid resistance at the analysis vehicle speed.

(b) With the intervention skid resistance determined in the last step, obtain the terminal state permeability from the skid resistance-permeability plot derived in Step 2(b).

Figure 6-1 shows the flow diagram of the above analysis. The data to be obtained in Step 1 are required for the skid resistance analysis in Steps 2 and 3. The skid resistance test in Step 1(d) can be performed following a standard test procedure, such as the ASTM standard test method for skid resistance of paved surfaces using a full-scale tire (ASTM, 2011a). Step 1(f), 2 and 3 are unique to the proposed procedure and will be explained in detail in the subsequent sections.

6.4 Measurement of Permeability of Porous Pavement Surface Layer

The degree of clogging of a porous pavement can be expressed in terms of the percentage of its air voids filled by clogging materials (Tan et al., 2003, Fwa et al., 2015). The degree of clogging of a porous layer is in general negatively correlated with the permeability of the layer (Izevbekhai and Maloney, 2011, Fwa et al., 2015). Hence, permeability is indicative of the degree of clogging even though their relationship may not be linear. For the purpose of the present study, besides being the parameter that can be more conveniently measured on-site as compared with the degree of clogging,

permeability is also an engineering parameter that can be used to compute and monitor the changes in the drainage capacity of the porous pavement layer. More importantly, it is a key input parameter to the skid resistance simulation model (to be described in Section 6.5) for the calculation of porous pavement skid resistance.

The on-site measurement of the permeability of a porous pavement surface course can be made by means of a falling-head test. It has been demonstrated by Tan et al. (1999) and Fwa et al. (2001) that a falling-head test apparatus, equipped with a pressure sensor to measure the height of falling head with time, provides the necessary data for permeability determination of a porous surface layer. For a porous pavement surface layer with a known thickness, its coefficient of permeability can be calculated using the falling-head test results by the following modified Darcy equation that describes the non-laminar flow in the porous material (Scheidegger, 1963),

$$v = k \cdot i^m \tag{6-1}$$

where v is the flow speed, i the hydraulic gradient, k the coefficient of permeability, and m an experimental constant. k and m are determined using falling-head test results. For a typical porous surface course with permeability of 10 mm/s or higher, the test will be completed in less than two minutes.

6.5 Determination of Skid Resistance of Porous Pavement

The proposed procedure of terminal service state determination requires an analytical model that can predict the skid resistance of a porous pavement surface with a known coefficient of permeability. The following two forms of skid resistance prediction models are currently available: (i) Empirical relationships that relate skid resistance with various forms of pavement characteristics such as surface macrotexture and aggregate type (Masad et al.

2010, Meegoda and Gao); or (ii) Mechanistic simulation models that derive skid resistance from theoretical consideration of the interaction among pavement surface, runoff and tire (Zhang et al. 2013, 2016).

In the present study, the three-dimensional finite-element simulation model of porous pavement skid resistance developed by Zhang et al. (2013, 2016) is adopted. The calculation of skid resistance consists of the following two parts: (i) the water film thickness on the surface of the porous pavement under the analysis rainfall intensity is determined; and (ii) with the computed water film thickness, the skid resistance for the vehicle speed of interest is computed.

6.5.1 Calculation of Water Film Thickness

Water film thickness is calculated for the porous pavement of interest with the following input variables:

- Rainfall intensity – A logical choice is the design rainfall intensity for the roadway section, although a different rainfall intensity could be used if deemed to be more appropriate by the highway agency concerned.
- Thickness of porous surface course of the pavement section considered.
- Cross slope of the pavement section considered.
- Coefficient of permeability of the porous surface course – This coefficient of permeability is obtained from on-site falling-head test as explained in Section 6.4.

A number of methods are available for computing the water film thickness of runoff during a rainfall (Anderson et al., 1998, Ranieri et al., 2012). The present study adopts the computation program PAVDRN developed by Anderson et al. (1998) to calculate the thickness of steady–state water flowing on a porous pavement surface as follows:

$$t_w = [\frac{nL(i-f)}{\alpha S^{0.5}}]^{0.6} - MTD \quad (6\text{-}2)$$

where t_w is water film thickness (mm), n the Manning's roughness coefficient, L the drainage path length (m), i the rainfall intensity (mm/h), f the infiltration rate into the porous pavement (mm/h), α is a model constant, S is the slope of drainage path (m/m), and MTD the mean texture depth (mm). PAVDRN provides recommended values of n for different types of pavement materials, and values of porous pavement MTD ranging from 1.0 to 4.0 mm.

The infiltration rate f of porous pavement in Equation (6-2) is estimated by the following relationship:

$$f = \frac{khS}{L} \quad (6\text{-}3)$$

where k is the coefficient of permeability of the porous pavement layer (mm/h), and h is the thickness (m) of the porous layer. Based on the recommendation of the PAVDRN program, a MTD value of 2.5 mm was used in the calibration of the skid resistance simulation model to be described in the next section.

6.5.2 Computation of Skid Resistance

6.5.2.1 Consideration of Water Film Thickness in Skid Resistance Determination

Depending on whether surface water film is present or absent on a porous pavement surface, there can be two different skid resistance generation scenarios. According to Equation (6-2), when the rainfall intensity is less than the infiltration rate, or when the rainfall intensity is higher than the infiltration rate, but still not high enough for the first term of Equation (6-2) to be larger than MTD of the porous pavement, the skid resistance is equal to that of a wetted porous pavement surface with zero water film thickness. This is the scenario

with water film thickness t_w equal to zero. The next scenario occurs when the rainfall intensity is high enough to have water film thickness t_w larger than zero.

In the first scenario where $t_w = 0$, the skid resistance is governed by the microtexture of the pavement surface material, and is not dependent on vehicle speed. Since skid resistance measurements by most commercial skid resistance test devices are made at a water film thickness of about 0.5 mm on non-porous pavements (Henry, 2000), such measurements when made on porous pavements fall in the scenario of $t_w = 0$ because typical MTD values of porous pavements are larger than 1.0 mm. For instance, if the ASTM E274 standard test method for skid resistance of paved surfaces using a full-scale tire (ASTM, 2011a) is employed to test a porous pavement, the test result will be SN_0 which refers to a skid number measured at zero water film thickness.

In the second scenario with $t_w > 0$, the skid resistance of a porous pavement is affected by the following three main factors: water film thickness, vehicle speed, permeability of porous pavement. The standard skid resistance tests alone do not provide sufficient information to reveal the complex effects these factors have on skid resistance. The skid resistance measured is a result of interaction among vehicle tire, water and pavement surface. In this study, as explained in the next section, a 3-dimensional finite-element skid resistance simulation model developed by Zhang et al. (2013) is adopted to predict the skid resistance of a locked wheel sliding on a porous pavement with $t_w > 0$.

6.5.2.2 Simulation Model for Computation of Skid Resistance

The 3-dimensional finite-element skid resistance simulation model developed by Zhang et al. (2013) employs theories of solid mechanics and fluid dynamics to analyze tyre-fluid interaction, tyre-pavement interaction, and fluid-pavement interaction. Figure 6-2 shows a schematic representation of the

analysis involved in the model. The model comprises three sub-models, namely the tyre sub-model, pavement sub-model, and the fluid sub-model.

The tyre sub-model consists of three structural components, namely the tyre rim, tyre sidewalls and tyre tread. The tyre is in contact with the pavement surface under a downward concentrated load acting on the tyre rim, and a uniformly distributed tyre inflation pressure acting on the inside tyre walls. In the fluid sub-model, fluid behavior is represented by the full Navier-Stokes equations (Pinkus and Sterlicht, 1961), and the standard k - ε model is adopted to model turbulent flow around the tyre and inside porous pavement layer.

The pavement sub-model is a rigid porous structure. The contact mechanism between the tyre and pavement surface is assumed to follow the Coulomb's theory of friction. The porous structure of the pavement layer is represented by a simplified pore network structure with straight channels in longitudinal, transverse and vertical directions. The dimension of the cubic pores and spacing of the pores are determined by trial and error to achieve the permeability required (Zhang et al., 2012).

The solution of the simulation analysis is obtained through an iterative process of analyzing the interactions among the three sub-models. Fluid stresses acting on the tyre and pavement are first computed. Next, the tyre deformations resulted from the fluid stresses are calculated. With the new deformed shape of the tyre, fluid stresses are re-calculated. This iterative process is continued until convergence is reached. The final output of the simulation analysis is the skid number SN_V at speed v defined by the following equation:

$$SN_v = \frac{F_x}{F_z} \times 100 = \left[\frac{F_t + F_d}{F_z} \right] \times 100 = \left[\frac{\mu \left(F_z - F_u \right) + F_d}{F_z} \right] \times 100 \qquad (6\text{-}4)$$

where F_x is the total resisting forces acting on the wheel, F_t the traction force, F_z the vertical wheel load, F_u the fluid uplift force, F_d the fluid drag force, and μ the friction coefficient of tyre-pavement interface. The friction coefficient is given by the SN_0 measured in the preceding sub-section.

6.6 Identifying Skid Resistance Intervention Level

Section 3.3.2 has explained the concept of skid resistance interventional level adopted by highway agencies, with examples highlighted in Table 3-3. It should be noted that although the skid resistance intervention levels of the various agencies were established based on the conventional non-porous pavements, the magnitude of skid resistance indicated as the intervention level by each agency is the value of skid resistance required for safe driving in wet weather. This magnitude of skid resistance requirement for safe driving remains unchanged regardless of the type of pavement or materials used. Hence, the concept and value of intervention skid resistance are equally applicable for porous pavements.

The skid resistance intervention level indicated in Table 3-3 is a single-point representation of skid resistance requirement at the standard test speed of 64 km/h and test water film thickness of 0.5 mm (Henry, 2000). It is possible to identify the equivalent skid resistance of this requirement at other vehicle speeds. That is, for a pavement with a given intervention level skid resistance at 64 km/h vehicle speed, the corresponding skid resistance values at other vehicle speeds could be indicated. In other words, as illustrated in Chapter 3, the one-point skid resistance intervention level can be represented by a skid resistance intervention curve to cover the entire range of operating vehicle speeds. This concept of skid resistance intervention curve is illustrated in Figure 6-3.

For a given single-point skid resistance intervention level, such as those given in Table 3-3, the corresponding skid resistance intervention curve can be derived using a finite-element skid resistance simulation model for non-porous pavements (Ong and Fwa, 2007; Fwa and Ong, 2008). The simulation model for non-porous pavements is a special case of the porous pavement skid resistance simulation model described in Section 6.5.2.2.

6.7 Determination of Terminal Service State of Clogged Porous Pavement

This is the last step of the overall procedure of determining the terminal service state of clogged porous pavement. First, it involves calculating the skid resistance at different permeability values using the skid resistance simulation model, and plotting the skid resistance-permeability curve, as illustrated in Figure 6-4(a). Next, the intervention skid resistance at the analysis vehicle speed is obtained from the skid resistance intervention curve, as shown in Figure 6-4(b). Finally, from the resistance-permeability curve of the porous pavement, the terminal service state of clogged porous pavement is given by the permeability at which the skid resistance is equal to the intervention level skid resistance.

6.8 Illustrative Example

6.8.1 Problem Description

This example problem considers the standard porous pavement design adopted in Singapore. The pavement consists of a porous asphalt layer of 50 mm thick supported on a 100 mm layer of dense graded asphalt course. The porous asphalt mix has 5% binder content of modified polymer asphalt and a top aggregate size of 19.0 mm (Fwa et al., 2002). The straight road section analysed has 2 lanes in each direction. The main purpose of having the porous

asphalt layer is to provide a safe wet-weather driving surface during rainy days. The analysis is to determine the terminal service state of the porous pavement.

The pavement section has a constant cross-slope of 2% across the two lanes in each direction. The width of each traffic lane is 3.5 m. The porous asphalt layer has an initial porosity of 23%, and an initial coefficient of permeability of 15.2 mm/s. The skid resistance of the initial unclogged porous pavement is SN = 50 measured using the ASTM E274 standard test with smooth tyre (ASTM, 2011a). The terminal service state of the porous pavement is to be determined for a rainfall intensity of 80 mm/h. The rainfall intensity is selected as the 90th percentile value of rainfall intensity data for Singapore's annual rainfalls having durations equal to or longer than 10 minutes (Goh, 2015).

6.8.2 Computation of Water Film Thickness

For the selected condition of rainfall intensity, the water film thicknesses for different stages of clogging (represented by their respective values of permeability coefficient) can be calculated from the PAVDRN program using Equations (6-2) and (6-3). For the present problem, the outermost wheel path of the outer lane is considered for water film thickness calculation. This represents the worst condition with respect to water film thickness for the pavement section. The initial 15.2 mm/s coefficient of permeability represents the unclogged condition, while a value close to zero indicates a condition when the porous pavement is fully clogged.

6.8.3 Determination of Terminal Service State Permeability

Knowing the water film thickness, the initial skid resistance, a vehicle speed and a given permeability, the available skid resistance of the porous pavement with the given permeability can be calculated using the finite-element skid resistance simulation model. For illustration purpose in this example

problem, the data for the skid resistance versus porous pavement permeability relationships at the following three vehicle speeds were generated from the simulation model: 80, 70 and 60 km/h. The computed skid resistance-permeability curves for the three speeds are shown in Figure 6-5.

Next, Figure 6-5 illustrates how the terminal service state of the porous pavement is determined. First, consider a case where the analysis vehicle speed is chosen to be 80 km/h. This is the 85th percentile wet-weather traffic speed. Assuming that the skid resistance intervention curve of Figure 6-3 is applicable for the present problem, the intervention skid resistance value at 80 km/h is equal to SN = 24. With this SN value, the corresponding coefficient of permeability is k = 4.2 mm/s (see Figure 6-5(a)). This is the minimum permeability of the porous pavement needed to satisfy the required skid resistance for wet-weather driving safety. That is, the terminal service state of the porous pavement is reached when its coefficient of permeability falls to k = 4.2 mm/s.

For illustration purpose, the effects of changing the analysis vehicle speed to 70 km/h and 60 km/h, respectively, are also shown in Figure 6-5(b). At 70 km/h, the intervention skid resistance is SN = 28, and the terminal service state is reached at coefficient of permeability k = 2.3 mm/s. At 60 km/h, the intervention skid resistance is SN = 31.5, and the coefficient of permeability at the terminal service state is found to be k = 1.0 mm/s.

6.8.4 Discussion of Results

The following observations may be made from the results of the example problem:

(1) The results show that, for a given porous pavement subject to clogging, its terminal service state is dependent on the choice of analysis vehicle

speed. A higher analysis vehicle speed will require a higher pavement permeability at the terminal service state, i.e. the terminal service state will be reached sooner. For instance, a highway agency may impose a lower wet-weather speed limit to extend the safe service life of a porous pavement. For the example problem, if one lowers the maximum wet-weather speed from 80 km/h to 70 km/h, the terminal permeability coefficient is reduced from 4.2 mm/s to 2.3 mm/s. This means that maintenance intervention can be activated later when the coefficient of permeability reaches 2.3 mm/s.

(2) The analysis presented can be used to determine the safe vehicle speed allowed on a clogged porous pavement by measuring its coefficient of permeability. For instance, if the porous pavement in the example problem is found to have a coefficient of permeability of 1.1 mm/s, then it would not be safe for vehicles traveling at 70 km/h or higher, and a suitable speed limit to be imposed would be 60 km/h.

(3) Knowing the terminal service state and the corresponding permeability of a porous pavement will permit the highway agency concerned to plan for its de-clogging maintenance. A highway agency can set a permeability level slightly higher than the terminal permeability to be the de-clogging activation threshold to provide sufficient lead time for de-clogging maintenance work. By monitoring the rate of deterioration of permeability through periodic surveys, a highway agency is able to plan and schedule de-clogging maintenance in advance.

(4) It is of interest to have an idea of the degree of clogging at the terminal state in terms of porosity even though it is not practical to monitor porosity in the field. For the porous asphalt mix used in Singapore,

laboratory studies (Fwa et al., 2015) indicated that for the permeability coefficient values of 4.2, 2.3 and 1.0 mm/s, the corresponding mix porosities are approximately 12, 10.5, and 7.5%.

6.9 Summary

The current practice of pavement condition survey does not have the capability to set a threshold state for maintenance of porous pavements subject to clogging, nor to track and monitor the development of clogging and the associated deterioration rate of permeability of the porous layer. A quantitative procedure has been proposed in this chapter to measure the permeability of a porous pavement as an engineering basis to determine the terminal service state of the pavement with respect to wet-weather driving safety.

With the knowledge of the permeability of a porous pavement and water film thickness, the skid resistance performance of the porous pavement at different vehicle speeds under a given rainfall intensity can be derived using a skid resistance simulation model. The analysis can be repeated for different pavement permeability levels to develop the skid resistance-permeability relationship of the porous pavement. From this relationship, the terminal permeability can be identified as one that gives a skid resistance equal to a pre-determined skid resistance intervention level. This terminal permeability defines the terminal service state of the porous pavement with respect to wet-weather driving safety.

The proposed procedure enables highway agencies to determine the terminal service state of a porous pavement quantitatively on a rational engineering basis. It helps to extend the capability of the current practice of pavement condition survey to cover porous pavements more adequately. It is

also useful as a tool for effective de-clogging maintenance management of porous pavements.

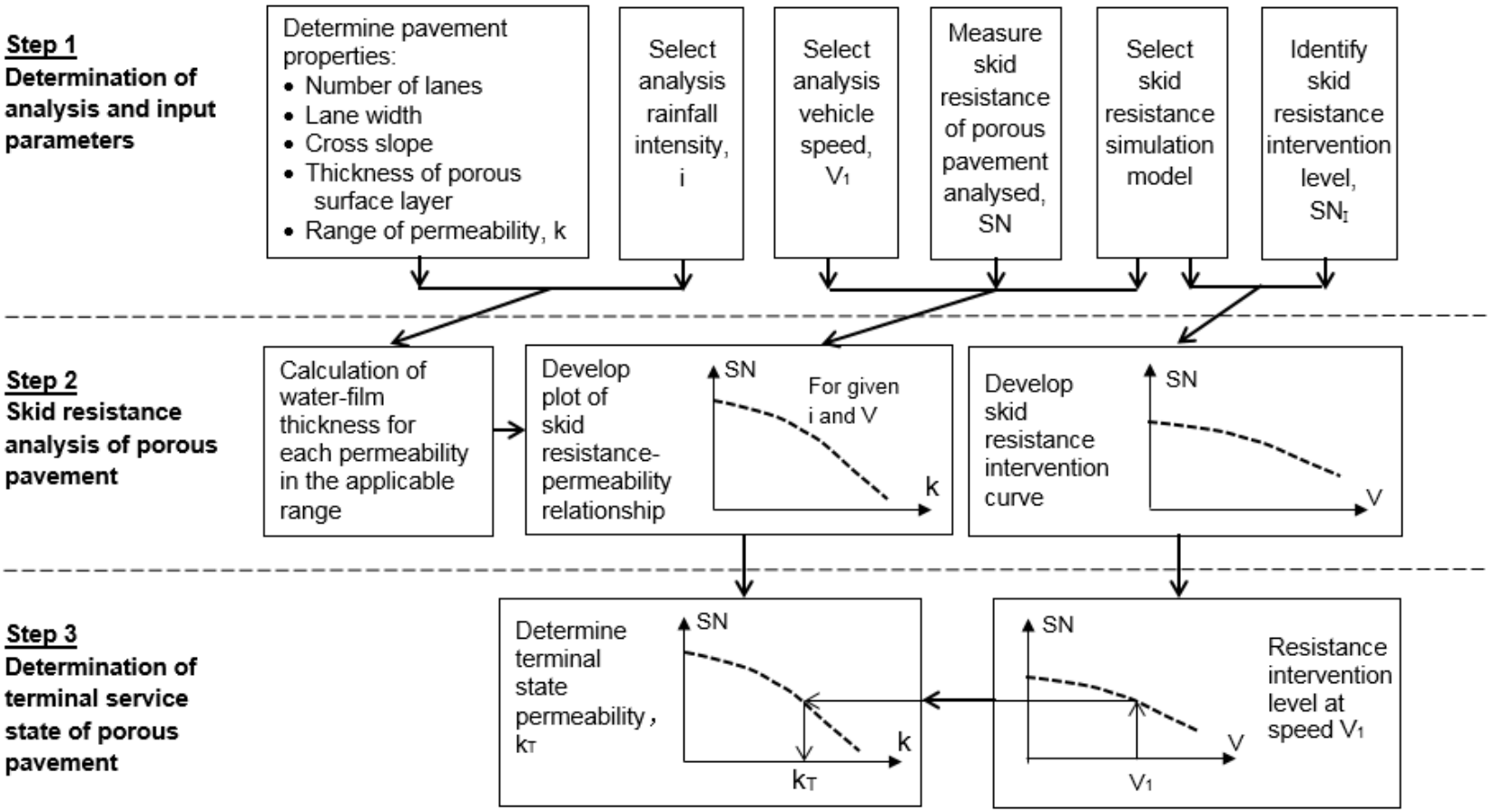

Figure 6-1 Flow Diagram for Determination of Terminal Service State of Porous Pavement

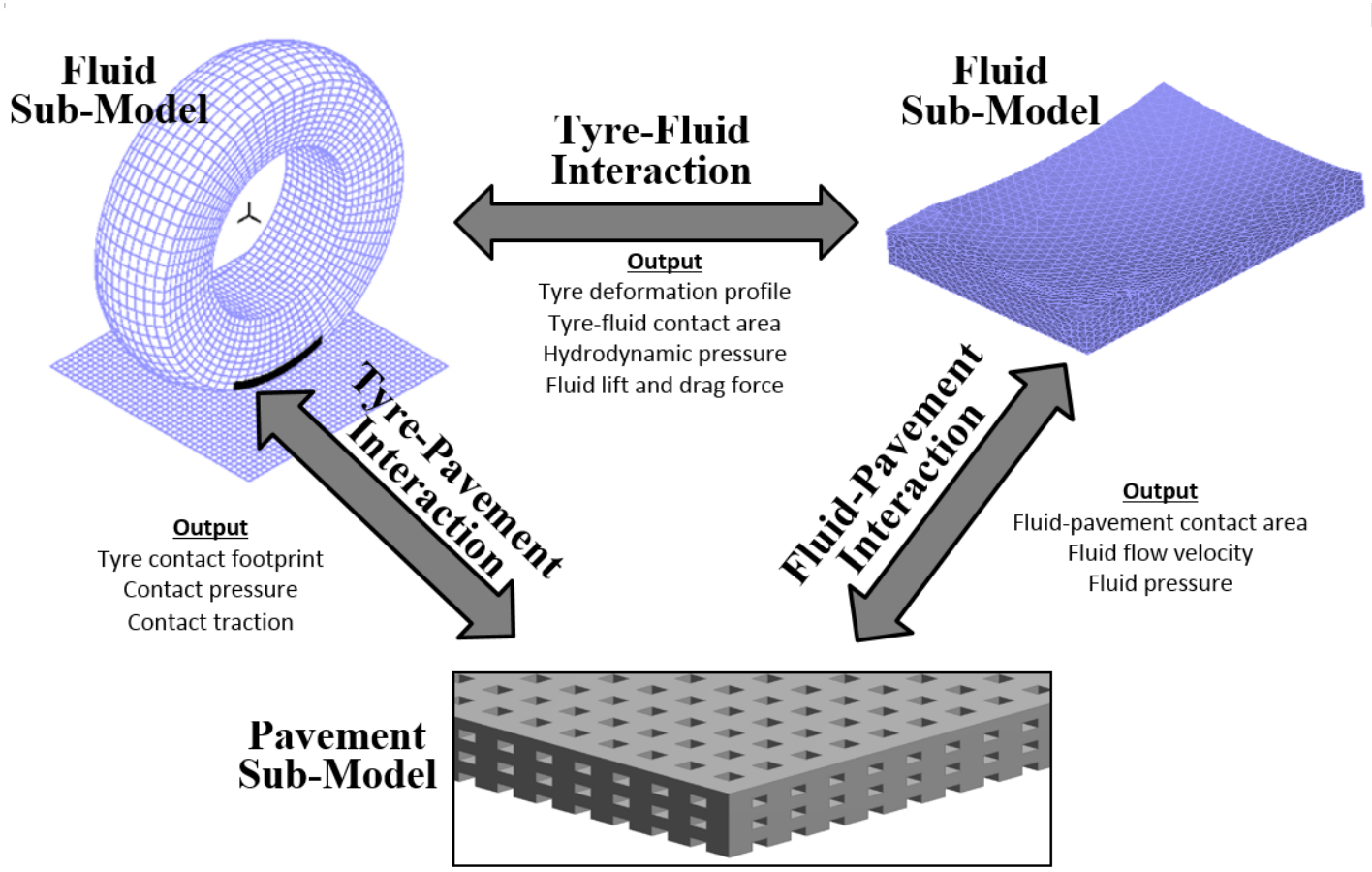

Figure 6-2 Schematic Representation of Mechanistic Modeling for Skid Resistance Simulation of Porous Pavement

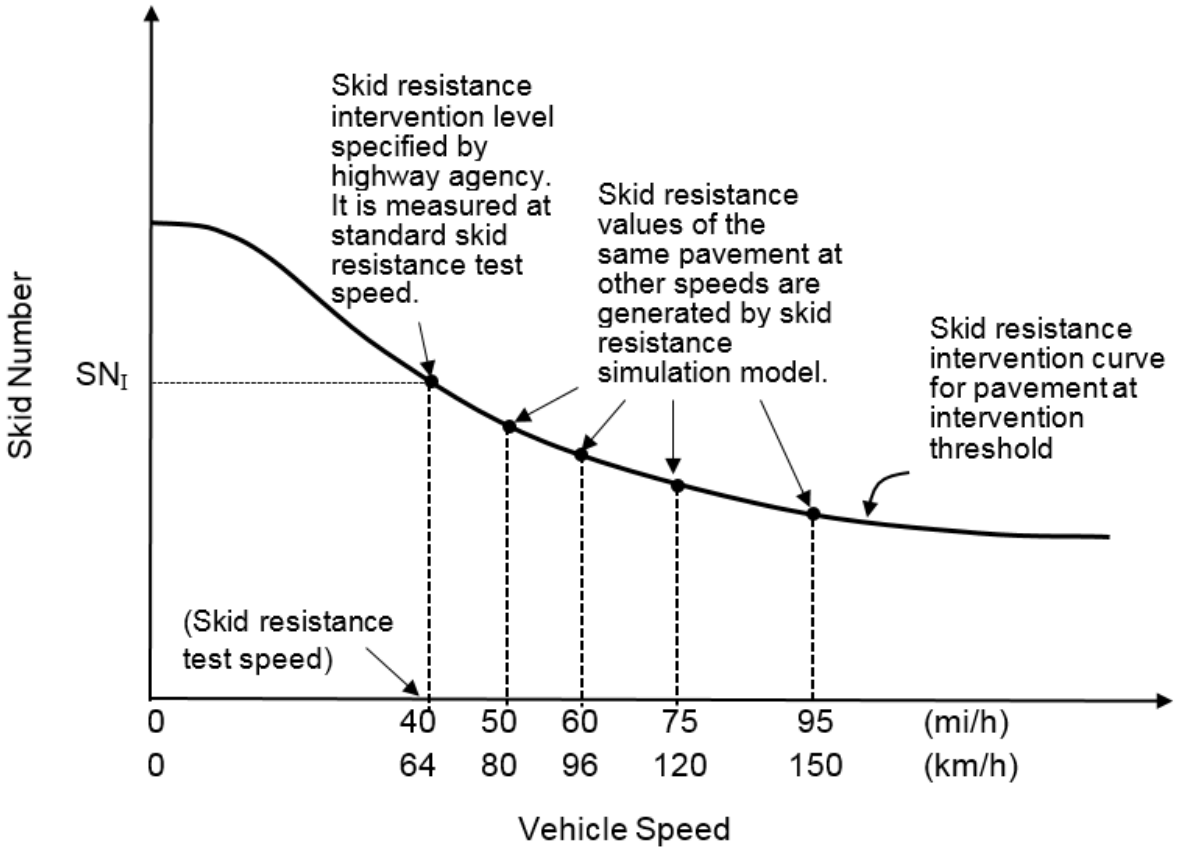

Figure 6-3 Schematic Representation of the Concept of Skid Resistance Intervention Curve

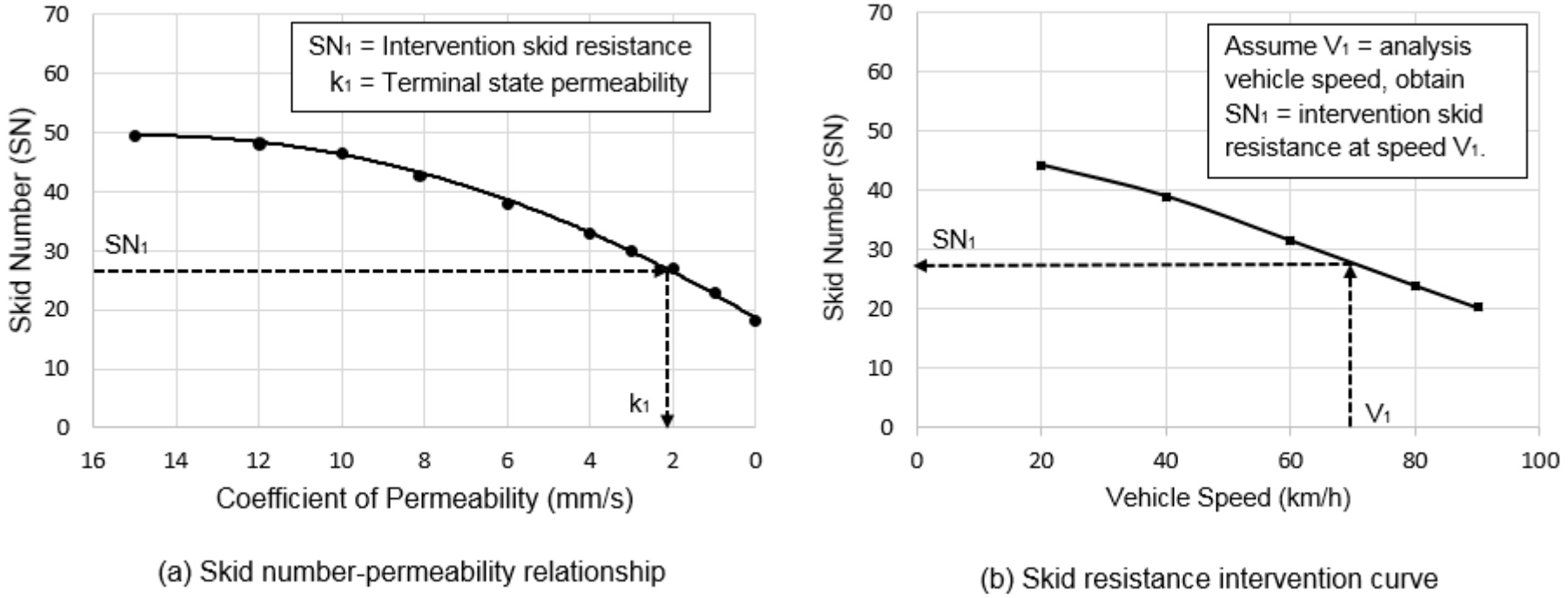

Figure 6-4 Determination of Terminal State Permeability of Porous Pavement

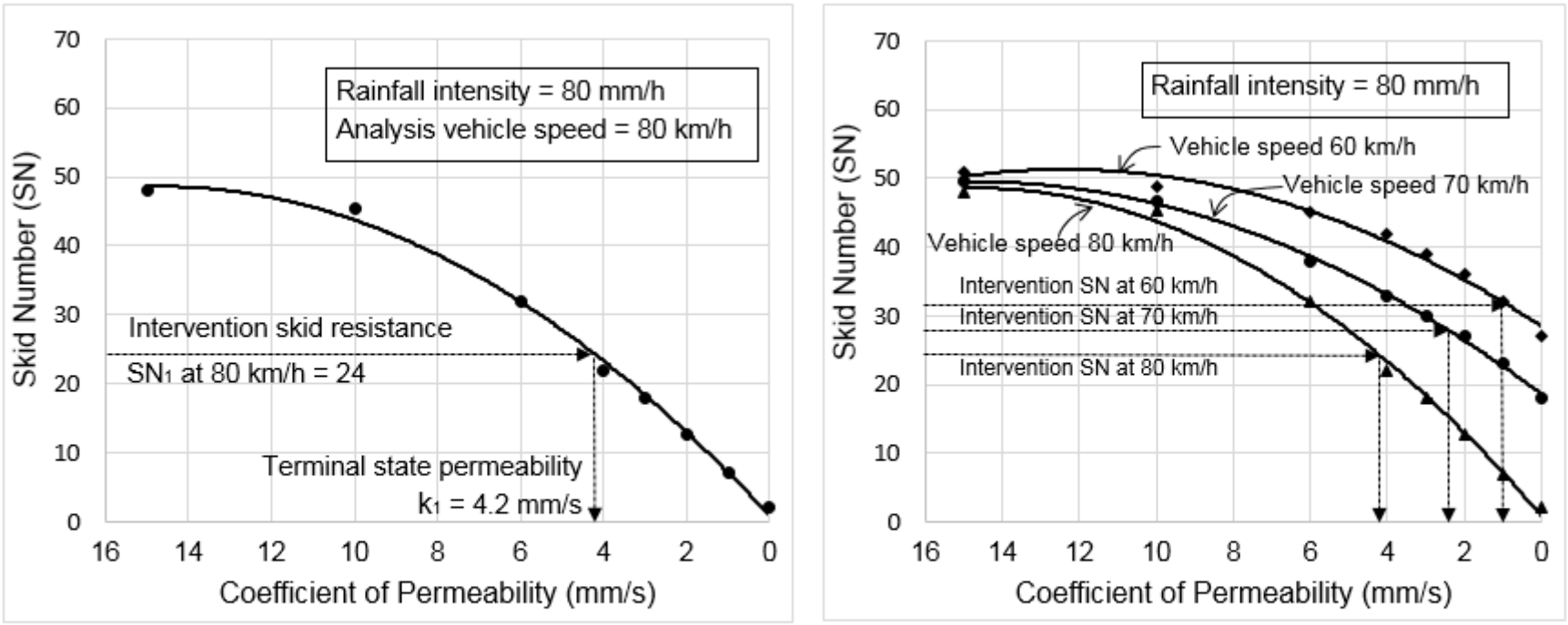

(a) Terminal state permeability at analysis vehicle speed of 80 km/h

(b) Comparison of terminal state permeability at different analysis vehicle speeds

Figure 6-5 Terminal State Permeability Determination for Illustrative Example

CHAPTER 7 CONSIDERATION OF SOUND ABSORPTION PROPERTIES IN MIX DESIGN OF POROUS ASPHALT MIXTURES

7.1 Introduction

Porous asphalt pavements are known to be effective as a form of quiet pavement because of their porous structure. The connected pores in the porous asphalt structure reduce tire-pavement noise through the higher sound absorption property of the structure, and the weakening of noise generation mechanisms (such as air sucking, air pumping, air resonant and horn effect) by acting as air channels to relieve air pressures (Sandberg and Ejsmont, 2002; Donavan and Lodico, 2009).

In the mix design of porous asphalt mixture, a point of interest to pavement engineers is to determine how the choice of different mix designs would help to reduce tire-pavement noise. Currently such quantitative information is unavailable to guide pavement engineers in the mix design of porous asphalt pavement mixtures. There are also no recommended laboratory procedures for assessing the tire-pavement noise reduction of a design mix of porous asphalt mixture. This chapter presents an attempt to develop a laboratory procedure and a method of analysis to assist pavement engineers in estimating the contribution to tire-pavement noise reduction by the porous structure of a porous asphalt design mix.

The proposed laboratory procedure consists of two main steps. In the first step, by means of acoustic impedance tubes, the sound absorption coefficients of laboratory specimens of a test mix and a reference dense graded mix are measured. Next, with the measured sound absorption coefficients, the tire-pavement noise reduction of the test mix is estimated using a simplified method. For illustration of the proposed procedure, the proposed laboratory

procedure was applied to test four porous asphalt mix designs used in Singapore. The sound absorption characteristics of the test mixtures with respect to the following properties were examined: percent porosity of mixture, degree of clogging, and thickness of specimen. The test results are analyzed to show how each of these properties affects the sound absorption properties of the test mixtures, and to estimate the effectiveness of the sound absorption and tire-pavement noise reducing capability of the porous asphalt mixtures studied. The calculated noise reductions using the proposed simplified method are compared with those measured from a field trial to assess the applicability of the proposed method.

7.2 Objective and Scope of Study

Technological improvements in automobile exhaust system and engine design have made tire-pavement noise the most dominant contributor to road traffic noise (Shimeno et al., 2010; Abbott et al., 2010; Sandberg and Ejsmont, 2002). Pavement engineers and researchers have explored different pavement wearing course designs to mitigate tire-pavement noise. A porous asphalt wearing course helps to reduce tire-pavement noise through its porous structure to dissipate sound energy, and its surface pores and macrotexture to lessen the generation of noise at the tire-pavement contact (Sandberg and Ejsmont, 2002; Donavan and Lodico, 2009). This chapter focuses on the first mechanism by examining the sound absorption characteristics of asphalt porous mixture. The main objective is to demonstrate that during the mix design phase of an asphalt mixture, it is possible to conduct acoustic tests on laboratory specimens to determine the sound absorption characteristics of the specimens, and perform analysis on the measured acoustic properties of the specimens to estimate the tire-pavement noise reduction achievable. To achieve this objective, a

laboratory test and an analysis procedure is proposed in this chapter. The proposed procedure is developed to provide useful information to pavement engineers for the selection of suitable materials and porosity level in the design of porous asphalt mixtures to meet tire-pavement noise reduction requirements.

To illustrate the details involved in the testing and analysis of the proposed procedure, a laboratory test program was conducted on four porous asphalt mixtures with different porosity levels. The other two factors included in the test program were the degree of clogging and the thickness of test specimens. These three properties are of interest to pavement engineers because besides pavement surface texture, they are the main pavement-related factors that affect the tire-pavement noise generated by traffic traveling on a porous pavement. The values of the three properties tested in the experimental program were:

Percent porosity of mixture: 12%, 16%, 20% and 25%.
Degree of clogging: 0%, 28%, 53%, 76%, and 100%.
Thickness of specimen: 63 mm, 100 mm, and 200 mm.

The effects of clogging and specimen thickness were tested for the porous mixture with 20% porosity.

In addition to the porous mixtures, a dense graded mix was also tested in the study. The dense graded mix had an air void content of about 4%. It served to provide a reference to facilitate the effectiveness assessment of the sound absorption and tire-pavement noise reducing capability of the porous asphalt mixtures tested.

Following the acoustic testing of the test mixtures, an approximate simplified calculation method was proposed to estimate the magnitude of noise reduction based on the sound absorption properties measured. A field trial of

the test mixtures were laid to provide actual tire-pavement noise measurements for comparison with the calculated values.

7.3 Laboratory Test Program

7.3.1 Preparation of Test Specimens

Specimens of five different mixtures were prepared for the laboratory tests program, namely four porous asphalt mixes designated as PA-13, PA-16, PA-20 and PA-25, and a dense graded asphalt mix designated as DG. The gradations of these mixtures are shown in Table 7-1. The test mixes were selected for the purpose of the present study so that the porosity (i.e. percent air voids) covers a range from 4 to 25%. The porosity of a mix can be varied by adjusting its asphalt binder content and compaction effort. As shown in Table 7-1, an asphalt content of 5% was used for all the mix designs tested in this study. Marshall size test specimens of 102 mm in diameter and about 63 mm in height (ASTM, 2010a) were used for the study. Following the local practice in Singapore, drop hammer compaction in accordance with the ASTM standard procedure D6926-10 (ASTM, 2010a) was adopted. Three replicate specimens were prepared for each specific test. The porosity level of the test specimens are summarized in Table 7-2.

7.3.2 Laboratory Clogging Procedure

To study the effect of clogging, a laboratory clogging procedure developed by Fwa et al. (Fwa et al., 2015) was adopted to produce clogged specimens with the following target degrees of clogging: 25%, 50%, 75%, and 100%. The procedure used a local residual soil in Singapore as the clogging agent. 5.3 g of the residual soil was applied in stages to a test specimen. At the end of each stage of clogging, the permeability coefficient of the specimen was measured. The clogging procedure developed by Fwa et al. (Fwa et al., 2015)

permitted clogging treatment and permeability measurements to be made in sequence in the same test setup.

The percent clogging achieved is calculated according to the following definition,

$$\%\ \text{clogged after clogging stage n} = \frac{\text{Permeability coefficient after clogging stage n}}{\text{Permeability coefficient before clogging treatment}} \quad (7\text{-}1)$$

An alternative definition of percent clogged is to take the ratio of porosity after clogging stage n and the initial porosity before clogging treatment. Equation (7-1) is considered to be a more practical definition as it is relatively easy to perform permeability measurements both in the laboratory and in the field (Fwa et al., 1998). In comparison, it is practically impossible to measure changes in porosity in the field in a nondestructive manner.

7.3.3 Acoustic Absorption Measurements

The acoustic absorption coefficients of test specimens were measured using an acoustic impedance tube following the ASTM 1050-10 standard test procedure (ASTM, 2010b). Measurements were carried out based on the standing wave method in which a loudspeaker was employed to set up a sound field from one end of the tube, and the other end of the tube was terminated by the specimen to be tested. A pure tone signal was supplied to the loudspeaker and a plane wave was generated in the tube in the direction of the specimen. The wave was partially reflected from the specimen and the interference between the incident and reflected waves gave rise to a standing wave pattern. By measuring the ratio between the maximum and minimum sound pressure, the sound absorption coefficient of the sample for zero degree incident sound can be calculated.

Past research studies and field measurements of tire-pavement noise spectra have found that the most significant frequency range of sound intensity is between 630 and 2000 Hz (Buratti and Moretti, 2010; Rasmussen and Sohaney, 2012; Caltrans, 2011). Hence, the frequency range of 100 to 2,500 Hz was selected for the acoustic absorption measurements in the present study. In accordance with ASTM 1050-10 standard specification (ASTM, 2010b), for low frequencies below 500 Hz, the measurements were made using a 100 mm diameter impedance tube. For higher frequency, an impedance tube of 29 mm was used. The choice of the impedance tube size was to maintain a plane wave across the width of the tube for the test.

7.3.4 Method of Analyzing Sound Absorption and Noise Reduction of Test Mixtures

The noise generated by interaction of tire and pavement is the combined effect of the noise component transmitted directly through the air and the component reflected from the pavement. This is schematically represented in Figure 7-1. In the case of porous pavement, the reflected sound waves consist of those reflected from the pavement surface as well as those reflected after penetrating into the porous pavement. The tire-pavement noise measured by the OBSI (On-Board Sound Intensity) method (AASHTO, 2015) or the CPX (Close Proximity) method (BS ISO, 2015) is the total sound intensity with contributions from sound energy of both the direct and reflected sound waves.

In the estimation of tire-pavement noise, it is useful to know the relationship between the incident sound energy and the reflected sound energy. When the incident sound waves strike a pavement surface, some of their energy may be absorbed or lost, and the energy of the reflected sound waves is less than the energy of the original incident sound wave. The relationship can be

expressed in terms of sound intensity in dBA (A-weighted decibel) as follows (Davis and Patronis, 2006; Moser, 2009),

$$L_I = 10 \log_{10} (p^2/p_{ref}^2) \quad (7\text{-}2)$$

$$L_R = 10 \log_{10} [(1 - \alpha) (p^2/p_{ref}^2)] \quad (7\text{-}3)$$

where L_R and L_I are reflected and incident sound intensity in dBA respectively, α is the sound absorption coefficient of the pavement, p is the sound pressure in Pa, and P_{ref} is the reference sound pressure equal to 2×10^{-5} Pa. The sound absorption coefficient is the ratio of sound energy absorbed by the pavement material to the sound energy incident upon the pavement surface. When a pavement material absorbs sound waves perfectly (i.e. no reflected waves), its 'α' value would be 1.0; where it does not absorb sound at all, its 'α' value becomes zero (i.e. total reflection with $L_R = L_I$) (Davis and Patronis, 2006; Moser, 2009).

Referring to Figure 7-1, assuming that the component of tire-pavement interaction sound waves that travels through air has intensity L_I, and the other component of the same intensity L_I strikes the pavement surface and reflected with an intensity of L_R , then the total combined sound intensity L_T is given by (Davis and Patronis, 2006; Moser, 2009),

$$L_T = 10 log_{10}(10^{L_I/10} + 10^{L_R/10})$$

$$= 10 log_{10}\left[(p^2 / {p_{ref}}^2) + (1-\alpha)(p^2 / {p_{ref}}^2)\right] \quad (7\text{-}4)$$

$$L_T = 10 log_{10}(2-\alpha) + L_I \quad (7\text{-}5)$$

From Equations (7-5), it can be seen that for a known source of generated sound (e.g. tire-pavement interaction sound), the magnitude of the total combined sound intensity depends on the value of the sound absorption coefficient 'α' of the pavement material. It shows that the difference between

an excellent sound absorbing material ('α' value approaching 1) and a poor sound absorbing material ('α' value approaching 0) can be as much as 3 dBA.

It should be noted that since the sound absorption property of a material varies with frequency, the sound absorption coefficient values at different frequencies have to be measured to obtain the sound absorption spectrum that shows the variation of sound absorption coefficient with frequency. Typically, sound absorption coefficients are determined at one-third octave frequencies, and Equations (7-2) and (7-3) are then applied to obtain the sound intensity L_T spectrum in one-third octave frequencies. Next, the overall L_T in dBA is calculated by means of the following equation:

$$Overall\ L_T = 10\log_{10}[10^{L_1/10} + 10^{L_2/10} + 10^{L_3/10} + ... + 10^{L_n/10}] \quad (7\text{-}6)$$

in which L_i is the sound intensity at one-third octave frequency i, for i = 1, 2, ……, n, where L_n represents the sound intensity at the n^{th} one-third octave frequency.

Given the same sound source with intensity L_I, the dBA difference of the reflected sounds of two mixtures in a specific third-octave frequency band j can be computed from Eq. (7-5) as,

$$\Delta L_{Ti} = 10log_{10}\frac{2-\alpha_1}{2-\alpha_2} \quad (7\text{-}7)$$

where α_1 and α_2 are the sound absorption coefficients of mixture type 1 and 2 respectively in the given third-octave frequency band. This equation can be used to calculate the noise reduction achieved by mixture type 1 with reference to mixture type 2. Therefore, the contribution of sound absorption to the noise reduction of mixture type 1 can be calculated by setting $\alpha_2 = 0$ (i.e. zero sound absorption) as follows,

$$\Delta L_{Ti} = 10log_{10}(1 - \frac{\alpha_1}{2}) \quad (7\text{-}8)$$

Equation (7-8) is applicable only for a single frequency band j. To determine the overall noise reduction, Equation (7-6) must be used to compute the overall sound intensities of mixture types 1 and 2 respectively. An approximate method of estimating the overall sound reduction achieved by mixture type 1 with reference to mixture type 2 is adopted in this study by the use of either of the following two sound absorption ratings defined by ASTM (ASTM, 2009b):

(i) Noise reduction coefficient (NRC) – NRC is the average of the sound absorption coefficients of a material for 250, 500, 1000 and 2000 Hz rounded to the nearest 0.05:

$$NRC = (\alpha_{250Hz} + \alpha_{500Hz} + \alpha_{1000Hz} + \alpha_{2000Hz}) / 4 \quad (7\text{-}9)$$

(ii) Sound absorption average (SAA) – SAA is the average of the sound absorption coefficients of a material for the twelve one-third octave bands from 200 through 2500 Hz, inclusive, rounded to the nearest 0.01:

$$SAA = \sum_{i=1}^{12} (\alpha_{f_i}) / 12 \quad (7\text{-}10)$$

where the twelve one-third octave frequencies fi are 250, 315, 400, 500, 630, 800, 1000, 1250, 1600, 2000 and 2500 Hz.

The average sound absorption value NRC or SAA can be used as an approximate method to estimate noise reduction of the mixtures tested. The errors of noise reduction calculations using this approximate method are assessed by comparing with actual measured dBA values obtained from trial pavement sections constructed using the various test mixes.

7.4 Analysis of Test Results

The sound absorption test results are analyzed for the following two aspects:

(A) The sound absorption spectra characteristics of test mixtures in terms of the magnitudes and trends of variation of their sound absorption coefficients; and

(B) The magnitudes of tire-pavement noise reduction resulting from sound energy absorbed by the test mixtures.

The analysis is performed to examine for the effects of the following three factors: (i) porosity of test mixtures, (ii) effect of clogging, and (iii) effect of specimen thickness.

7.4.1 Effect of Porosity Level of Test Mixtures

The impedance tube test results of the five test mixtures PA-13, PA-16, PA-20, PA-25, and DG (see Table 7-1) are plotted in Figure 7-2. The measured sound absorption coefficients at one-third octave frequencies are shown in this figure. Each data point is the average of test results from three replicate specimens. The following patterns of the measured sound absorption coefficient spectra of the test mixtures can be observed:

- All four porous asphalt mixtures with porosity varying from 12 to 25% had substantially higher sound absorption capability than the dense graded mix with percent air voids of about 4%.
- The improved sound energy absorption of the porous asphalt mixtures, as compared with the dense graded mixture, is most significant within the frequency range of 250 to 1250 Hz. This is of physical significance because tire-pavement noise is most prevalent to the human ear in the range of 800 to 1200 Hz (Morgan et al., 2003).
- As the porosity level of the porous mixture decreases, there is a tendency for the significant sound absorption range to move toward the lower

frequency end. This finding is consistent with past research observations reported in the literature (Mun, 2010).

Table 7-3(a) presents the calculated NRC and SAA values, as well as the corresponding noise reduction dBA obtained using Equation (7-8). Overall, for each mix type, there are little differences between the NRC and SAA values, and between the NRC- and SAA-based calculated noise reductions. Generally, the NRC and SAA values of the porous mixes varied between 0.4 and 0.5, which are considerably higher than the dense graded mix value of 0.15. The estimated noise reduction resulting from the sound absorption of the porous mixes is about 1.2 dBA, which is nearly 1 dBA higher than noise reduction of the dense graded mix.

7.4.2 Effect of Clogging

The porous structure of a porous asphalt pavement has contributed to its ability to absorb sound. When clogging of the pores occurs, the sound absorption effectiveness of the porous mixture structure will be affected. In this study, the effect of clogging on the sound absorption property of the porous mixture PA-20 (see Table 7-1) with porosity of 20% was investigated.

The test results are plotted in Figure 7-2(b). Sound absorption coefficients were measured at 0%, 28%, 53%, 76% and 100% clogged condition. Figure 7-2(b) clearly shows that the sound absorption capability of the porous mixtures decreased progressively as the percent clogging increased, and eventually dropped to practically the same level as that of the dense graded DG mix. The sound absorption capability of the mixtures within the frequency range of 250 to 1000 Hz was most affected by clogging of the mixture.

Table 7-3(b) shows the calculated NRC and SAA as well as the estimated noise reductions for different percentages of clogging. The effects of

percent clogging on these properties can be examined from the plots in Figure 7-3. The sound absorption and noise reduction capability of the porous structure was little affected by clogging when the percent clogging was less than about 50%. Beyond 50% clogging, the rates of deterioration of the two properties increased markedly.

It is interesting to note that when the percent clogging of the porous mixture increased toward 100% (i.e. fully clogged according to the definition of Equation (7-1)), its sound absorption spectrum as well as the NRC and SAA values, and the noise reduction achieved, approached the corresponding levels of the dense graded DG mixture, instead of zero. It is likely that although the permeability of either the dense graded mixture or the 100% clogged porous asphalt mixture is practically zero, there are still pores in the mixtures that contribute to sound energy absorption.

7.4.3 Effect of Specimen Thickness

Another point of interest is the effect of asphalt layer thickness on sound absorption and noise reduction. This was examined in this chapter by testing test specimens of three thicknesses: 63, 100 and 200 mm. Figure 7-2(c) shows that the peak range of frequencies moved toward the lower frequency end as the thickness of test specimens increased. This shifting trend of sound absorption spectra has been observed and reported by earlier researchers (Li et al., 2015). Despite this difference, Table 7-3(c) reveals that there are negligible differences in the magnitudes of sound absorption ratings NRC and SAA, and also the values of noise reductions.

7.5 Comparison of Laboratory Estimated Noise Reductions with Field Data

To assess the errors involved in using the laboratory determined sound absorption ratings NRC and SAA in estimating noise reductions achieved by

porous asphalt mixtures, trial sections of the wearing course mix designs tested in this study (see Table 7-1) were constructed. Each trial section measured 100 m long with a wearing course thickness of 60 mm. The tire-pavement noise of these trials sections were measured at 80 km/h by means of the OBSI method in accordance with the AASHTO standard test procedure AASHTO TP76 Standard Method of Test Measurement of Tire/Pavement Noise Using the On-Board Sound Intensity (OBSI). With the measured sound absorption coefficients of the mix designs given in Figure 7-2(a), and the measured sound intensity spectra, the overall sound intensity and the contribution of noise reduction for each mix design can be calculated using Equations (7-2), (7-3) and (7-6).

The main difference between the above method based on actual measurements and the approximate method of calculating noise reduction is that while the approximate method applies either NRC or SAA, this more exact method based on actual measurements makes use of the sound absorption coefficients in each frequency band to calculate the reflected sound intensity in the individual frequency bands, and applies Equation (7-6) to calculate the overall noise reduction taking into account of the sound intensity contributions from each frequency band. Table 7-4 summarizes the results of the analysis using the more exact method and makes comparisons with the noise reductions calculated earlier using the proposed approximate method.

Table 7-4 shows that the proposed approximate method underestimates the noise reduction by about 30% for the porous asphalt mix designs, but is accurate for the case of dense graded mix. This is because the sound absorption coefficients of the dense graded mix remain more or less the same for different frequency bands, while those of the porous asphalt mixes varies substantially

with the frequency bands. The use of SAA by averaging the sound absorption coefficients introduces errors. An attempt to use a revised SAA by taking the root-mean-square value of the sound absorption coefficients produced negligible change to the estimated noise reductions.

Notwithstanding the fact that the proposed approximate method underestimates the noise reduction achievable for a mix design, it is still useful as an approximate procedure for providing a conservative estimate of the noise reduction capability of mixture during the laboratory mix design phase. This is because the method does not require the knowledge of the tire-pavement noise frequency spectrum, but only the sound absorption coefficients that can be determined relatively easily in the laboratory using standard Marshall size specimens.

The results in Table 7-4 can also be used to provide an estimate of percent contribution of the porosity of a porous mixture to its total noise reduction. Taking the dense graded mix DG as reference, the difference between the OBSI values (column 2 of Table 7-4) of a porous mix and the dense grade mix gives the total noise reduction resulting from the use of porous asphalt wearing course. The corresponding difference of the noise reduction values in column 3 of Table 7-4 represents the contribution from sound energy absorption by the porous structure of the porous mix. The ratio would provide an estimate of the percent contribution of sound absorption capability of the porous mixture. The results are summarized in Table 7-5. It is seen from the table that the estimated percent noise reduction contribution due to sound energy absorption of the porous asphalt mixtures tested varied from 23 to 33%.

7.6 Summary

This chapter has demonstrated a laboratory procedure to determine the sound absorption characteristics of porous asphalt pavement wearing course mix designs, and estimate their contributions to tire-pavement noise reduction. Four porous asphalt mix designs with porosity varying from 12 to 25% were tested to study the effect of porosity level. Also studied were the effects of percent clogging and specimen thickness. A dense graded mix was included in the test program to serve as a reference for comparison. Using Marshall size specimens, the sound absorption coefficients of the test specimens were measured by means of standard laboratory acoustic test equipment in the form of impedance tube.

It was found that the sound energy absorption of the porous asphalt mixtures tested was most significant within the frequency range of 250 to 1250 Hz. As the porosity level of the porous mixture decreases from 25 to 12%, there was a tendency for the significant sound absorption range to move toward the lower frequency end. However, there were negligible differences in the noise reduction contributions from sound absorption for the range of porosity studied. On the other hand, clogging of the pores in the mixtures resulted in significant reductions in both the sound absorption coefficients and the overall tire-pavement noise. The sound absorption capability of the porous mixtures decreased progressively as the percent clogging increased, and eventually dropped to practically the same level as that of the dense graded DG mix. The sound absorption capability of the mixtures within the frequency range of 250 to 1000 Hz was most affected by clogging of the mixture. On the effect of layer thickness, the test results showed that changing the thickness of test specimens from 63 mm to 200 mm had no significant effect on sound absorption and tire-

pavement noise reduction. A field trial was conducted to verify the laboratory analysis of noise reduction.

This chapter has proposed an approximate method to estimate the noise reduction capability of mix designs based on either of the ASTM sound absorption ratings NRC (noise reduction coefficient) and SAA (sound absorption average). Although the approximate method underestimates noise reductions by about 30% as compared with the more exact method of calculation using actual measured tire-pavement noise spectra from a field trial, it is still a practical tool for laboratory mix design by giving a conservative estimate of noise reduction achievable based on the relatively easily obtainable laboratory measured sound absorption coefficients. The field trial also indicated that about 23 to 33% of the total tire-pavement noise reduction achieved by the porous asphalt mixtures could be attributed to their sound absorption capability. Such information obtainable from the laboratory sound absorption measurements can offer valuable guidance to pavement engineers in the mix design of quiet pavement mixtures.

Table 7-1 Aggregate Gradation and Mix Composition of Porous Asphalt Mix Designs and Other Mixes Studies

Sieve Size	Mix Design (% passing)				
	PA-13	PA-16	PA-20	PA-25	DG
20mm	-	-	100	100	100
16mm	-	100	95	90	-
13.2mm	100	70	85	75	90
9.5mm	85	59	72	55	72
4.75mm	45	33	22	19	54
2.36mm	30	22	18	15	36
1.18mm	25	16	-	-	26
600um	20	10	13	10	-
300um	13	6	9	8	14
150um	10	4	7	6	-
75um	4	3	6	4	6
Asphalt Binder	Performance grade polymer-modified binder PG76-22				Penetration grade Pen 60/70
% Asphalt by Weight of Total mix	Allowable range: 4.5 to 5.5%; 5.0% selected for present study.				
Target % Air Voids	10%	15%	20%	25%	4%
Actual Specimen % Air Voids	12%	16%	20%	25%	4%

Note: PA = porous asphalt mix, DG = dense graded mix.

Table 7-2 Porosity Values of Porous Asphalt Test Specimens

Mix Design	Target Porosity (%)	Porosity of Specimens (%)	Average Rounded-Off Porosity for Reporting (%)
PA-13	10%	11.86	12%
		12.32	
		13.10	
PA-16	15%	16.12	16%
		16.76	
		17.33	
PA-20	20%	20.85	20%
		21.76	
		19.98	
PA-25	25%	25.44	25%
		25.89	
		26.12	

Table 7-3 Estimated Noise Reductions Using Approximate Method Based on Noise Reduction Coefficient (NRC) and Sound Absorption Average (SAA)

Mix	Target Porosity (%)	Noise Reduction Coefficient (NRC)	Sound Absorption Average (SAA)	Noise Reduction (dBA)	
				Based on NRC	Based on SAA
PA-25	25	0.415	0.435	-1.0	-1.1
PA-20	20	0.440	0.474	-1.1	-1.2
PA-16	16	0.498	0.498	-1.2	-1.2
PA-13	12	0.448	0.473	-1.1	-1.2
DG	4	0.150	0.152	-0.3	-0.3

(a) Noise reduction contributions from structure mixtures

Mix	Percent Clogged (%)	Noise Reduction Coefficient (NRC)	Sound Absorption Average (SAA)	Noise Reduction (dBA)	
				Based on NRC	Based on SAA
PA-20	0	0.440	0.474	-1.1	-1.2
	28	0.413	0.440	-1.0	-1.1
	53	0.385	0.412	-0.9	-1.0
	76	0.283	0.282	-0.7	-0.7
	100	0.165	0.173	-0.4	-0.4

(b) Sound absorption and noise reductions as a function of degree of clogging

Mix	Specimen Thickness (mm)	Noise Reduction Coefficient (NRC)	Sound Absorption Average (SAA)	Noise Reduction (dBA)	
				Based on NRC	Based on SAA
PA-20	63	0.440	0.474	-1.1	-1.2
	100	0.428	0.443	-1.0	-1.1
	200	0.480	0.503	-1.2	-1.3

(c) Noise reductions of porous asphalt as a function of specimen thickness

Table 7-4 Comparison of Noise Reductions Computed from Field OBSI Measurements and Estimated Noise Reductions from Laboratory Data

Mix Type	Field Measurements		Approximate Method by Estimating Noise Reduction from Laboratory Measured SAA (dBA)	Percent Difference (%)
	Measured OBSI (dBA)	Computed Noise Reduction (dBA)		
PA-25	97.4	1.6	1.1	-31.3
PA-20	97.5	1.6	1.2	-25.0
PA-16	98.2	1.7	1.2	-29.4
PA-13	98.9	1.7	1.2	-29.4
DG	103.1	0.3	0.3	0

Table 7-5 Estimated Percent Contribution of Sound Absorption to Total Tire-Pavement Noise Reduction

Mix Type	Measured OBSI (dBA)	Total Noise Reduction with respect to DG mix (dBA)	Noise Reduction due to Sound Absorption (dBA)		Percent Noise Reduction Contribution due to Sound Absorption (%)
			With respect to $\alpha = 0$	With respect to DG mix	
PA-25	97.4	5.7	1.6	1.3	22.8
PA-20	97.5	5.6	1.6	1.3	23.2
PA-16	98.2	4.9	1.7	1.4	28.6
PA-13	98.9	4.2	1.7	1.4	33.3
DG	103.1	--	0.3	--	--

Note: α = sound absorption coefficient

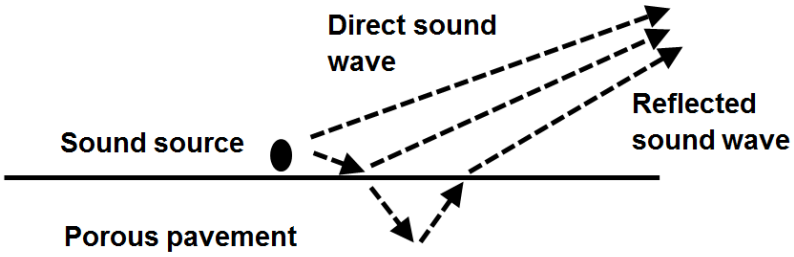

Figure 7-1 Schematic Representation of Reflection of Sound Wave

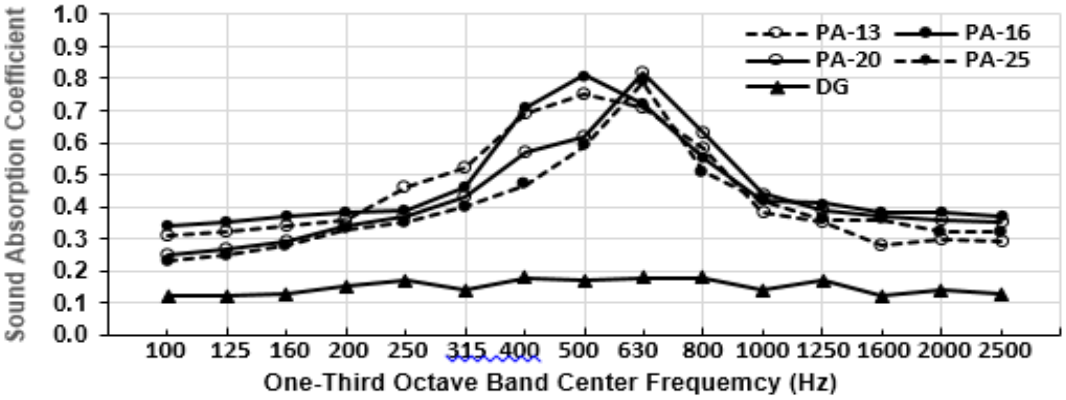

(a) Effect of mixture porosity on sound absorption coefficient spectra

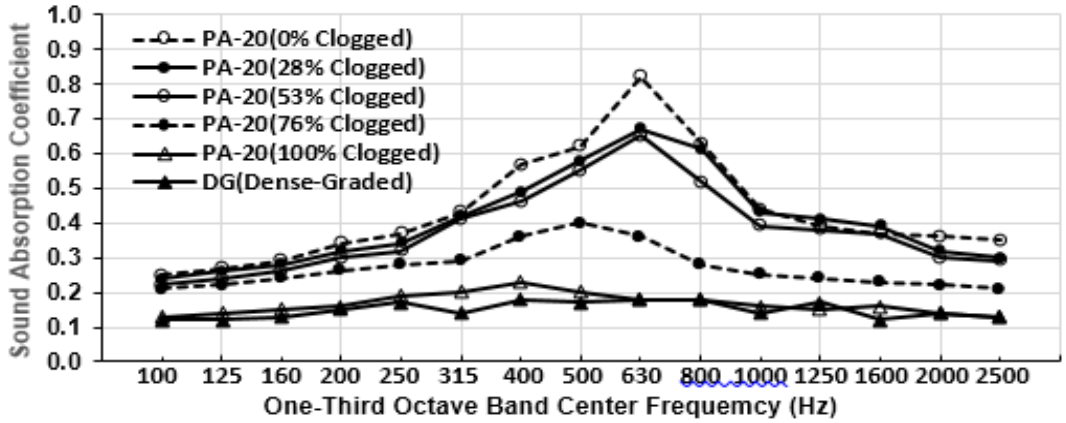

(b) Effect of percentage clogged on sound absorption coefficient spectra

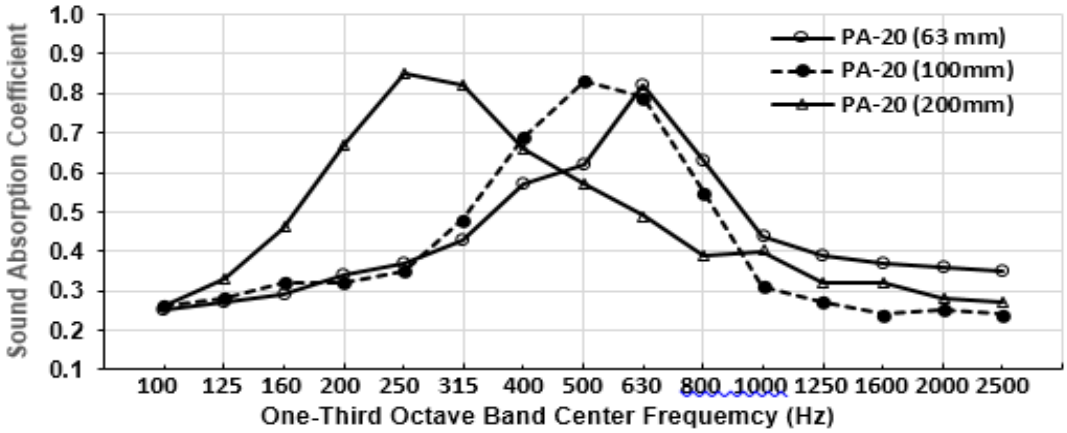

(c) Effect of specimen thickness on sound absorption coefficient spectra

Figure 7-2 Sound Absorption Coefficient Spectra as a Function of (a) Test Mixture Porosity Levels, (b) Percentage Clogged, and (c) Specimen Thickness

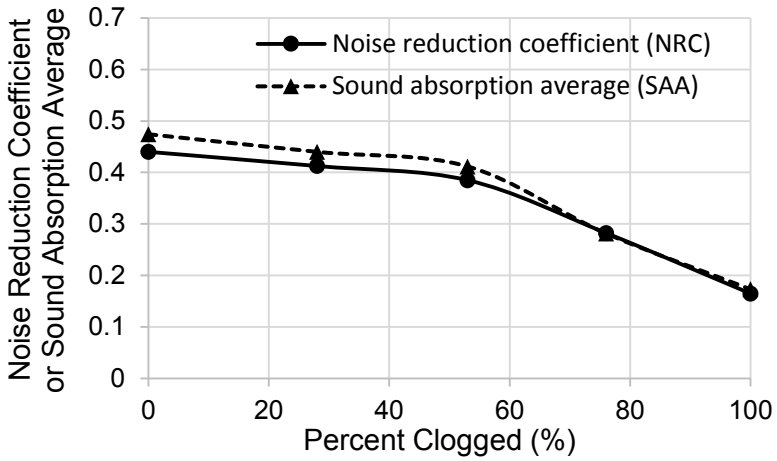

(a) Effect of percent clogging on noise reduction coefficient (NRC) and sound absorption average (SAA)

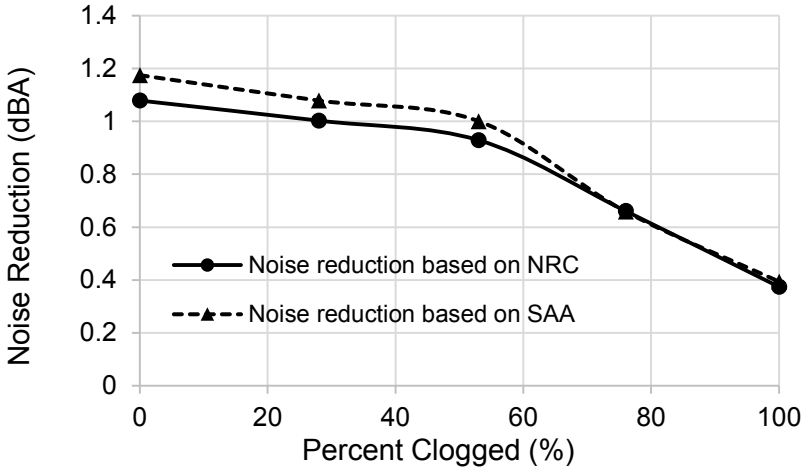

(b) Effect of percent clogging on noise reduction

Figure 7-3 Effects of Percent Clogging of Porous Asphalt Mixture on (a) NRC and SAA and (b) Noise Reduction

CHAPTER 8 CONCLUSIONS AND RECOMMENDATIONS

8.1 Achievements and Contributions of Research

The current pavement design method puts much of its effort on structural analysis to provide a pavement with an adequate structural capacity against different design failure modes. Unfortunately, the functional performance of pavements is not adequately addressed. There are also similar inadequacy in the current pavement management practice. To overcome some of these limitations, this research has been conducted to incorporate several important functional considerations into pavement design and management to improve (a) highway operational efficiency, (b) safe traffic operation, and (c) environmental sustainability.

The academic achievements and contributions of this research can be summarized as follows:

(1) The current pavement design procedures in use today either ignore the problem of rutting or are unable to provide a definite terminal rut depth as a design criterion. Similarly, there is no sound engineering basis of terminal rut depth to guide pavement engineers in planning their pavement management programs. This research has developed a theoretically sound procedure to derive quantitatively a terminal rut depth based on wet-weather driving safety considerations, to fill the knowledge gap in pavement design and pavement management.

(2) The current methods of selecting aggregates for asphalt paving mix design could not address the skid resistance requirements covering the entire life cycle of a pavement mixture. An improved framework of asphalt paving mix design procedure consisting of a laboratory phase

and an analytical evaluation phase has been developed in this research to enhance the rigor and completeness of the aggregate selection process.

(3) No rational procedures are available today in determining speed limits advisory for wet-weather driving. Based on the considerations of safe skid resistance, hydroplaning risk, and braking distance requirements, a theoretically sound engineering procedure for determining rain-related wet-weather speed limits for use in a variable speed advisory system has been derived.

(4) Porous pavements have been widely used to improve wet-weather skid resistance performance of pavements. However, no mechanistically derived procedure has been available to guide pavement engineers in determining the terminal state of a clogged porous pavement. This research has established such a procedure based on sound engineering consideration of skid resistance to arrive at a rational criterion of defining the terminal state of a clogged porous pavement.

(5) Another important benefit of porous pavement is to reduce tire-pavement noise. Conventional porous mix design does not address this requirement specifically in the mix design phase. This research proposes a laboratory procedure to measure the sound absorption characteristics of trial mixes, to serve as a useful guide on the likely tire-pavement noise reduction potential of the trial mixes.

8.1.1 Terminal Rut Depth for Pavement Design and Management

In the first part of this research work, a quantitative engineering procedure for establishing a terminal rut depth and a rut depth maintenance activation level for a rutted pavement, taking into consideration the actual pavement skid resistance characteristics and traffic operating speeds was

developed. This procedure first identifies the minimum skid resistance adopted by the highway agency concerned. Next, by using a finite element simulation model to derive the skid resistance intervention level curve and skid resistance-vehicle speed curves under different ponded rut depths, the terminal rut depth can be determined for a given pavement with the consideration of skidding risk, hydroplaning risk, and safe braking distance.

With this procedure, a terminal rut depth for pavement design and a rut depth maintenance intervention level can be established for a road section according to its unique design and operating conditions. This proposed procedure will provide the highway agency and the pavement engineer with a more effective pavement design and management tool to design and manage pavements according to their respective driving safety risks.

8.1.2 Improved Selection Procedure of Aggregates for Asphalt Pavement Considering Skid Resistance and Hydroplaning

Guidelines have been established by highway agencies in many parts of the world for the selection of aggregates in asphalt mix design. Such aggregate selection guidelines based on laboratory friction testing of polished aggregates or asphalt mixtures provide useful criteria for pavement engineers. However, the results obtained from laboratory tests do not provide one with all the information required to evaluate the skid resistance available from the pavement surface under actual road operating conditions. This part of the research presents a rational analytically sound procedure to select the mix design for an asphalt pavement when the aggregates are polished due to repeated traffic loading. It is based on three critical criteria, namely the braking distance of the pavement section concerned, the skid resistance and hydroplaning speeds on road

segments of the pavement section with different design speeds and under different weather conditions.

The procedure consists of a laboratory and evaluation phase. The laboratory phase measures the frictional resistance of the polished surface prepared with the aggregates to be evaluated at two selected test speeds. The evaluation phase applies the laboratory measured data to estimate field skid numbers at the desired speeds and calibrate a three dimensional finite element skid resistance simulation model for the purpose of predicting in-service field skid resistance performance, hydroplaning speed and also the braking distance of the polished mixture.

This procedure enables a pavement design engineer to check if the pavement designed can fulfil (i) the design maximum braking distance allowed, (ii) the acceptable minimum skid resistance adopted by the highway agency, and (iii) the maximum traffic speed allowed when the pavement has reached the polished state due to the repeated traffic.

8.1.3 Improved Procedure for Determining Rain-Related Wet-Weather Speed Limits

The maximum posted speed limit is commonly set at the 85th percentile operating speed or at a certain value below this speed. However, the maximum speed limit adopted by most of highway agencies does not differentiate between dry weather and wet weather and hence the maximum posted speed limit is not applicable during wet weather. This part of the research has been conducted to determine the maximum safe speed limit under different rainfall intensities for a given road section considering skidding and hydroplaning safety issues, and also the vehicle braking distance control.

A three-dimensional finite simulation model is first applied to compute the skid resistance available under different speeds. Next the speed limit is determined based on the two criteria mentioned below:

(a) Speed limit based on stopping distance — Based on the stopping sight distance of the road section considered, a speed limit can be computed in order to stop a vehicle within a safe distance when required.

(b) Speed limit based on minimum skid resistance — The speed limit based on the minimum skid resistance chosen by the highway agency concerned is determined using the skid resistance curves of the in-service pavement derived from finite simulation model under different water film thicknesses.

For each water film thickness, two speed limits based on the above two criteria can be obtained and the lower of these two speed limits is taken as the posted speed limit for the water film thickness. The process is repeated for other water film thickness until obtaining the speed limits for the full range of water film thickness as required.

8.1.4 Functional Approach for Determining Terminal Service State of Porous Pavement

The benefits of porous pavements in improving wet-weather driving safety are attributed to their high porous structure. The most serious form of distress affecting porous pavements' service life is clogging. The current pavement condition survey practices focus on distresses that relate basically to conventional non-porous pavements. This research has developed a rational engineering procedure based on the consideration of wet-weather driving safety

requirements to determine the terminal service state of a porous pavement affected by clogging.

The proposed procedure consists of a finite element skid resistance simulation model for porous pavements. This model is able to compute the skid resistance of a clogged porous pavement with a known permeability under a given rainfall intensity and vehicle speed. By applying this model, the minimum porous pavement permeability that can still produce an acceptable safe skid resistance can be identified. This terminal permeability defines the terminal service state of the porous pavement with respect to wet-weather driving safety. The proposed procedure helps to extend the capability of the current practice of pavement condition survey to cover porous pavements more adequately. It is also useful as a tool for effective de-clogging maintenance management of porous pavements.

8.1.5 Asphalt Mix Design Considering Sound Absorption Properties of Asphalt Mixtures

This part focuses on the choice of different mix designs that would help to reduce tire-pavement noise. Currently, such quantitative information is not available to guide pavement engineers in the mix design of porous asphalt pavement mixtures. There are also no recommended laboratory procedures for assessing the tire-pavement noise reduction of a design mix of porous asphalt mixture. This research develops a laboratory procedure and a method of analysis to assist pavement engineers in estimating the contribution to tire-pavement noise reduction by the porous structure of a porous asphalt design mix.

The proposed laboratory procedure consists of two main steps. In the first step, by means of acoustic impedance tubes, the sound absorption

coefficients of laboratory specimens of a test mix and a reference dense graded mix are measured. Next, with the measured sound absorption coefficients, the tire-pavement noise reduction of the test mix is estimated.

The procedure allows pavement engineers to examine the influence of the following mix properties on the sound absorption characteristics of the design mix: percent porosity of mixture, degree of clogging and thickness of specimens.

8.2 Recommendations for Further Research

This research has developed several procedures to address some deficiencies of the current pavement design methods and pavement management practices in their consideration of pavement functional requirements. More research works are needed before a comprehensive pavement design procedure and management system could be developed, giving full and complete consideration to all important functional requirements of a pavement. Listed below are some recommendations for further research in this direction:

(a) Besides traffic noise, this research does not address any other environmental sustainability issues in pavement design and management. Works are needed in the following four areas:

- Use of construction wastes or any other forms of waste as pavement materials.
- Recycling of pavement materials for new pavement construction.
- Use of recyclable pavement materials in pavement design.
- Use of materials that possess no risk of causing environmental pollution.

For each of the four applications highlighted above, the research required is likely to involve the development of new laboratory test

procedures to evaluate the suitability of the material in question for the intended application.

(b) The treatment of tire-pavement noise in the present research addresses only one aspect of the problem. It does not examine the effect of pavement surface macrotexture on the magnitude of tire-pavement noise generated. To study this problem, it is necessary to model the detailed three-dimensional geometric properties of the pavement surface, and their interaction with vehicle tires.

(c) All the safety requirements addressed in this thesis are related to skidding risk, hydroplaning potential, and braking distance adequacy along straight pavement sections. There are different safety requirements for pavement sections located along horizontal curves. This will require the analysis of skid resistance hydroplaning speed involving rolling tires with slip angles. The finite element models used in this thesis have to be extended to cover the cases of rolling tires with slip angles.

(d) The analyses presented in this thesis focus on asphalt pavements. Similar analyses could be applied to concrete pavements which have very different microtexture and macrotexture characteristics from those of asphalt pavements. For example, practically all concrete pavements will require their top surfaces to be textured or grooved. Some changes in the finite element modeling might be necessary to study the effects of these artificially created textures or grooves.

(e) For each of the new procedures proposed in this research, there is a need to conduct a detailed error analysis to ensure that the resulting controls recommended will be generating practically implementable and

achieving its intended objectives of providing a functional pavement design. Such an analysis requires detailed assessment of the accuracy and reliability of the parameter values and input data of the proposed procedure.

REFERENCES

AASHO (1961). AASHO Interim Guide for the Design of Rigid and Flexible Pavements. American Association of State Highway Officials, Washington D.C., USA.

AASHTO (1972). AASHTO Interim Guide for Design of Pavement Structures-1972. American Association of State Highway and Transportation Officials, Washington D.C., USA.

AASHTO (1976). Guidelines for Skid Resistant Pavement Design. Task Force for Pavement Design, American Association of State Highway and Transportation Officials, Washington, D.C., USA.

AASHTO (1985). AASHTO Guide for Design of Pavement. Structures. Pavements, Pavements. American Association of State Highway Officials, Washington D.C., USA.

AASHTO (1989). Report of the AASHTO Joint Task Force on Rutting. American Association of State Highway and Transportation Officials, Washington D.C., USA.

AASHTO (1993). AASHTO Guide for Design of Pavement. Structures. Pavements, Pavements. American Association of State Highway Officials, Washington D.C., USA.

AASHTO (2008a). Mechanistic-Empirical Pavement Design Guide, Interim Edition: A Manual of Practice. American Association of State and Highway Transportation Officials, Washington, D.C., USA.

AASHTO (2008b). Guide for Pavement Friction. American Association of State Highway Transportation Officials, Washington, D.C..

AASHTO (2011). A Policy on Geometric Design of Highways and Streets, 6th Edition, American Association of State Highway and Transportation Officials, Washington, D.C., USA.

AASHTO (2012). Pavement Management Guide. American Association of State Highway and Transportation Officials, Washington, DC.

AASHTO (2015). TP76 Standard Method of Test Measurement of Tire/Pavement Noise Using the On-Board Sound Intensity (OBSI). American Society of State and Highway Transportation Officials, Washington D.C., USA.

Abbott, P. G., and S. M. Phillips (1996). Vehicle Noise Levels Derived from the Statistical Pass-By Method and Road Surface Texture. NOISE-CON 1996, Seattle, Washington.

Abbott, P. G. and Watts (2004). The relationship between coast-by and close-proximity car tyre noise levels for different road surfaces. In Proceedings of INTER-NOISE 04, Prague, Czech Republic, pp. 531.

Abbott, P. G., P. A. Morgan and B. McKell (2010). A Review of Current Research on Road Surface Noise Reduction Techniques. Transport Research Laboratory, Wokingham, UK.

Agostinacchio, M. and Cuomo, G., (2006). Noise Emission Comparison between Porous Concrete and Porous Asphalt Road Pavements. Proceedings 10th International Symposium on Concrete Roads, Brussels, Belgium, 8-22 September 2006, pp. 1-10.

Ahammed, M. A. and S. L. Tighe (2011). Asphalt Pavements Surface Texture and Skid Resistance – Exploring the Reality. Published by NRC Research Press. Can. J. Civ. Eng. 39: pp. 1-9.

Ahlvin R. G. (1991). Origin of Developments for Structural Design of Pavements. Technical Report GL-91-26, USAE Waterways Experiment Station, US Army Corps of Engineers, Vicksburg, MS.

Al-Kaisy, A., L. Ewan and D. Veneziano (2012). Evaluation of a Variable Speed Limit System for Wet and Extreme Weather Conditions: Phase 1. Report No. FHWA-OR-RD-12-14, Oregon Department of Transportation, Salem, OR.

American Association of State Highway Transportation Officials (AASHTO) (2008). Guide for Pavement Friction. AASHTO, Washington, D.C..

Anderson, D. A., R. S. Huebner, J. R. Reed, J. C. Warner and J. J. Henry (1998). Improved surface drainage of pavement", National Cooperative Highway Research Program Web Document 16, Transportation Research Board, National Research Council.

Anfosso-Lédée, F. (2004). Modeling the local propagation effects of tire-road noise: Propagation filter between CPX and CPB measurements. In Proceedings of INTER-NOISE 04, Prague, Czech Republic, pp. 2543.

Asphalt Institute (1981). Cause and Prevention of Stripping in Asphalt Pavements. Educational Series No. 10, Asphalt Institute, College Park, MD.

ASTM (1996). Test Method for Determining the Polishability of Bituminous Pavement Surfaces and Specimens by Means of the Penn State

Reciprocating Polishing Machine (Withdrawn 1997). ASTM E1393-90, ASTM International, West Conshohocken, PA.

ASTM (1999). Calculating International Friction Index of a Pavement Surface. Vol.04.03, ASTM E-1960, ASTM International, West Conshohocken, PA.

ASTM (2000). Standard Specification for Standard Smooth Tire for Pavement Skid-Resistance Tests, ASTM E524-88, ASTM International, West Conshohocken, PA, USA.

ASTM (2002). Standard Test Method for Skid Resistance Measurements Using the North Carolina State University Variable-Speed Friction Tester (Withdrawn 2006). ASTM E707-90, ASTM International, West Conshohocken, PA.

ASTM (2005). Standard Guide for Examination of Documents Produced with Liquid Ink Jet Technology (Withdrawn 2014), ASTM E2389-05, ASTM International, West Conshohocken, PA.

ASTM (2008a). Standard Specification for Standard Rib Tire for Pavement Skid-Resistance Tests, ASTM E501-08, ASTM International, West Conshohocken, PA.

ASTM (2008b). Standard Specification for Smooth Tire for Pavement Skid-Resistance Tests, ASTM E524-08, ASTM International, West Conshohocken, PA.

ASTM (2009a). Standard Test Method for Measuring Paved Surface Frictional Properties Using the Dynamic Friction Tester. ASTM E1911-09ae1, ASTM International, West Conshohocken, PA.

ASTM (2009b). Standard Test Method for Sound Absorption and Sound Absorption Coefficients by the Reverberation Room Method. ASTM C423-09a, ASTM International, 2009, West Conshohocken, PA.

ASTM (2010a). Standard Practice for Preparation of Bituminous Specimens Using Marshall Apparatus. International Standard D6926-10, ASTM International, West Conshohocken, PA.

ASTM (2010b). Standard Test Method for Impedance and Absorption of Acoustical Materials using a Tube, Two Microphones and a Digital Frequency Analysis System. ASTM E1050-10, ASTM International, West Conshohocken, PA.

ASTM (2011a). Standard Test Method for Skid Resistance of Paved Surfaces Using a Full-Scale Tire. ASTM E274/E274M – 11, ASTM International, West Conshohocken, PA.

ASTM (2011b). Standard Practice for Accelerated Polishing of Aggregates or Pavement Surfaces Using a Small-Wheel, Circular Track Polishing Machine. ASTM E660-90, ASTM International, West Conshohocken, PA.

ASTM (2013a). Standard Practice for Accelerated Polishing of Aggregates Using the British Wheel. ASTM D3319-11, ASTM International, West Conshohocken, PA.

ASTM (2013b). Standard Test Method for Measuring Surface Frictional Properties Using the British Pendulum Tester. ASTM E303-93, ASTM International, West Conshohocken, PA.

ASTM (2014). Standard Test Method for Skid Resistance of Paved Surfaces Using a Full-Scale Tire. ASTM E274-11, ASTM International, West Conshohocken, PA, USA.

ASTM (2015a). Standard Test Method for Measuring Pavement Macrotexture Depth Using a Volumetric Technique. ASTM E965-15, ASTM International, West Conshohocken, PA.

ASTM (2015b). Standard Test Method for Measuring Pavement Macrotexture Properties Using the Circular Track Meter. ASTM E2157-15, ASTM International, West Conshohocken, PA.

ASTM (2015c). Standard Practice for Calculating Pavement Macrotexture Mean Profile Depth, ASTM E1845-15, ASTM International, West Conshohocken, PA.

ASTM (2015d), Standard Test Method for Testing Side Force Friction on Paved Surfaces Using the Mu-Meter, ASTM E670-09, ASTM International, West Conshohocken, PA.

Baladi, G. (1987). Fatigue Life and Permanent Deformation Characteristics of Asphalt Concrete Mixes. Transportation Research Record 1227. Transportation Research Board. National Research Council. Washington, D.C..

Balmer, G. G. and B. E. Colley (1966). Laboratory Studies of the Skid Resistance of Concrete. American Society for Testing and Materials, Journal of Materials, Vol. 1-No. 3.

Balmer, G. G. and B. M. Gallaway (1983). Pavement Design and Controls for Minimizing Automotive Hydroplaning and Increasing Traction. In

Frictional Interaction of Tire and Pavement, ASTM STP 793, ed. by W. E. Meyer and J. D. Walters, American Society for Testing and Materials, Philadelphia. pp. 167-190.

Bathe, K. J. (1996). Finite Element Procedures, Prentice Hall, New Jersey.

Barksdale, R. D. (1972). Laboratory evaluation of rutting in base course materials. Proceedings of the Third international Conference on the Structural Design of Asphalt Pavements, Vol. 1, London, pp. 161-174.

Beale M. H., M. T. Hagan and H. B. Demuth (2015). Neural Network Toolbox™ User's Guide. The MathWorks, Inc., Natick, MA.

Beckenbauer, T. and A. Kuijpers (2001). Prediction of pass-by levels depending on road surface parameters by means of a hybrid model. In Proceedings of INTER-NOISE 01, pp. 2528.

Bendtsen, H. (1998). Porous Asphalt Pavement and Noise Reduction over a Long Period. EURO-NOISE, Munich, Germany.

Bergmann, M. (1980). Noise generation by tire vibrations. In Proceedings of INTER-NOISE 80, pp. 239, Miami, FL.

Bloem, D. L. (1971). Skid-Resistance: The Role of Aggregates and Other Factors. National Sand and Gravel Association Circular 109, Silver Spring, MD.

Bolton, J. S., H. J., Song, Y. K., Kim and J. K., Yeon (1998). The Wave Number Decomposition Approach to the Analysis of Tire Vibration. NOISE-CON 1998, Ypsilanti, Michigan.

Boscaino G., F. G. Praticò (2001). A Classification of Surface Mixture Indices of Pavement Surfaces. Bulletin des Laboratoires des Ponts et Chaussées, Issue 234, pp. 17-34, 123,125,127.

British Standard BS ISO 11819-2.2 (2015) Acoustics - Method for Measuring the Influence of Road Surfaces on Traffic Noise. British Standards Institution, London, UK.

British Standard BS 7941-1 (2006). Methods for Measuring the Skid Resistance of Pavement Surfaces. Sideway-Force Coefficient Routine Investigation Machine. British Standards Institution, Bristol, UK.

British Standard BS 812 (1960). Methods for Sampling and Testing Mineral Aggregates, Sands and Fillers. British Standard Institution, Bristol, UK.

British Standard BS 812 (1989). Testing aggregates - Part 114: Method for determination of the polished-stone value. British Standards Institution, Bristol, UK.

Brosseaud, Y., J. L. Delorme and R. Hiernaux (1993). Use of LPC Wheel Tracking Rutting Tester to Select Asphalt Pavements Resistant to Rutting. Transportation Research Record #1384, TRB, National Research Council, Washington, D.C..

Browne, A. L. (1975). Mathematical Analysis for Pneumatic Tire Hydroplaning. In Surface Texture verses Skidding: Measurements, Frictional Aspects, and Safety Features of Tire-pavement Interaction. ASTM STP 583, ed. by J. G. Rose, American Society for Testing and Materials, Philadelphia, pp. 75-94.

Brown, R. (1996). Physical Testing of Rubber, Chapman & Hall, London, UK.

Bschorr, O. (1985). Reduction of Tire Noise. INTER-NOISE 85, Munich, Germany.

BS EN 12697-49 (2014). Bituminous mixtures. Test methods for hot mix asphalt. Determination of friction after polishing. British Standards Institution, Bristol, UK.

BSI (2014). BS EN 12697-49:2014 Test methods for hot mix asphalt. Determination of friction after polishing. British Standards Institution, Bristol, UK.

Buratti C. and E. Moretti (2010). Traffic Noise Pollution: Spectra Characteristics and Windows Sound Insulation in Laboratory and Field Measurements. Journal of Environmental Science and Engineering, Volume 4, No.12.

Burnett, W.C., J. L. Gibson, and E. J. Kearney (1968). Skid Resistance of Bituminous Surfaces. Highway Research Record No. 236, pp. 49-60.

California Department of Transportation (Caltrans) (2006). Maintenance Manual, Volume 1. Caltrans, Sacramento, CA.

Caltrans (2011). Eight Year Evaluation of the Noise Performance of the Caltrans Asphalt Research Pavements on LA 138. Report prepared by Illingworth and Rodkin, Inc. for Caltrans.

Carey, W. N. and P. E. Irick (1960). The pavement serviceability performance concept. Highway Research Bulletin No. 250, Transportation Research Board, Washington D. C., USA.

Central Massachusetts Regional Planning Commission (CMRPC) (2006). Pavement Management Field Guide to Road Surface Distresses. CMRPC, Worcester MA.

Chakroborty, P., D. Animeshs (2003). Principles of Transportation Engineering. PHI Learning Pvt. Ltd.

Chu, L. and Fwa T.F. (2016). Incorporating Pavement Skid Resistance and Hydroplaning Risk Considerations in Asphalt Mix Design. Journal of Transportation Engineering, 142(10), 04016039-1-10. DOI: 10.1061/(ASCE)TE.1943-5436.0000872.

Corwill, D. M. (1989). Antiskid properties of road surfacing. Proc., Int. Proceedings Symposium on Road Development and Safety, Luxembourg, Belgium.

Coulomb, C. A. (1785). Theorie des Machines Simpes, En Ayant Egard au Frottement de Leurs Parties, et la Roideur des Ordages. Mem Math Phys Paris, x, pp. 161-342.

Crouch, L., J. Gothard, G. Head, and W. Goodwin (1995). Evaluation of Textural Retention of Pavement Surface Aggregates. Transportation Research Record 1486:124–129.

Crouch, L., J. Gothard, G. Head and W. Goodwin (1995). Evaluation of Textural Retention of Pavement Surface Aggregates. Transportation Research Record 1486, Transportation Research Board, Washington, D.C., pp. 124-129.

Csathy, T.I., W. C. Burnett and M. D. Armstrong (1968). State-of-the-Art of Skid Resistance Research. Highway Research Board Special Report 95,

Highway Research Board, National Research Council, Washington, D.C..

Cybenko, G. (1989). Approximations by Superpositions of Sigmoidal Functions. Mathematics of Control, Signals, and Systems, 2(4), 303-314.

Dahir, S. H., J. J. Henry and W. E. Meyer (1979). Final Report: Seasonal Skid Resistance Variations. Pennsylvania Department of Transportation (PENNDOT), Harrisburg.

Dahir, S. H., W. E. Meyer and R. R. Hegmon (1976). Laboratory and Field Investigation of Bituminous Pavement and Aggregate Polishing. Transportation Research Record 584, Transportation Research Board, TRB, National Research Council, Washington, D.C.

Dare, T. P. (2012). Generation Mechanisms of Tire-Pavement Noise. Ph.D. thesis, Purdue University, West Lafayette, Indiana.

Davis D. and E. Patronis (2006). Sound System Engineering. Third Ed. Focal Press (Elsevier imprint), Burlington, MA.

DCCD (2012). Porous Asphalt. Best Management Practices Fact Sheet, Dauphin County Conservation District, PA.

Descornet, G., and U. Sandberg (1980). Road Surface Influence on Tire Noise. INTER-NOISE 80, Miami, Florida.

Descornet, G. and U. Sandberg (1980). Road surface influence on tire noise - II. In Proceedings of INTER-NOISE 80, pp. 267, Miami, FL.

Dewey, G. R., A. C. Robords, B. T. Armour and R. Muethel (2001). Aggregate Wear and Pavement Friction. Presented at 80th Transportation Research Board Annual Meeting, Washington, D.C..

Dillard, J. H. and R. A. Alwood (1957). Providing Skid-Resistant Roads in Virginia. Association of Asphalt Pavement Technologists (AAPT) Proceedings, Volume 26, pp. 1-22.

Do, M.-T., Z. Tang, M. Kane and F. de Larrard (2007). Pavement polishing – Development of a dedicated laboratory test and its correlation with road results. Wear, Volume 263, pp. 36-42.

Domenichini, L., M. Crispino, M. D'Apuzzo, R. Ferro, G. Boscanino, F. la Torre, F. G. Praticò (1998). Rumore e Vibrazinoi da traffic – L' influenza delle caratteristiche superficiali delle pavimentazioni – PIARC book, National Italian Committee, Vernoa.

Donavan, P. R., and D. M. Lodico (2009). Tire/Pavement Noise of Test Track Surfaces Designed to Replicate California Highways. INTER-NOISE 09, Ottawa, Canada.

Dorman, G. M. (1962). The extension to practice of a fundamental procedure for design of flexible pavements, Proceedings of 1st International Conference of Structural Design of Asphalt Pavements, pp. 785-793.

Donavan, P. R. (2008). Comparative Measurements of Tire/Pavement Noise in Europe and the United States - NITE I. INTER-NOISE 08, Shanghai, China.

DOTD (2006). Standard Specifications for Roads and Bridge Manual. Louisiana Department of Transportation and Development (DOTD), Baton Rouge, LA.

Donavan, P. R. (2008). Comparative Measurements of Tire/Pavement Noise in Europe and the United States - NITE I. INTER-NOISE 08, Shanghai, China.

Donavan, P. R., and D. M. Lodico (2009). Measuring Tire-Pavement Noise at the Source. Transportation Research Board of the National Academies, Washington D.C. .

Donavan, P. R., and L. J. Oswald (1980). The Identification and Quantafication of Truck Tire Noise Sources under on-Road Operating Conditions. INTER-NOISE 80, Miami, Florida.

Eberhardt, A. C. (1984). Development of a Transient Response Model for Tire/Pavement Interaction. INTER-NOISE 84, Honolulu, Hawaii.

Ejsmont, J. A. (1982). Comparison of Road and Laboratory Measurements and Influence of Some Tire Parameters on Generation of Sound. Swedish Road and Transport Research Institute, Borlänge, Sweden.

Ergun, M., S. Iyinam and A. F. Iyinam (2005). Prediction of Road Surface Friction Coefficient Using Only Macrotexture and Microtexture Measurements. Journal of Transportation Engineering, Vol. 131, No. 4.

Erin, L. D. and B. B. Courtney (2003). Measurement of automobile tire tread vibration and radiated noise. In Proceedings of Noise-Con 03, pp. 168, Cleveland, OH.

Erukulla, S. (2011). Refining a Laboratory Procedure to Characterize Change in Hot-Mix Asphalt surface Friction. Master of Science Thesis, Auburn University, Auburn, AL.

EU (1996). Future Noise Policy - European Commission Green Paper. European Commission, Brussels, Belgium.

FCPA (1990). Pervious Pavement Manual, Florida Concrete and Products Association, Orlando, FL, pp. 57.

Federal Highway Administration (FHWA) (2010a). Pavement Friction Management. Technical Advisory T 5040.38, FHWA, Washington, D.C..

Federal Highway Administration (FHWA) (2010b). Pavement Management Roadmap. Report FHWA-HIF-11-011. Federal Highway Administration, Washington, D.C..

Feighan, K. (2006). Pavement Skid Resistance Management. In T. F. Fwa (Ed.), Handbook of Highway Engineering, Taylor & Francis Group, Boca Raton, FL, pp. 21.1-21.32.

Fitzpatrick, K., P. Carlson, M. A. Brewer, M. D. Wooldridge and S. P. Miaou (2003). Design Speed, Operating Speed, and Posted Speed Practices. NCHRP Report 504, National Cooperative Highway Research Program, Transportation Research Board, Washington, D.C..

Flintsch, G.W., E. De Leon, K.K. McGhee and I.L. Al-Qadi (2003). Pavement Surface Macro-texture Measurement and Application. Transportation Research Board (TRB), Washington, D.C..

Flintsch, G.W., Y. Luo and I. L. Al-Qadi (2005). Analysis of the Effect of Pavement Temperature on the Frictional Properties of Flexible Pavement Surfaces. Presented at 84th Transportation Research Board Annual Meeting, Washington, D.C..

Forster, S. W. (1989). Pavement Micro-texture and its Relation to Skid Resistance. Transportation Research Record 1215, Transportation Research Board, TRB, National Research Council, Washington D.C..

Freitas, E. F. (2012). The Effect of Time on the Contribution of Asphalt Rubber Mixtures to Noise Abatement. Noise Control Engineering Journal, 60 (1).

French design manual for pavement structures (1997). Guide Technique, LCPC and SETRA, Union Des Synducates, De L'industrie Routiere, Francaise.

Fujikawa, T., H. Koike, Y. Oshino and H. Tachibana (2006). Road Texture for Abating Truck Tire Noise Generation. INTER-NOISE 06, Honolulu, Hawaii.

Fwa, T. F., Chu, L. and Tan, K. H. (2016). Rational procedure for determination of rut depth intervention level in network-level pavement management. Transportation Research Record, No. 2589, 59-67.

Fwa, T. F., E. Lim and K. H. Tan (2015). Comparison of Permeability and Clogging Characteristics of Porous Asphalt and Pervious Concrete Pavement Materials. Transportation Research Record, No. 2511, Transportation Research Board, pp. 72-80.

Fwa, T. F. and G. P., Ong (2008). Wet-pavement hydroplaning risk and skid resistance: analysis. Journal of Transportation Engineering, 134(5), pp. 182-190.

Fwa T. F., Pasindu, H. R. and G. P. Ong (2012). Critical Rut Depth for Pavement Maintenance Based on Vehicle Skidding and Hydroplaning Consideration. Journal of Transportation Engineering, Vol. 138, No. 4, pp. 423-429.

Fwa T. F., S. A. Tan, and C. T. Chuai (1998). Permeability Measurement of Base Materials using Falling-Head Test Apparatus. Transportation Research Record No. 1615, Transportation Research Board, pp. 94-99.

Fwa, T. F., Tan S. A. and Guwe Y. K. (2001). Expedient Permeability Measurement for Porous Pavement Surface. International Journal of Pavement Engineering, 2(4), 2001, 259-270.

Fwa, T. F., Tan S. A. and Guwe, Y. K. (2002). Laboratory Evaluation of Clogging Potential of Porous Asphalt Mixtures. Transportation Research Record, No. 1681, 43-49.

Gert, H. (1997). Hysteresis friction of sliding rubbers on rough and fractal surfaces, Rubber Chem. Technol. 70 (1) pp. 1–14.

Gibbs, D., R. Iwasaki, R. Bernhard, J. Bledsoe, D. Carlson, C. Corbisier, K. Fults, T. Hearne, J. K. McMullen, D. Newcomb, C. P. Roberts, J. Rochat, L. Scofield and M. Swanlund (2005). Quiet Pavement Systems in Europe. Federal Highway Administration, Washington D.C..

Goh, K. J. (2015). Analysis of spatial envelope rainfall-intensity-duration-frequency curves for Singapore. Bachelor of Civil Engineering thesis, School of Civil And Environmental Engineering, Nanyang Technological University, Singapore.

Goodwin, L. C. (2003). Best Practices for Road Weather Management, Version 2.0. Report No.FHWA-OP-03-081, Federal Highway Administration, Washington, D. C..

Gough, V. E. (1959). Discussion of Paper by D. Tabor. Revue Generale Du Caoutchouc, Vol.36, No. 10, pp. 1409.

Gray, J. E. and F. A. Renninger (1965). The Skid Resistant Properties of Carbonate Aggregates. Highway Research Record 120, Highway Research Board, National Research Council, Washington, D.C.

Gough, V. E. (1958). Friction of Rubber. The Engineer, pp701-704.

Haider, M., G. Descornet, U. Sandbery, F. G. Pratico (2007). Road Traffic Noise Emission: Recent developments and Future Prospects, International SIIV Congress, Palermo.

Hall J. W., K. L. Smith, L. Titus-Glover, J. C. Wambold, T. J. Yager and Z. Rado (2009). Guide for Pavement Friction. NCHRP Web-Only Document 108, National Cooperative Highway Research Program, Washington D.C..

Han, C., J. Luk, V. Pyta and P. Cairney (2009). Best Practices for Variable Speed Limits: Literature Review. Report AP-R342-09, Austroads, Sydney, Australia.

Harald, A. (1990). Skid Resistance and Road Surface Texture. Proceedings Symposium on Surface Characteristics of Roadways. American Society of Testing and Materials (ASTM), Philadelphia, PA.

Henry, J.J. (2000). Evaluation of Pavement Friction Characteristics. NCHRP Synthesis 291, National Cooperative Highway Research Program (NCHRP), Washington, D.C..

Henry J. J. (1986). The Wet-Pavement Traction Measurement: A State-of-the-Art Review. ASTM STP No. 929, Ed. Potting M. G. and T. J. Yager, American Society for Testing and Materials, West Conshohocken, PA, pp. 3-25.

Henry J. J. and M. C. Leu (1978). Prediction of Skid Resistance as a Function of Speed from Pavement Texture. Transportation Research Record 666, pp. 7-10.

Henry, J. J., H. Abe, S. Kameyama, A. Tamai, A. Kasahara and K. Saito (2000). Determination of the International Friction Index (IFI) Using the Circular Texture Meter (CTM) and the Dynamic Friction Tester (DFT). Permanent International Association of Road Congresses (PIARC) IVth Symposium on Surface Characteristics, Nantes, France, Publication No. 109.01.06.B- 2000.

Henry, J.J., and K. Saito (1983). Skid-Resistance Measurements with Blank and Ribbed Test and Their Relationship to Pavement Texture. Transportation Research Record, ISSN 0361-1981, (946): pp. 38-43.

Hicks, R. G., S. Seeds, D. G. Peshkin (2000). Selecting a Preventive Maintenance Treatment for Flexible Pavements. Report No. FHWA-IF-00-027, Federal Highway Administration, Washington, D.C..

Highways England (2006). UK Design Manual for Roads & Bridges (DMRB). Highways England, Guildford, UK.

Highway Research Board (1972). Skid resistance, National Cooperative Highway Research Program Synthesis of Highway Practice, No. 14, Washington, D.C..

Hinze, J. O. (1975). Turbulence. Second edition, McGraw-Hill, New York.

Highways England (2006). UK Design Manual for Roads & Bridges (DMRB). Highways England, Guildford, UK.

Hogervorst, D. (1974). Some Properties of Crushed Stone for Road Surfaces. Bulletin of the International Association of Engineering Geology, Vol. 10, No.1, Springer.

Horne, W. B. (1969). Results from Studies of Highway Grooving and Texturing at NASA Wallops Station. In Pavement Grooving and Traction Studies, NASA SP-5073. National Aeronautic and Space Administration, Washington D.C., USA, pp. 425-464.

Horne, W. B., J. L. McCarty and J. Tanner (1976). Some Effects of Adverse Weather Conditions on Performance of Airplane Antiskid Braking Systems, NASA Technical Note D-8202, National Aeronautic and Space Administration, Washington D.C..

Horne, W. B. and R. C. Dreher (1963). Phenomena of Pneumatic Tire Hydroplaning, NASA Technical Note D-2056, National Aeronautics and Space Administration, Washington D.C.

Horne, W. B. and T. J. W. Leland (1962). Influence of Tire Tread Pattern and Runway Surface Condition on Braking Friction and Rolling Resistance of a Modern Aircraft Tire. NASA TND-1376, NASA, USA.

Horne, W. B. and U. T. Joyner (1965). Pneumatic Tire Hydroplaning and Some Effects on Vehicle Performance. SAE Paper 970C.

Hossain, M. S., F. Parker and P. S. Kandhal (2000). Comparison and Evaluation of Tests for Coarse Aggregate Particle Shape, Angularity, and Surface Texture. J. of Testing and Evaluation, Vol. 28, No. 2, 2000, pp. 77-87.

Ibrahim, A. T. and F. L. Hall (1994). Effect of Adverse Weather Conditions on Speed-Flow-Occupancy Relationships. Transportation Research Record 1427, pp. 184-191.

Ibrahim, M. A. (2007). Evaluation Skid Resistance of Different Asphalt Concrete Mixes. Building and Environment, Elsevier Ltd. Vol. 42, pp. 325-329.

Institute of Highway Planning and Design (IHPD) (1997). Specifications for design of highway asphalt pavement, People's Communication Press, Beijing.

International PIARC Experiment to Compare and Harmonize Texture and Skid Resistance Measurements (1995). PIARC Report 01.04.T. The World Road Association, Paris.

IRC:37-2001 (2001). Guidelines for the design of flexible pavements, 2nd revision, IRC.

Isenring, T., H. Koster and I. Scazziga (1990). Experiences with porous asphalt in Switzerland. Transportation Research Record: Journal of the Transportation Research Board, No. 1265, pp. 41-53.

ISO (1997). Acoustics - Measurement of the Influence of Road Surfaces on Traffic Noise - Part 1: Statistical Pass-By Method. ISO 11819-1, International Organization for Standardization, Geneva, Switzerland.

ISO (2003). Tyres - Coast-By Methods for Measurement of Tyre-to-Road Sound Emission. ISO 13325, International Organization for Standardization, Geneva, Switzerland.

ITE (2009). Traffic Engineering Handbook, 6th Edition, Publication No. TB-010B, Institute of Traffic Engineers (ITE), Washington, D.C..

Iwai, S., Y. Miura, H. Koike and G. Levy (1994). Influence of Porous Asphalt Pavement Characteristics on the Horn Amplification of Tire/Road Contact Noise. INTER-NOISE 94, Yokohama, Japan.

Izevbekhai, B. I. and Maloney, M. (2011). Maintenance and Evaluation of Porous Pavement Infrastructure in Minnesota. [CD-ROM] 90th Annual Transportation Research Board Meeting, January 25-28, 2011.

Jayawickrama, P.W., B. Thomas (1998). Correction of field skid measurements for seasonal variations in Texas. Transportation Research Record (1639). pp. 147-154.

Jayawickrama, P. W., R. Prasanna and S. P. Senadheera (1996). Survey of state practices to control skid resistance on hot-mix asphalt concrete pavements. Transportation Research Record No. 1536, pp. 52-58.

Jonkers, E., G. Klunder, R. van der Horst, and R. de Rooy (2008). Development of an Algorithm for Using Weather-Dependent Dynamic Speed Limits to Enhance Safety. Proceedings of 15th World Congress on ITS, 16-20 November 2008, New York, NY, pp. 2100-2109.

Kandhal, P., and F. Jr. Parker (1998). Aggregate Tests Related to Asphalt Concrete Performance in Pavements. National Cooperative Highway Research Program Report 405, Transportation Research Board, National Research Council, Washington, D.C..

Kandhal, P. S. (2004). Tire/ Pavement Noise. Hot Mix Asphalt Technology. National Asphalt Pavement Association, pp. 22-31.

Karol, J. K., S. M. Rebecca, O. Jan and S. Ayesha (2010). Determination of the Binder Content of Hot Mix Asphalt Containing Dolomitic Aggregates

Using the Ignition Oven, Report No. FHWA/IN/JTRP-2010/13, SPR-2862. Federal Highway Administration, U.S. Department of Transportation Office of Safety, Washington D.C..

Katz, B., C. O'Donnell, K. Donoughe, J. Atkinson, M. Finley, K. Balke, B. Kuhn, D. Warren (2012). Guidelines for the Use of Variable Speed Limit Systems in Wet Weather, Report No. FHWA-SA-12-022, Federal Highway Administration, U.S. Department of Transportation Office of Safety, Washington D.C..

Kawamura, A., M. Takahashi, and T. Inoue (2001). Basic Analysis of Measurement Data from Japan in EVEN Project, Transportation Research Record, No. 1764, TRB, Washington, DC.. pp. 232-242.

Kennedy, C. K., A. E. Young and I. C. Buttler (1990). Measurement of Skidding Resistance and Surface Texture and the Use of Results in the United Kingdom. Proceedings Symposium on Surface Characteristics of Roadways. American Society of Testing and Materials (ASTM), Philadelphia, PA.

Khasawneh, M. A. (2008). The Development and Verification of New Accelerated Polishing Machine. Ph. D Dissertation, Graduate Faculty of the University of Akron, Akron, OH.

Kinsler, L. E., A. R. Frey, A. B. Coppens and J. V. Sanders (2000). Fundamentals of Acoustics, John Wiler & Sons, Inc, New York.

Koiki, H., T. Fujikawa, Y. Oshino and H. Tachibana (1999). Generation Mechanism of Tire/Road Noise Part 2: Pipe Resonance in Tread Groove of Tire. INTER-NOISE 99, Fort Lauderdale, Florida.

Kokkalis, A. G., G. H. Tsohos and O. K. Panagouli (2002). Consideration of Fractals in Pavement Skid Resistance Evaluation. Journal of Transportation Engineering, Vol. 128, No. *6*, pp. 591-595.

Kowalski, K., R. S. McDaniel, A. Shah and J. Olek (2009). Long-Term Monitoring of Noise and Frictional Properties of Three Pavements: Dense-Graded Asphalt, Stone Matrix Asphalt, and Porous Friction Course. Transportation Research Record, 2127, pp. 12-19.

Kroger, M., M. Lindner and K. Popp (2004). Influence of Friction on Noise and Vibrations of Tyres. INTER-NOISE 04, Prague, Czech Republic.

Kropp, W., F. X. Bécot and S. Barrelet (2000). On the Sound Radiation from Tires. Acta Acoustica, 86(5), pp. 769-779.

Kropp, W., K. Larsson, F. Wullens, P. Andersson, F. X. Becot, and T. Beckenbauer (2001). The modelling of tyre/road noise - A quasi three-dimensional model. In Proceedings of INTER-NOISE 01, The Hague, Holland, pp. 2322.

Kubiak E. J., P. G. Dierstein and F. K. Jacobson (1972). Modification and Calibration of the Illinois Skid Test System. Research and Development Report No. 41, Illinois Department of Transportation, Springfield, IL.

Kulakowski, B.T. and W. E. Meyer (1990). Skid Resistance of Adjacent Tangent and Nontangent Sections of the Roads. Transportation Research Record 1215, Transportation Research Board, TRB, National Research Council, Washington, D.C.

Kummer, H.W. and W. E. Meyer (1963). Penn State Road Surface Friction Tester as Adapted to Routine Measurement of Pavement Skid Resistance. Road Surface Properties, 42nd Annual Meeting.

Larson R. N. and K. D. Smith (2008). Relationship between Skid Resistance Numbers Measured with Ribbed and Smooth Tire and Wet-Accident Locations. Report FHWA/OH-2008/11, Ohio Department of Transportation, Columbus, OH.

Larsson, K. and W. Kropp (1999). A high frequency range tyre model based on two coupled elastic plates. In Proceedings of INTER-NOISE 99, pp. 131, Fort Lauderdale, FL.

Launder, F. T., D. B. Spalding (1974). The numerical computation of turbulent flows. Computation Methods in Applied Mechanics in Engineering, 3, pp. 269-289.

Leu, M. C. and J. J. Henry (1983). Prediction of Skid Resistance as a Function of Speed from Pavement Texture. Transportation Research Record 946, Transportation Research Board, National Research Council, Washington, D.C..

Li, M., W. van Keulen, H. Ceylan, G. Tang, M. van de Ven, and A. Molenaar (2015). Influence of Road Surface Characteristics on Tire-Road Noise for Thin-Layer Surfacing. Journal of Transportation Engineering, Vol. 141, No. 11, pp. 04015024 1-10.

Liang, R. (2013). Long Term Validation of an Accelerated Polishing Test Procedure for HMA Pavements. Final Report, ODOT Project No.

FHWA/OH-2013/3, Ohio Department of Transportation, Columbus, OH.

Liang, R.Y. (2003). Blending Proportions of High Skid and Low Skid Aggregate. Final Report prepared for Ohio Department of Transportation (ODOT), Columbus, Ohio.

Lister, N.W., and R. R. Addis (1977). Field observations of rutting and practical implications. Transportation Research Record 640, Transportation Research Board, Washington, D.C., pp. 28-34.

Liu, Q., and Cao, D. (2009). Research on Material Composition and Performance of Porous Asphalt Pavement. Journal of Materials in Civil Engineering, 21(4), 135-140.

Luce, A., E. Mahmoud, E. Masad and A. Chowdhury (2007). Relationship of Aggregate Micro-texture to Asphalt Pavement Skid Resistance. Journal of Testing and Evaluation, ASTM 35(6), pp. 578–588.

MaClean, D. J. and F. A. Shergold (1958). The polishing of roadstone in relation to the resistance to skidding of bituminous road surfacings. Road Research Technical Paper No. 43, Department of Scientific and Industrial Research, Her Majesty's Stationery Office, London, pp. 1-29.

Manual for asphalt pavement (1989). Japan Road Association, Japan.

Masad. E., A. Luce and E. Mahmoud (2006). Implementation of Aims in Measuring Aggregate Resistance to Polishing, Abrasion and Breakage. FHWA Report FHWA/TX-06/5-1707-03-1, Texas Department of Transportation, Austin, Texas.

Masad. E., A. Luce, E. Mahmoud and A. Chowdhury (2007). Relationship of Aggregate Texture to Asphalt Pavement Skid Resistance Using Image Analysis of Aggregate Shape. Final Report for Highway IDEA Project 114. Texas Department of Transportation, Austin, Texas.

Masad. E., R. Arash, A. Chowdhury, and P. Harris (2008). Predicting Asphalt Mixture Skid Resistance Based On Aggregate Characteristics. FHWA Report FHWA/TX-09/0-5627-1, Texas Department of Transportation, Austin, Texas.

Masad, E., A. Rezaei, and A. Chowdhury (2010). Field evaluation of asphalt mixture skid resistance and its relationship to aggregate characteristics. Report FHWA/TX-11/0-5627-3, Texas Department of Transportation, Austin, TX.

McGhee, K.K. and G.W. Flintsch (2003). High Speed Texture Measurement of Pavements. Final Report, Report No. VTRC 03-R9, Virginia Transportation Research Council (VTRC), Charlottesville, Virginia.

McGovern, C., P. Rusch, and D. Noyce (2011). State Practices to Reduce Wet Weather Skidding Crashes, FHWA Report FHWA-SA-11-21, Department of Transportation, Federal Highway Administration, Washington, D.C..

Meiarashi, S. and F. Oishi (2007). Noise reduction effect of porous elastic road surface measured by CPX method. In Proceedings of INTER-NOISE 07, Istanbul, Turkey, pp. 702.

Ministry of Transportation and Infrastructure, British Columbia (BC MTI), (2009). Pavement Surface Condition Rating Manual. 3rd Edition, British Columbia, Canada.

Monismith, C.L., K. E. Secor and W. Blackmer (1961). Asphalt mixture behaviour in repeated flexure, Proceedings of Association of Asphalt Paving Technologists, Vol. 30, pp. 188-222.

Moore, D. F. (1966). Prediction of Skid-resistance Gradient and Drainage Characteristics for Pavements, Highway Research Record 131, pp. 181-203.

Moore, D.F. (1969). Recommendations for an International Minimum Skid-Resistance Standard for Pavements. Highway Research Board Special Report 101, Highway Research Board, National Research Council, Washington, D.C..

Moore, D. F. (1975). Principles and Applications of Tribology, Pergamon Press, Oxford, UK.

Morgan P. A., P. M. Nelson and H. Steven (2003). Integrated Assessment of Noise Reduction Measures in the Road Transport Sector. TRL Project Report PR SE/652/03. Transport Research Laboratory, Wokingham, U.K..

Moser, M. (2009). Engineering Acoustics: An Introduction to Noise Control. Springer, London.

Mun, S. (2010). Sound Absorption Characteristics of Porous Asphalt Concrete Pavements. Canadian J. of Civil Engineering, Vol. 37, pp. 273-278.

Norsemeter (2015). Norsemeter Friction. http://www.norsemeter.no/Technology/. Accessed 16 October 2015.

Mullen, W.G., S. H. M. Dahir and N. F. El Madani (1974). Laboratory Evaluation of Aggregates, Aggregate Blends, and Bituminous Mixes for Polish Resistance. Transportation Research Record 523, Transportation Research Board, TRB, National Research Council, Washington, D.C..

NCHRP (2000). NCHRP Synthesis 291: Evaluation of Pavement Friction Characteristics, National Cooperative Highway Research Program, Washington D.C. Permanent International Association of Road Congress (PIARC).

NCHRP (1978). Open-graded friction courses for highways. NCHRP Synthesis of Highway Practice 49, Transportation Research Board, National Research Council, Washington D.C..

Neithalath, N., A. Marolf, J. Weiss and J. Olek (2005). Modeling the Influence of Pore Structure on the Acoustic Absorption of Enhanced Porosity Concrete. Journal of Advanced Concrete Technology, 3(1),pp. 29-40.

Newton, P. W., S. Baum, K. Bhatia, S. K. Brown, S. Cameron, B. Foran, T. Grant, S. L. Mak, P. Memmott, V. G. Mitchell, K. Neate, N. C. Smith, R. Stimson, A. Pears, S. Tucker and E. D. Yencken (2001). Australia State of the Environment Report 2001: Human Settlements Theme Report. The Commonwealth Scientific and Industrial Research Organisation, Canberra, Australia.

Nichols, F.P., Jr., J. H. Dillard and R. L. Orwood (1957). Skid Resistant Pavement in Virginia. Virginia Council of Highway Investigation and Research. Reprint No. 18.

Nicholls, J.C. (1998). Asphalt surfacing. CRC Press, London, UK.

Nilsson, N. A. (1979). Possible Method of Reducing External Tyre Noise. The International Tire Noise Conference 1979, Stockholm, Sweden.

Nilsson, N. A. (1980). External Tire/Road Noise from Trailing Contact Edge - the Excitation Process. IFM Akustikbyran AB, Stockholm, Sweden.

Nilsson, N. A., O. Bennerhult, and S. Soederqvist (1980). External tire/road noise: its generation and reduction. In Proceedings of INTER-NOISE 80, pp 245, Miami, FL.

Nilsson, N. A. (1982). Principles in the Control of External Tire/Road Noise. INTER-NOISE 82, pp. 123, San Francisco, California.

Nitta, N., K. Saito and S. Isozaki (1990). Surface Characteristics of Roadways: International Research and Technologies. *A*STM Special Technical Publication 1031*,* American Society for Testing and Materials, pp. 113-126.

NZ Transport Agency (2010). NZTA T10:2010. Specification for State Highway Skid Resistance Management. New Zealand Transport Agency, Wellington, New Zealand.

Ohio State Department of Transportation (ODOT) (2006). Pavement Condition Rating System. ODOT, Columbus, OH.

Ong, G. P. (2006). Hydroplaning and Skid Resistance Analysis Using Numerical Modelling. PhD Thesis of the National University of Singapore.

Ong, G. P. and T. F. Fwa (2010). A Mechanistic Interpretation of Braking Distance Specifications and Pavement Friction Requirements. Transportation Research Record, 2155, pp. 145-157.

Ong, G. P. and T. F. Fwa (2007). Wet-pavement hydroplaning risk and skid resistance: modeling. Journal of Transportation Engineering, 133(10), pp. 590-598.

Oswald, L. J., and A. Arambages (1983). The Noise Mechanisms of Cross Groove Tire Tread Pattern Elements. NOISE-CON 83, New York.

Pavement design (2004), Austroads, Sydney.

PIARC (2013). Quiet Pavement Technologies. Report 2013R10EN. F.G. Practicò and M. Swanlund (eds.). World Road Association (PIARC), La Défense, France.

Permanent International Association of Road Congresses (PIARC) (1995), International PIARC Experiment to Compare and Harmonize Texture and Skid Resistance Measurements, Report No. AIPCR-01.040.T, PIARC, Brussels, Belgium.

Phillips, S. M., P. A. Morgan and G. R. Watts (1999). Development of Methods for Understanding Tyre/Road Noise Generation and Propagation. INTER-NOISE 99, Fort Lauderdale, Florida.

Pilli-Sihvola, Y. and P. Rama (1997). Speed limits. ITS International, Issue No. 13, Nov/Dec. pp. 72-73.

Pinkus, O. and B. Sterlicht (1961). Theory of Hydrodynamic Lubrication. McGraw-Hill, New York.

Ponniah, J., S. Tabib, B. Lane, and C. Raymond (2010). Evaluation of the Effectiveness of Different Mix Types to Reduce Noise Level at the Tire/Pavement Interface. Proceedings of the Annual Conference of the Transportation Association of Canada, Halifax, Nova Scotia, Canada.

Raaberg, J., B. Schmidt and H. Bentsen (2001). Technical Performance and Long-Term noise Reduction of Porous Asphalt Pavement. Report 112, Road Directorate, Danish Road Institute.

Ranieri, V., G. Ying, and J. J. Sansalone (2012). Drainage Modeling of Roadway Systems with Porous Friction Courses. Journal of Transportation Engineering, 138(4), pp. 395-405.

Rasmussen R. O. and R. C. Sohaney (2012). A Tire-Pavement and Environmental Traffic Noise Research Study. Report No. CDOT-2012-5, Colorado Department of Transportation, Denver, CO.

Rasmussen, R. O., R. J. Bernhard, U. Sandberg, E. P. Mun (2007). The Little Book of Quieter Pavements. Report No. FHWA-IF-08-004, Federal Highway Administration, Washington, D. C..

Rasmussen, R. O., Sohaney, R., P. Wiegand, D. Harrington (2011). Measuring and Analyzing Pavement Texture. Concrete Pavement Surface Characteristics Program. National Concrete Pavement Technology Center; Iowa State University, Institute of Transportation, Tech Brief.

Rasmussen, R. O., R. Sohaney, and P. Wiegand (2011). Measuring and Reporting Tire-Pavement Noise Using On-Board Sound Intensity

(OBSI). National Concrete Pavement Technology Center, Iowa State University, Ames, Iowa.

Rado, Z. (1994). Analysis of Texture Models. PTI Report No. 9510, Pennsylvania Transportation Institute (PTI), Penn State University, State College, Pennsylvania.

Rezaei A., E. Masad and A. Chowdhury (2011). Development of a Model for Asphalt Pavement Skid Resistance Based on Aggregate Characteristics and Gradation. Journal of Transportation Engineering, 137(12), pp. 863-873.

Rezaei A., E. Masad (2012). Experimental-Based Model for Predicting the Skid Resistance of Asphalt Pavements. International Journal of Pavement Engineering. Taylor & Francis Group. Vol. 14, No. 1, pp. 24-35.

Richard, J., R. J. Ruhala and C. B. Burroughs (1998). Separation of Leading Edge, Trailing Edge, and Sidewall Noise Sources from Rolling Tires. NOISE-CON 1998, Ypsilanti, Michigan.

RN-29 (1970). A guide to the structural design for new roads, Department of the Environment, HMSO, London.

Roberts, F. L., P. S. Kandhal, E. R. Brown, D. Y. Lee, and T. W. Kennedy, (1996). Hot Mix Asphalt Materials, Mixture Design, and Construction. National Asphalt Pavement Association Education Foundation. Lanham, MD.

Road Research Laboratory (1960). Instructions for using the portable skid resistance testers. Road Note No. 27, Department of Scientific and Industrial Research, Her Majesty's Stationery Office, London.

Rozaei A., E. Masad and A. Chowdhury (2011). Development of a Model for Asphalt Pavement Skid Resistance Based on Aggregate Characteristics and Gradation. Journal of Transportation Engineering, 137(12), pp. 863-873.

RstO 2000 (1999). Richtlinien für die Standardisierung des Oberbaues von Verkehrsflächen, Entwurf,

Runkle, S. N. and D. C. Mahone (1980). Variation in Skid Resistance over Time. Virginia Highway & Transportation Research Concil, pp. 10-13.

Ryszard, W. (2001). Measurement of Tyre/Road Noise in Longitudinal Slip Conditions. INTER-NOISE 01, the Hague, the Netherlands.

Saemann, E. U. and H. Schmidt (2002). Schallmessungen bei der Entwicklung von Reifen mit Geringem Vorbeifahrtpegel. Zeitschrift für Lärmbekämpfung, 49(2), pp. 59-62.

Saito, K., T. Horiguchi, A. Kasahara, H. Abe and J. J. Henry (1996). Development of Portable Tester for Measuring Skid Resistance and Its Speed Dependency on Pavement Surfaces." Transportation Research Record 1536, Transportation Research Board, TRB, National Research Council, Washington D.C..

Sandburg, U. (1998). Influence of Road Surface Texture on Traffic Characteristics Related to Environment, Economy, and Safety: A State-of-the-Art Study Regarding Measures and Measuring Methods. VTI Report 53A-1997, Swedish National Road Administration, Borlange, Sweden.

Sandburg, U. and J. A. Ejsmont (2002). Tyre/Road Noise Reference Book. ISBN 91-631- 2610-9, Informex, Kisa, Sweden.

Scavuzzo, R. W., L. T., Charek, P. M., Sandy and G. D. Shteinhauz (1994). Influence of Wheel Resonance on Tire Acoustic Cavity Noise. SAE Technical Paper, Series No. 940533.

Schaaf, K. and D. Ronneberger (1982). Noise radiation from rolling tires – sound amplification by the “horn-effect". In Proceedings of INTER-NOISE 82, pp. 131, San Francisco, CA.

Scheidegger, A. E. (1963). The Physics of Flow through Porous Media. University of Toronto Press, Toronto, Canada.

Senior, S.A. and C. A. Rogers (1991). Laboratory Tests for Predicting Coarse Aggregate Performance in Ontario." In Transportation Research Record No. 1301. Transportation Research Board, Washington, D.C..

Shaffer, S. J., A. C. Christiaen, M. J. Rogers Battelle (2006). Assessment of friction-based pavement methods and regulations. Heavy Vehicle Research Centre.

Shahin, M. Y. (1994). Pavement Management for Airports, Roads and Parking Lots, Chapman and Hall, New York, NY.

Shell pavement design manual – asphalt pavements and overlays for road traffic (1978). Shell International Petroleum Company Limited, London.

Shimeno, S., Oi, A. and T. Tanaka (2010). Evaluation and Further Development of Porous Asphalt Pavement with 10 Years Experience in Japanese Expressways. Proceedings 11th Int Conf on Asphalt Pavements, 1-6 August, Nagoya, Japan, Vol. 1, pp. 43-52.

Skerritt, W.H., 2004. Notes from February 19 (2004) teleconference with Mr. Bill Skerritt of the New York Department of Transportation, Engineering Geology section of the Materials Bureau.

Smith, B., and G. Fager (1991). Physical Characteristics of Polish Resistance of Selected Aggregates. Transportation Research Record 1301, Transportation Research Board, Washington, D.C.. pp. 117-126.

Smith, L., R. Beckman, D. Anson, K. Nagel and M. E. Williams (1995). TRANSIMS: Transportation Analysis and Simulation System. Fifth National Conference on Transportation Planning Methods Applications-Volume II: A Compendium of Papers, Seattle, Washington.

Sousa, J. B., J. Craus and C. L. Monismith (1991). Summary report on permanent deformation in asphalt concrete. SHRP-A/IR-91-104, Strategic Highway Research Program (SHRP). Washington D.C..

Speir R., T. P. R. Barcena and P. Desaraju (2009). Development of Friction Improvement Policies and Guidelines for the Maryland State Highway Administration. Report MD-07-SP708B4F, Maryland State Highway Administration, Baltimore, MD.

Subedi, Y. P. (2015). Evaluation of Louisiana Friction Rating Table by Field Measurements. MSc thesis, Department of Civil and Environmental Engineering, Louisiana State University.

Tan, S. A., T. F. Fwa and C. T. Chuai (1999). Automatic field permeameter for drainage properties of porous asphalt mixes. Journal of Testing and Evaluation, 27(1), 57-62.

Tan, S. A., T. F. Fwa and C. T. Han (2003). Clogging evaluation of permeable bases. Journal of Transportation Engineering, 129(3), 309-315.

Tarrer. A. R. and V. Wagh (1991). The effect of the physical and chemical characteristics of the aggregate on bonding. SHRP-A/UWP-91-510, Strategic Highway Research Program (SHRP). Washington D.C..

Technical committee report on road surface characteristics. Proc., 19th World Congress, Marakesh, Morocco.

The Highways Agency (2006). Design Manual for Roads and Bridges. Volume 7 Section 5. London, United Kingdom.

Theyse, H. L., M. Beer and F. C. Rust (1996). Overview of the South African mechanistic pavement design analysis method, Transportation Research Record, 1539, TRB, National Research Council, Washington, D.C., pp. 6-17.

Thickness design – asphalt pavements for highways and streets (1999). The Asphalt Institute, Manual Series No. 1 (MS-1), 9th edition.

Tomiyama, K., A. Kawamura, T. Ishida, and J. Masakazu (2010). Wavy Characteristics and Its Evaluation Index Determining Ride Quality of Rut Profile. Pavement Evaluation Conference, Roanoke, VA.

Tyfour, W. R. (2009). Tire Skid Resistance on Contaminated Wet Pavement. Jordan Journal of Mechanical and Industrial Engineering. Volume 3, Number 2, pp. 119-124.

Ulf Sandberg (1982). Will tire/road noise limit vehicle noise reductions? In Proceedings of INTER-NOISE 82, Washington, D.C., pp. 127.

Ulf Sandberg and J. A. Ejsmont (2002). Tyre/Road Noise Reference Book. INFORMEX, Kisa, Sweden.

van der Zwan, J. T. (2011). Developing Porous Asphalt for Freeway in the Netherlands: Reducing Noise, Improving Safety, Increasing Service Life. TR News 272, pp. 22-29.

Villani, M., I. Artamendi, M. Kane and A. Scarpas (2011). The Contribution of the Hysteresis Component of the Tire Rubber Friction on Stone Surfaces, Journal of the Transportation Research Board, No. 2227, Transportation Research Board of the National Academies, Washington, D.C., pp. 153–162.

Voller, T. W. and D. I. Hanson (2006). Development of Laboratory Procedure for Measuring Friction of HMA Mixtures – Phase I. Final Report of NCAT No. 06- 06, National Centre for Asphalt Technology.

von Meier, A. (1992). Thin Porous Surface Layers - Design Principles and Results Obtained. The Mitigation of Traffic Noise in Urban Areas, Nantes, France.

von Meier, A., G. J. van Blokland and J. C. P. Heerkens (1990). Noise Optimized Road Surfaces and Further Improvements by Tyre Choice. INTROC 90, Gothenburg, Sweden.

Walker, D., L. Entine, S. Kummer (2002). Pavement Surface Evaluation and Rating (PASER), Asphalt Roads." Wisconsin Transportation Information Center, Madison, WI.

Wallman, C.G. and H. Astrom (2001). Friction Measurement Methods and the Correlation between Road Friction and Traffic Safety. Swedish National

Road and Transport Research Institute, VTI Meddelande 911 A, Linkoping, Sweden.

Wambold, J. C., C. E. Antle, J. J. Henry and Z. Rado (1995). International PIARC Experiment to Compare and Harmonize Texture and Skid Resistance Measurements. Final Report, PIARC, Paris, France.

Wambold, J. C., J. J. Henry and A. Anderson (1998). Third Year Joint Winter Runway Friction Program. National Aeronautics and Space Administration (NASA), Washington, D.C..

Washington State Department of Transportation (WSDOT) (1999). Pavement Surface Condition Field Rating Manual for Asphalt Pavements. Olympia, Washington.

Williams, M. L., R. F. Landel and J. D. Ferry (1955). Temperature Dependence on Relaxation Mechanisms in Amorphous Polymers. Journal of American Chemical Society, 77, 3701-3707.

Wilson D. J. (2013). The Effect of Rand Contaminants on Road Pavement Skid Resistance. Research Report 515, New Zealand Transport Agency, Wellington, New Zealand.

Wilson D. J. and R. C. M. Dunn (2005). Polishing aggregates to equilibrium skid resistance. ARRB Road & Transport Research Journal 14, No.2, pp. 1-17.

Wu, C. L. and M. Nagi (1995). Optimizing Surface Texture of Concrete Pavement. Portland Cement Association, Skokie, Ill.

Yum, K. and J. S. Bolton (2004). Sound radiation modes of a tire on a reflecting surface. In Proceedings of Noise-Con 04, page 161, Baltimore, MD.

Yum, K., K. Hong, and J. S. Bolton (2006). Experimental relationship between tire structural wave propagation and sound radiation. In Proceedings of INTER-NOISE 06, page 5605, Honolulu, HI.

Younger, K.,R. G. Hicks and J. Gower (1994). Evaluation of Porous Pavements Used in Oregon, Final Report. Oregon Department of Transportation, Salem, Oregon.

Zhang, L. (2014). Analyzing Skid Resistance and Tire/ Road Noise on Porous Pavement Using Numerical Modeling. Ph.D. thesis. National University of Singapore.

Zhang, L., T. F. Fwa, G. P. Ong and L. Chu (2016). Analysing effect of roadway width on skid resistance of porous pavement. International Journal of Road Materials and Pavement Design, 17(1), 1-14.

Zhang, L., G. P. Ong and T. F. Fwa (2013). Developing an analysis framework to quantify and compare skid resistance performances on porous and non-porous pavements. Transportation Research Record: Journal of the Transportation Research Board, No. 2369, pp. 77-86.

Zhang, L., G. P. Ong and T. F. Fwa (2012). Three dimensional modeling of porous pavement permeability using a simplified pore network structure. Proceedings of the 7th International Conference on Maintenance and Rehabilitation of Pavements and Technological Control, Auckland, New Zealand.

Zheng, C. C., Z. D. Chen and J. L. D. (2001). Pavement Design in Takalimakan Desert. Journal of Transportation Engineering, Vol. 127, No. 2, ISSN 0733-947X/01/0002-0112–0115, pp. 16272.